Influence of Enteric Microbiota on Human Rotavirus and Human Norovirus Infection, and Rotavirus Immunity in Gnotobiotic Pigs

Erica L. Twitchell

Dissertation submitted to the faculty of the Virginia Polytechnic Institute and State University in partial fulfillment of the requirements for the degree of

Doctor of Philosophy
In
Biomedical and Veterinary Sciences

Lijuan Yuan, Committee Chair
Irving Coy Allen
Liwu Li
Xiang-Jin Meng

November 15, 2018
Blacksburg, VA

Keywords: rotavirus, norovirus, microbiome, gnotobiotic, pigs

Influence of Enteric Microbiota on Human Rotavirus and Human Norovirus Infection, and Rotavirus Immunity in Gnotobiotic Pigs

Erica L. Twitchell

ACADEMIC ABSTRACT

Enteric microbiota influences enteric viral infections, and host response to these pathogens and vaccines. Using gnotobiotic (Gn) pigs transplanted with human gut microbiota (HGM), we studied the effects of HGM on the immune response to oral rotavirus vaccination and rotaviral disease. We also used HGM transplanted Gn pigs to determine the effects of HGM on human norovirus infection. Despite commercially available vaccines, human rotavirus is a leading acute gastroenteritis in children, especially those in developing countries. Human norovirus (HuNoV) is a leading cause of acute gastroenteritis in all age groups worldwide, and no vaccines are commercially available. Further understanding of how enteric microbiota influences these viral diseases may identify therapeutic targets.

In our rotavirus study, pigs were colonized with HGM from an infant with low fecal concentrations of enteropathy biomarkers and responded well to their first dose of oral rotavirus vaccine (healthy human gut microbiota "HHGM"); or pigs were colonized with HGM from an infant with high fecal concentrations of enteropathy biomarkers and a poor response to the first dose of oral rotavirus vaccine (unhealthy human gut microbiota "UHGM"). HHGM colonized pigs had stronger cell-mediated and mucosal immune response to oral rotavirus vaccine compared to UHGM pigs based on the number of rotavirus-specific IFN-γ producing T cells in the ileum, spleen, and blood, and trends towards higher rotavirus specific antibody titers in intestinal contents, respectively. Significant correlations between multiple Operational Taxonomic Units (OTUs) of bacteria and frequencies of IFN-γ producing T cells at the time of human rotavirus challenge existed, suggesting that certain members of the microbiota influenced the immune response to the vaccine. After the vaccinated pigs were challenged with human rotavirus, HHGM pigs had less severe and shorter duration of viral shedding and diarrhea compared to UHGM pigs, suggesting that HHGM facilitated development of stronger protective immunity. These results demonstrated that composition of the enteric microbiota influenced host immune response to oral vaccination.

In the norovirus study, Gn pigs were colonized with HHGM to determine the effects of microbiota on HuNoV infection. Colonized pigs shed more virus for a longer duration than non-colonized pigs, and also had higher viral titers in the duodenum and distal

ileum. Diarrhea was more severe 4-10 days post-infection and lasted longer in colonized compared to non-colonized pigs. Twenty-seven genes related to the immune system were highly upregulated in HuNoV infected, colonized pigs compared to non-colonized controls. These result showed that HHGM influenced infectivity of HuNoV in the Gn pig model and altered host gene expression related to the immune system.

These studies showed that HHGM can improve the host immune response and efficacy of rotavirus vaccine, but it can also enhance infection and clinical disease in HuNoV infected Gn pigs. Depending on the virus, gut microbiota may be beneficial or detrimental to the host. Those developing future treatments aimed at altering microbiota to prevent or ameliorate one viral pathogen need to consider the potential for enhancing a different pathogen. These studies demonstrated the usefulness of HGM transplanted Gn pigs for evaluation of microbiota influence on infection and immunity of enteric viral pathogens.

Influence of Enteric Microbiota on Human Rotavirus and Human Norovirus Infection, and Rotavirus Immunity in Gnotobiotic Pigs

Erica L. Twitchell

GENERAL AUDIENCE ABSTRACT

Gut microbiota influences intestinal viral infections, and host response to these pathogens and vaccines. Using gnotobiotic (Gn) pigs transplanted with human gut microbiota (HGM), we studied the effects of HGM on the immune response to oral rotavirus vaccination and rotaviral disease. We also used HGM transplanted Gn pigs to determine the effect of HGM on human norovirus infection. Despite commercially available vaccines, human rotavirus is a leading acute gastroenteritis in children, especially those in developing countries. Human norovirus (HuNoV) is a leading cause of vomiting and diarrhea in all age groups worldwide, and no vaccines are commercially available. Further understanding of how gut microbiota influences these viral diseases may identify therapeutic targets.

In our rotavirus study, pigs were colonized with HGM from an infant without evidence of intestinal disease based on fecal analysis, and who responded well to the first dose of oral rotavirus vaccine (healthy human gut microbiota "HHGM"); or pigs were colonized with HGM from an infant with evidence of potential intestinal dysfunction and a poor response to the first dose of oral rotavirus vaccine (unhealthy human gut microbiota "UHGM"). HHGM colonized pigs had a stronger immune response to the oral rotavirus vaccine compared to UHGM pigs. Significant correlations between multiple Operational Taxonomic Units (OTUs) of bacteria and frequencies of rotavirus-specific immune cells at the time of human rotavirus challenge existed, suggesting that certain members of the microbiota influenced the immune response to the vaccine. After the vaccinated pigs were challenged with human rotavirus, HHGM pigs had less severe and shorter duration of viral shedding and diarrhea compared to UHGM pigs, suggesting that HHGM enhanced vaccine efficacy. These results demonstrated that composition of the gut microbiota influenced host immune response to oral vaccination.

In the norovirus study, GN pigs were colonized with HHGM to determine the effects of microbiota on HuNoV infection. Colonized pigs shed more virus for a longer duration than non-colonized pigs, and also had higher viral titers in sections of small intestine. Diarrhea was more severe 4-10 days after infection and lasted longer in colonized compared to non-colonized pigs. Twenty-seven genes related to the immune system were highly upregulated in HuNoV infected, colonized pigs compared to controls. These result showed that HHGM influenced infectivity of HuNoV in the Gn pig model and altered host gene expression related to the immune system.

These studies showed how HHGM improved the host immune response and efficacy of rotavirus vaccine, but conversely enhanced infection and clinical disease in HuNoV infected pigs. Depending on the virus, gut microbiota may be beneficial or detrimental to the host. Those developing future treatments aimed at altering microbiota to prevent or ameliorate one viral pathogen need to consider the potential for enhancing a different pathogen. These studies showed the usefulness of HGM transplanted Gn pigs for evaluation of microbiota influence on infection and immunity of intestinal viruses.

Dedicated to my family

.

ACKNOWLEDGEMENTS

I consider myself very fortunate to have Dr. Lijuan Yuan as a mentor. She is an exemplary professional and personal role model. Dr. Yuan has always been supportive, patient, and eager to share her knowledge. I cannot thank her enough.

It has been a privilege to work with Yuan lab members, past and present. I could not have completed this without their help. Thank you Dr. Shaohua Lei, Ashwin Ramesh, Dr. Tammy Castellucci, Mariah Weiss, Christine Tin, Dr. Xingdong Yang, Dr. Guohua Li, Dr. Ke Wen, Libby Majette, and Dr. Erika Olney.

I thank current and former committee members, Dr. Coy Allen, Dr. Liwu Li, Dr. X.J. Meng, and Dr. Nanda Nanthakumar for sharing their knowledge, and providing guidance and support.

I am thankful for the efforts of Yuan lab collaborators, Dr. Sylvia Becker-Dreps, Dr. Andrea Azcarate-Peril, Dr. Samuel Vilchez, Dr. Stacey Schultz-Cherry, Dr. Husen Zhang, Dr. Song Li, and Jiyoung Lee. The studies presented in this dissertation would not have been possible without them.

The BMVS administration has been very supportive. I am extremely appreciative of the assistance provided by Dr. Ansar Ahmed and Dr. Roger Avery. I also thank Becky Jones and Susan Rosebrough.

This work could not have been completed without the veterinary and animal care provided by Dr. Sherrie Clark-Deener, Dr. Kevin Pelzer, Dr. Nicole Lindstrom, and TRACCS staff members.

TABLE OF CONTENTS

LIST OF FIGURES

Chapter 2

Chapter 3

LIST OF TABLES

Chapter 1

Chapter 2

Chapter 1 Literature review

Enteric viral infections and the intestinal microbiome

Erica Lynn Twitchell

Department of Biomedical Sciences and Pathobiology

Virginia-Maryland College of Veterinary Medicine,
Virginia Tech, Blacksburg, VA 24061, USA.

Partially published as a book chapter in *Mechanisms underlying host-microbiome interaction in pathophysiology of human disease*. Edited by Sun J and Dudeja PK (2028). Used with permission.

Introduction to the microbiome

The enteric microbiome is known to influence host heath in a variety of ways. The focus of this work is to investigate the influence of enteric microbiome on human rotavirus and human norovirus infection and rotavirus immunity in Gn pigs.

Enteric microbiota is composed of bacteria, viruses, fungi, protozoa and archaea, but for the purposes of this work, only bacteria will be considered. In humans, the enteric microbiota is estimated to contain over 35,000 species of bacteria, and the colon has up to 10^{12} bacteria per gram of contents (1, 2). According to the Human Microbiome Project and the Metagenome of the Human Intestinal Tract (MetaHit), studies suggested there may be over 10 million non-redundant genes in the microbiome (1). The microbiome, the collective genomes of all members of the microbiota, has a role in development of the immune system and enteric nervous system, metabolism of nutrients and pharmaceutical agents, and protection from enteropathogens. An altered microbiome may lead to immune dysfunction; altered metabolism, and increased risk of conditions such as diabetes and inflammatory bowel disease; and increased risk of enteropathogen infection (1)

The definition of healthy gut microbiota varies by source. It has been stated "healthy" gut microbiota is mainly composed of the phyla Firmicutes and Bacteroidetes, followed by Actinobacteria and Verrucomicrobia (1). The Firmicutes: Bacteroidetes ratio has been implicated in predisposition to disease, but the true importance of these findings is questionable as there is significant variability in microbiome composition, even in healthy individuals (1). Some define healthy gut microbiota as having the low relative abundance of the phylum Proteobacteria and high relative abundance of the genera

Bacteroides, *Prevotella*, and *Ruminococcus* (3). The MEtaHIT consortium has attempted to classify enteric bacteria into enterotypes, which are clusters of species present in the host (4). Enterotype 1 has high relative abundance of *Bacteroides*, enterotype 2 has high relative abundance of *Prevotella*, and enterotype 3 has high relative abundance of *Ruminococcus* (3).

Gut microbiota varies between individuals and is influenced by mode of delivery, diet, environment, genetics, and disease states. The infant gut is first colonized by facultative anaerobes such as *Lactobacillus*, *Enterobacter*, and *Enterococcus* (5). As the environment becomes more reduced due to depletion of oxygen by first colonizers, strict anaerobes such as *Bacteroides, Bifidobacterium,* and *Clostridium* increase in abundance (5). Children delivered vaginally have microbiota predominantly composed of *Lactobacillus, Prevotella,* and *Sneathia* while C-section derived babies have microbiota composed mostly of *Staphylococcus*, *Corynebacterium,* and *Propionibacterium* (6). At 24-months of age, infants delivered by C-section have less diverse gut microbiota than those delivered vaginally (7). Newborn diet also influences microbiota composition. *Bifidobacterium*, *Lactobacillus,* and *Streptococcus* are more abundant in breast fed infants than formula fed babies, who have more *Atopobium, Bacteroides*, *E. coli*, and *Klebsiella* (5, 8). Human milk oligosaccharides nourish colonic bacteria and provide a selective growth advantage for *Bifidobacterium* (9). As solid food is introduced, polysaccharides induce increase in abundance of *Bacteroides, Clostridium,* and *Ruminococcus*, while the abundance of *Bifidobacterium* and *Enterobacteriaceae* members decrease (7). While on a milk based diet, the metagenome contains many genes for simple sugar digestion, but after solid food transition, genes for polysaccharide

breakdown and vitamin production increase (10). By the age of 3 years, the gut microbiota stabilizes and diversifies, is similar to that of adults, and *Ruminococcaceae, Lachnospiraceae, Bacteroidaceae,* and *Prevotellaceae* become more abundant (7, 10, 11). Firmicutes and Bacteroides are the dominant phyla of the human enteric microbiota (5)

Microbiota composition varies geographically and may partly be due to diet. Gut microbiota of children from rural Burkina Faso with a high fiber diet, differed from urban Italian children with a diet high in processed sugar and fat (7). Children from Burkina Faso had more Bacteroidetes, and reduced Firmicutes, Proteobacteria, and Actinobacteria compared to the Italian children (7). A study comparing adults and children from the United States, Venezuela, and Malawi determined *Prevotella* was dominant in Malawians and Venezuelans, while *Bacteroides* dominated in people from the United States(7). Metagenomic analysis revealed enrichment in glycan and urease metabolic pathways in Venezuelan and Malawian people (7).

Intestinal microbiota aids in development and function of the immune system. Germ-free animals demonstrate the importance of microbiota in immune system development. Germ free animals have underdeveloped immune systems and compared to wild type animals, and have decreased numbers of lymphocytes in GALT, intestinal lamina propria, and mesenteric lymph nodes (12). Introduction of commensal bacteria can lead to induction of sIgA, increased CD4+ T cell numbers, and development of GALT (5). Gnotobiotic animals can also have altered immune responses. Germ-free mice are less efficient at clearing *Escherichia coli* K12 administered intravenously, have a decreased inflammatory response, and smaller myeloid pool when compared to

conventional mice (13). Microbiota regulates mucin production, which is important for trapping pathogens, concentrating bacterial metabolites, and protecting against gastric and duodenal secretions (12). Sphingolipids produced by *Bacteroides* species, are structurally similar to host lipid agonists of invariant natural killer (iNK) T cells, and can promote iNKT cell activation (14). Intestinal immunity can be regulated by microbiota modulating TLR expression, upregulation of costimulatory molecules on antigen presenting cells, and T cell activation (12). Intestinal microbiota induces synthesis of antimicrobial peptides such as cathelicidins, c-type lectins, and defensins by host Paneth cells (1). *Bacteroides thetaiotaomicron* and Lactobacillus *innocua* are examples of two important species inducing production of AMPs (1). Microbiota- host interaction cause *Lactobacillus* spp. to produce lactic acid, and enhances the function of host lysozyme (15). Bacterial metabolic products such as short chain fatty acids (SCFAs) and lithocholic acid induce expression of cathelicidin (1). Gram-negative organisms especially, can activate intestinal dendritic cells leading to expression of sIgA by plasma cell (1). Proteobacteria, a dominant phylum in human newborn gut microbiota, triggers Proteobacteria specific IgA, which has a role in controlling Proteobacteria levels in adults(16). Another study found that the number of *Bifidobacterium* spp. in early fecal samples correlated with total levels of salivary sIgA at 6 month, and bifidobacterial diversity may enhance maturation of mucosal sIgA system (17). *L. reuteri* metabolizes tryptophan to indole-3-aldehyde, which then promotes IL-22 transcription, leading to AMP expression, mucosal homeostasis and enterocyte fucosylation (13, 18). Segmented filamentous bacteria in the terminal ileum of mice promote differentiation of enteric Th17 cells, induce IgA production, stimulate germinal centers, and induce IgA secreting cells

in Peyer's patches (2, 4). Firmicutes are also essential for Th17 cell development, which promote intestinal mucosal barrier integrity (18). Intestinal colonization patterns may affect B cell maturation as early colonization with *E. coli* and *Bifidobacterium* were associated with higher numbers of CD20+ B cells that expressed memory marker CD27 at 4 and 18 months of age (19). SCFAs are bacterial metabolites from dietary fiber fermentation (13). Butyrate, a SCFA, has anti-inflammatory effects on bone marrow derived and colonic macrophages, and enhances intestinal mucosal barrier function (13). *Bacteroides fragilis* polysaccharide (PSA) is an immunomodulatory compound detected by TLR 2 and involved in T cell development, induction of regulatory T cells, and secretion of IL-10 by CD4+ T cells (5). When given to germ free animals, PSA will correct T cell deficiency and direct lymphoid organogesis (20).

Rotavirus and norovirus virology, epidemiology, and immunology

Rotaviruses are nonenveloped, double-stranded RNA (dsRNA) viruses in the *Reoviridae* family that infect humans and other animals. The genome codes for six structural proteins and six nonstructural proteins located on 11 segments of double stranded RNA (21). The VP6 protein determines the rotavirus species (type A-J) (21). Genotypes are determined by RNA segments 7 and 4, which encode for the glycoprotein VP7, and a protease-cleaved protein VP4, respectively (21). In subtype nomenclature, VP7 determines the G designation and VP4 determines the P designation (21). Type A rotaviruses, which are most common in humans, have 32 G genotypes and 47 genotypes (21). Approximately 90% of severe infections are caused by six strains in humans (22).

Rotaviruses infect and replicate in mature enterocytes of the middle and distal intestinal villus and enteroendocrine cells of the small intestine (23). Viral binding

occurs via the VP8* domain of outer capsid protein VP4 to host glycan receptors such as sialoglycans and HBGAs (21, 24). Following VP8* binding, VP7 and the VP5* domain of VP4 bind with co-receptors to mediate entry (21). Potential co-receptors include integrins, heat shock protein 70, and junctional proteins (21). Viral internalization occurs via clathrin-dependent or -independent and caveolin-independent endocytic pathways (21, 24). Loss of the outer capsid layer and release of the double layered particle (DLP) into the cytoplasm is triggered by low calcium levels in the endosome (25). Viral mRNA is used for translation of proteins or RNA synthesis. RNA is packaged into new DLPs in the viroplasm (25). Binding of new DLPs to NSP4, followed by budding into the ER, where outer capsid proteins VP4 and VP7 are added, leads to formation of the triple-layered particle and transient envelope (25). Progeny are released via cell lysis or vesicular transport.

Rotaviruses are transmitted by the fecal-oral route and are major cause of acute gastroenteritis in young children, characterized by diarrhea, dehydration, and vomiting. Symptoms last from 1 to 5 days. Viral shedding in children ranges from 4 to 57 days with cessation of shedding in 43% of children within 10 days, 70% within 20 days, and 30% within 25 to 57 days (26). Disease incidence peaks between 4 and 23 months of age (21). Almost all children have had at least one rotavirus infection by 5 years of age (22). Due to the presence of maternal antibodies, infections in the first 3 months of life are generally milder than those occurring later (22). While rotavirus infections cause 8-10% of diarrhea episodes worldwide, they are responsible for approximately 35-40% of diarrhea episodes requiring hospitalization (22). Rotavirus infections caused approximately 500,000 deaths a year in children under 5 years of age, mostly in low-

middle income countries, before the two commercial vaccines (Rotarix and RotaTeq) became available (27, 28). Although vaccines have decreased the incidence of rotavirus mortality, efficacy of the vaccines is decreased in low –middle income countries compared to high income countries. Rotavirus infection still causes over 200,000 deaths a year, with over 90% occurring in low income countries (29).

Rotaviruses cause non-bloody diarrhea by causing damage to enterocytes, intestinal villus ischemia, action of the NSP4 enterotoxin, and activation of the enteric nervous system (27, 28). Damaged enterocytes lead to malabsorption and secondary osmotic diarrhea, while NSP4 causes secretory diarrhea (21). Enteric nervous system activation secondary to increased 5-HT secretion from enteroendocrine cells and NSP-4 mediated intracellular calcium elevation lead to increased small intestinal motility (30).

Correlates of protection against rotavirus infection include rotavirus-specific serum IgA, serum IgG, and fecal IgA (27, 28); however in some studies there is lack of correlation between neutralizing antibody titers and protection (27). Serum rotavirus-specific IgA is the best indicator of rotavirus immunity and it is used as a marker of vaccine take (31). Rotavirus-specific T cells help eliminate virus after infection and memory B cells provide long term protection (27). Newborns are protected from rotavirus infection by transplacental and breast milk antibodies (28). In adult mice, protection against rotavirus infection is mediated mostly by intestinal IgA (21). These cells are not readily inducible in neonatal mice (21). Children also have a poor ability to develop neutralizing antibodies, and protection against reinfection is age dependent (21). Rotavirus specific CD4+ T cells in children may be a factor in prevention of recurrent illness and the response to vaccination (21).

The innate immune system provides protection against rotavirus infection with DDX58 (RIG-I), an ATP-dependent RNA helicase that recognizes 5'triphosphate uncapped RNA; and IFIH1, which recognizes dsRNA (21). DDX58 and IFIH1 stimulate the IRF3 and NF-kB pathways via MAVS to induce IFN responses (21). TLR3 cognizes dsRNA, as does NLRP9b, a component of the nucleotide binding oligomerization domain like receptor inflammasome (21). It has been demonstrated in vitro and in vivo, that NSP1 can inhibit NF-kB and STAT1 activation leading to blockade of type I and type III IFN responses (21). In vitro and in piglets, rotavirus has been shown to down regulate the adaptive immune response via induction of TGF-β (21).

Norovirus is a nonenveloped, positive-sense, RNA virus in the C*aliciviridae* family (32). The human norovirus genome is ~7.6 kb in length (32). Eight viral proteins are encoded on 3 ORFs (ORF-1,-2,-3) (32). In the mature virion, 90 VP1 dimers are arranged in icosahedral symmetry and create cup-like structures on the viral surface (32). Six nonstructural proteins are derived from a polyprotein encoded on ORF-1, and include a protease and RNA-dependent RNA polymerase (32). There are at least six genogroups (I to VI) based on VP1 amino acid sequence (32). Most human norovirus infections are caused by GII, especially GII.4, GI, and to a very limited extent GIV(32). Noroviruses are genetically diverse and in GII.4 strains, the VP1 amino acid sequence can differ from other GII genotypes by 5-7%, and from strains of an individual virus by 2.8% (32).

CD300lf, found on a type of intestinal epithelial cell called tuft cells, was recently identified as the receptor for murine norovirus (33). This receptor is contacted by the dimeric murine norovirus VP1 protruding (P) domain (34). Serine palmitoyltransferase, required for sphingolipid biosynthesis, is needed for CD300lf to obtain the conformation

needed for viral binding (35). Bile acids are co-factors for virus-host cell binding (34). Type 2 cytokines induce tuft cell proliferation and promote murine norovirus infection in vivo and these cytokines can replace the need for commensal microbiota, discussed in more detail below, in promoting viral infection (33).

Norovirus infection is detected frequently in all age groups and causes epidemic and sporadic cases of gastroenteritis (36). Although all ages are at risk of norovirus infection, the most severe morbidity and mortality occur in the young old. Noroviruses cause approximately 200,000 deaths in children under 5 years of age in developing countries (32). In the United States, norovirus is estimated to cause 400,000 emergency room visits and 71,000 hospitalizations a year (37). Transmission can occur via the fecal oral route, and by aerosolization of virus in vomitus (32). Some genotypes are more commonly associated with specific modes of transmission, i.e. GII.4 is more often associated with person to person transmission, and GI.7 and GII.12 are more often associated with foodborne disease (32).

Symptoms include diarrhea, nausea, vomiting, abdominal pain and cramps, and fever (36). Using Norwalk like virus as an example, symptoms last for a median of 5 days, and are characterized by diarrhea in the first 5 days (87% of patients), and vomiting on the first day (74% of patients) (36). The incubation period is 15 to 50 hours (36). Vomiting is less common in children under one year of age compared to children over one year of age (36). Shedding can occur after resolution of clinical signs and has been reported to occur up to 3 weeks in 26% of patients over one year of age, and up to 38% of patients less than one year of age (36). Long term shedding of norovirus is not associated with increased severity of disease or prolonged duration of clinical symptoms (36).

Norovirus infection symptoms may be more prolonged and severe in immunocompromised individual and can be associated with persistent viral excretion (36). Asymptomatic infection can occur with a prevalence of greater than 25% in children through 3 years of age, and greater than approximately 5% in individuals over 35 years of age (32, 38). Treatment is supportive as no specific antivirals or prophylactic vaccines exist.

Due to the lack of a small animal model and, until recently reproducible means to culture norovirus in vitro, there are gaps in knowledge regarding norovirus pathogenesis and immunology. Murine noroviruses (MNVs) are common in laboratory mice but cause little or no signs of infection in wild type mice (32). Various strains of knock out mice have shown that innate and adaptive immunity are important for control of MNV infection (32).

Some people are naturally resistant to norovirus infection due to the type of HGBA expressed on the mucosal surface epithelium in the gastrointestinal tract (39). Approximately 20% people with European ancestry lack HBGAs on their mucosal surfaces and in secretions (nonsecretor phenotype) because of homozygosity for inactive FUT2 alleles, and are thus protected from most norovirus infections (40, 41). Nonsecretor status does not protect against all norovirus infections as GII.2, GII.4, and GI.3 infections have been documented in nonsecretors (32). In one study, secretors were 9.9 times more likely to be infected with GII.4 noroviruses and genogroup II, non-4 noroviruses than nonsecretors(42).

Rotavirus vaccines

Two rotavirus vaccines are commercially available, RotaTeq (RV5) and Rotarix (RV1). Since the introduction of these vaccines, hospitalization and emergency room visits for rotavirus acute gastroenteritis have been reduced by a median of 67% overall, and 71%, 59%, and 60% in low, medium and high child mortality countries, respectively (43). RV1 is a monovalent, live attenuated vaccine, which uses rotavirus strain 89-12, initially isolated from a child with G1P[8] gastroenteritis(44). In the US this vaccine is given at 2 and 4 months of age (44). RV5 is a live attenuated pentavalent vaccine composed of 5 bovine-human reassortant rotaviruses(44). In the US this vaccine is given at 2, 4 and 6 months of age (44). Monovalent G1P[8] vaccines can protect against rotaviruses with different P and G types (21). In a study on RV1 it was 94% and 71% effective against homotypic and partly heterotypic strains, and 87% against fully heterotopic strains in high income countries (45). In middle income countries these numbers were 59%, 72%, and 47% (45). In high income countries, the RV5 vaccine was 83% effective against homotypic strains, 82% effective against partly heterotypic strains, and 75% against single-antigen, non-vaccine type strains, whereas in middle income countries the numbers were 70% against single-antigen vaccine type strains, 37% against partly heterotypic strains, and 87% against single-antigen non-vaccine type strains (45). Both vaccines are effective in preventing severe disease in high income countries and reduce the incidence by 50-60% in low income countries (21, 46). After vaccine introduction, there has been no evidence of selection pressure in strain prevalence from vaccine use (47).

Oral vaccine efficacy

Oral vaccines have decreased efficacy in low - middle income countries compared to high income countries. Two examples are vaccines for enteric viral pathogens, rotavirus and poliovirus. RV1 has a 1 year protective efficacy against severe rotavirus disease of over 95% in European infants but less than 50% in Malawian infants (48). The list of factors that likely have a role in oral vaccine failure is lengthy and include transplacental transfer of maternal antibodies, presence of antibodies and innate antiviral substances in breast milk, genetic risk factors (HBGA type), exposure to the pathogen before vaccination, previous or concurrent infections at the time of vaccination, environmental enteropathy, malnutrition and associated immune deficiencies, microbiome composition and dysbiosis, co-administration of oral vaccines, heterotypic strain exposure, geographic location, season of administration, patient age, and improper storage of vaccines (48, 49).

Environmental enteropathy is an asymptomatic inflammatory disorder of the proximal small intestine leading to environmental enteric dysfunction (EED) (50). Villus height is decreased, intestinal permeability is increased, and there is evidence of malabsorption, mucosal inflammation, microbial translocation, systemic inflammation, and changes in the microbiome (50). Malnutrition secondary to EED can lead to stunting, wasting, and unattained neurocognitive potential (50). Intestinal infections, malnutrition, and dysbiosis or a combination of these factors, are the suspected cause of EE (50). A study evaluating environmental enteropathy and vaccine response in Bangladeshi infants showed that it was negatively associated with oral vaccine immunogenicity (51). Oral rotavirus and poliovirus vaccine failed in 68.5% and 20.2% of infants with EED respectively (51). Parenteral vaccine failure was much lower at 0% 0.9%, 7.9% and

3.8% for tetanus, *Haemophilus influenzae* , diphtheria, and measles vaccines respectively (51). In another study, biomarkers associated with environmental enteropathy were associated with decreased seroconversion to RV5 in Nicaragua (52). Six week old Pakistani infants who responded to RV1 vaccine had higher relative abundance of bacteria belonging to *Clostridium* cluster XI and *Proteobacteria* than nonresponders (53). A study evaluating oral rotavirus vaccine in six-week-old infants from Ghana showed responders had microbiota composition more similar to healthy Dutch infants than Ghanaian nonresponders, and vaccine response correlated with increased relative abundance of *Streptococcus bovis* and decreased relative abundance of the phylum Bacteroidetes (54). In that study, there was no difference in the diversity of the enteric microbiota between responders and nonresponders (54). A study from Vellore India found that rotavirus shedding after 2 doses of RV1 was associated with more bacterial taxa prevaccination, however there was no consistent difference in composition or diversity of bacterial microbiota in regards to serologic response (55). A study evaluating responses to oral polio vaccine found that a higher relative abundance of the phyla Actinobacteria at 15 weeks of age was associated with improved vaccine immunogenicity, and a higher relative abundance of Pseudomonadales was negatively associated with oral poliovirus vaccine response (49).

Co-administration of oral vaccine may influence immunogenicity. When oral rotavirus and oral poliovirus vaccines were given together, there was a negative effect on the immunogenicity of the rotavirus vaccine (both RV1 and RV5) but not oral poliovirus vaccine, in a study conducted with Bangladeshi infants (48). Co-administration was

associated with decreased rotavirus seroconversion rate compared to when the vaccines were staggered (48).

Enteric infections may affect oral vaccine efficacy by interfering with live attenuated vaccines due to competition for receptor binding or cell factors needed for the viral life cycle (48). Enteric infections may also affect vaccines by induction of innate immunity, such as type I, II, or III interferon responses, which can subsequently inhibit replication of the vaccine virus (48). Non-polio enteroviruses can inhibit oral polio vaccine efficacy, and their presence at time of oral poliovirus vaccination is associated with reduced odds of seroconversion (48). Enterovirus infection at the time rotavirus vaccine administration is also associated with decreased rotavirus specific IgA, failure to seroconvert, and rotavirus diarrhea (56).

Other factors that can alter immunogenicity of vaccines include consumption of breast milk, host genetics such as HBGA, and season of vaccine administration (21, 48). Breast milk with high concentration of lactadherin, a milk fat protein with antiviral properties, was associated with failure to seroconvert after rotavirus vaccines in Zambian infants (57). Conversely, a study in Nicaraguan infants, did not show an association between breast milk lactadherin and rotavirus vaccine responses (58). RV1 had a lower immunogenicity in the cool dry season in Zambia (48). There is also a seasonal variation in breast milk rotavirus specific IgA with higher titers occurring in cool dry months (59). This may account for some of the seasonal variability in vaccine efficacy. Secretors, individuals with functional FUT2 genes, are 26.6 times more susceptible to infection from P[8] strains of rotavirus, which are components of RV1 and RV5 (48).

Nonsecretors may not respond as well to the oral rotavirus vaccines, but they are also less susceptible to infection from certain genotypes (48).

The microbiome and viral infection

During infection, microbiota can protect against or enhance viral pathogenicity. Norovirus, poliovirus and mouse mammary tumor virus (MMTV) have enhanced replication, persistence, pathogenesis and/or transmission in the presence of commensal bacteria (60, 61).

In mice, poliovirus replication, pathogenesis, and transmission are enhanced by intestinal bacteria and decreased in antibiotic treated mice (60-62). N-acetylglucosamine containing surface polysaccharides such as peptidoglycan and LPS on bacteria may enhance polio pathogenesis by binding to and stabilizing virions to prevent premature RNA release and limit heat inactivation (62, 63). One study found that LPS enhances binding of the virus to the poliovirus receptor on the host cell (62). An *in vitro* study demonstrated that poliovirus was more infectious in cells treated with fecal material containing microbiota than fecal material without microbiota (63, 64). This was not dependent on the bacteria being alive as surface polysaccharides had the same effect (60, 64).

Norovirus can bind extracellular glycans on certain intestinal bacteria and this may assist with attachment to enterocytes (61, 62). Noroviruses also bind HBGA-expressing bacteria such as *Enterobacter cloacae,* which potentially promote attachment and infection of B cells (13, 65). Some bacteria such as *Streptococcus aureus*, *Streptomyces griseus,* and *Aerococcus viridans* have proteolytic activity needed for effective viral replication and infectivity (66). Murine norovirus (MuNoV) pathology is

microbiota dependent (62). Enteric bacteria control persistent enteric MuNoV infection by an IFN- γ receptor-dependent mechanism as IFN- γ cured persistent MuNoV infection in mice lacking T and B cells (61).

MMTV is a retrovirus transmitted in milk. Germ-free mice infected with MMTV cannot pass infectious virus to their offspring because the immune response triggered by gut microbiota is needed for transmission (60, 62). MMTV binds LPS of commensal bacteria and uses it to trigger TLR4 induced tolerance via production of IL-10 and thus causes persistent infection (60, 67). Memory T cell responses are also inhibited (68).

A French research group pioneered the study of microbiota impact on rotavirus pathogenesis nearly thirty years ago (69). They compared intestinal absorption of macromolecules during murine rotavirus infection in conventional versus germ-free newborn mice derived from seronegative dams. The study showed that rotavirus infection caused a transient increase in gut permeability to undegraded proteins; this increase occurred earlier after infection in conventional pups and later in germ-free pups (69). Furthermore, rotavirus titers in intestinal homogenates were high at 8 days post-inoculation (dpi) in conventional mice, while they become very low in germ-free mice, suggesting that microbiota promotes rotavirus replication (69). However, there was no correlation between virus excretion and diarrhea in mice, since diarrhea was observed from 2 to 8 dpi in both conventional and germ-free mice; and no differences were detected on diarrhea kinetics (69). When intestinal microbiota was absent, clinical and physiological disturbance were more severe, i.e. greater weight loss after rotavirus infection, and a more marked and long lasting augmentation in intestinal permeability to intact proteins (69). This study indicates that intestinal microbiota has significant

impacts on both rotavirus replication and pathogenesis as supported by the timing, magnitude and duration of increased epithelial permeability and virus excretion (69).

A recent study showed that rotavirus infection was reduced by 42% and diarrhea was decreased in incidence and duration in germ-free mice (via ablation of microbiota by antibiotics) compared to mice with conventional microbiota (70). Based on the non-altered ratio of positive to negative sense rotavirus RNA strands, the authors suggested that the antibiotics used to ablate the microbiota affected entry of the virus into host cells (70). These antibiotic treated mice had more durable mucosal and systemic humoral immune response and the durability was correlated with small intestinal rotavirus specific IgA antibody-secreting cells (ASC) (70). Mice treated with low levels of dextran sodium sulfate to increase exposure of immune cells to microbiota had decreased rotavirus specific antibodies (70). Further studies are needed to understand how the microbiota and antibiotics interact to induce the immunologic differences between the mouse groups. The contradictory findings between the two studies on the role of microbiota in rotavirus infection and diarrhea are most likely due to the difference between using true germ-free newborn mice (69) versus using mice ablated of microbiota with antibiotics (70). In addition to killing bacteria, antibiotics have many effects on the physiology and immune cell development of the host, which need to be taken into consideration and should be properly controlled in these types of studies.

In order to identify the influence of microbiota in Gn pig's response to HRV and to more closely mimic human infants with the model, Gn pigs transplanted with newborn human gut microbiota (HGM) and infected with HRV have been evaluated (71). HGM successfully colonized the Gn pig intestine after three oral inoculations. Sequencing of

16S rRNA genes demonstrated that the pigs carried microbiota similar to that of the C-section delivered human infant donor (71). This model was used to test the effects of probiotics on the gut microbiome structure during a virulent HRV (VirHRV) infection and the development of attenuated HRV (AttHRV) vaccine-induced immune responses were compared between the HGM and non-HGM transplanted Gn pigs (72). The AttHRV vaccine conferred overall similar protection against rotavirus diarrhea and virus shedding in Gn pigs and HGM transplanted Gn pigs (72). HGM promoted the development of the neonatal immune system, significantly enhancing IFN-γ producing T cell responses and reducing Treg cell responses in the AttHRV-vaccinated pigs (72).

A Gn pig model of enteric dysbiosis and rotavirus immunity has been developed during my PhD program (Chapter 2 of this dissertation) (73). Using this model, we showed that after vaccination with AttHRV, pigs colonized by gut microbiota from children who had a good immune response to oral rotavirus vaccination and low enteropathy scores (healthy human gut microbiota, HHGM) had more rotavirus-specific IFN-γ T cells in ileum, spleen, and blood than pigs colonized by microbiota from children who did not respond well to the oral rotavirus vaccine and had evidence of enteropathy (unhealthy human gut microbiota, UHGM) (73). UHGM pigs had higher viral shedding titers and more severe clinical signs compared to HHGM pigs after challenge with VirHRV (73). There was a significant positive correlation between *Collinsella* and significant negative correlations between *Clostridium* spp. and *Anaerococcus* and frequencies of IFN-γ T cells at the time of challenge. HHGM pigs had an increased mean relative abundance of *Bacteroides* after VirHRV challenge (73). Since the only variable that differed between these groups was microbiota composition, this study we clearly

demonstrated that the differences in immune responses and clinical disease are due to the influence of the different microbiota.

It has been shown that human intestinal cells incubated with soluble factors from *Bacteroides thetaiotaomicron* and *Lactobacillus casei* were protected from rotavirus infection (74). The protection was attributed to increased cell surface galactose induced by the bacterial factors, which blocked rotavirus infection. This mechanism is significant in rotavirus infection because these viruses use glycan recognition to attach to enterocytes (74). Perhaps a similar mechanism was at play in the Gn pig enteric dysbiosis study and may partially explain why HHGM pigs had decreased viral shedding compared to UHGM pigs (73). Antibiotics can decrease rotavirus replication and disease severity in mice, giving further support that enteric bacteria influence rotavirus infection (70).

These studies suggest a modulatory role of certain bacterial components of microbiome in the development of rotavirus infection and immunity. Although, the underlying mechanisms of specific host-bacteria and virus-bacteria interactions that lead to the different outcomes in enteric viral diseases and immunity have not been identified, studies of probiotics shed some light on the mechanisms.

Models of rotavirus and norovirus infection

Animal models are important tools for the study of viral pathogenesis, immunity, and preventative and therapeutic measures. Germ free animals are a necessity to determine the role of bacteria on the pathogenesis and immunity to infectious agents and have been important in the study of rotaviruses and noroviruses.

In addition to humans, many animals are susceptible to rotavirus infection and disease, and can be used as models (i.e., pigs, calves, lambs, rats, rabbits, mice, and NHP)

to study rotavirus pathogenesis and immunity. The Gn pig model has many benefits over other animal models. Pigs and humans share high genomic and protein sequence homologies, omnivorous diet, similar gastrointestinal physiology and similar immune systems (75, 76). Additionally, there is no transfer of maternal antibodies across the porcine placenta and Gn pigs are deprived of sow colostrum/milk, which prevents maternal antibodies from interfering with studies. Inoculation of Gn pigs, up to at least 8 weeks of age with Wa strain (G1P1A[8]) HRV will result in diarrhea(77). Based on duodenal biopsies from children with acute rotavirus infection, the histopathologic changes are similar to those found in piglets (78-80). The Wa strain VirHRV allows assessment of host response to natural infection, while the AttHRV strain can be used to study vaccination (81, 82).

After oral inoculation with VirHRV, Gn pigs develop diarrhea, shed virus and develop nearly complete protection against subsequent clinical disease and viral shedding when challenged with VirHRV after recovery (83-85). Diarrhea develops approximately 13 hours after inoculation and is associated with viral antigen in enterocytes at villus tips; villus atrophy develops 24 hours post-infection and is correlated with peak fecal viral titers (80). Gn pigs orally inoculated with AttHRV will seroconvert but have little to no virus shedding or clinical signs, and protection from diarrhea and viral shedding after challenge is less efficacious than what is seen in pigs receiving primary VirHRV oral inoculation (83-85).

Gnotobiotic calves have also been used to study rotavirus; however, reports are not as numerous as those in Gn pigs. Gn calves can be infected with some HRV strains, but clinical illness does not always develop (86). In a study where calves successfully

developed diarrhea after administration of an HRV strain, they had histologic lesions consistent with rotavirus infection (87). In addition to the fact that Gn calves are not as consistent as Gn pigs as a model of HRV infection and disease, ruminant physiology and microbiota is very different from humans, therefore calves are not a proper model for the study of the role of microbiota in HRV infection and immunity.

Despite the close genetic relationship between NHP and humans, they are not a superior rotavirus animal model compared to Gn pigs. Often, HRV strains are naturally attenuated in NHP (88). There have been reports of oral inoculation of simian (SA11) or human (Wa) rotavirus into different NHP with the development of diarrhea, however it is usually during the first week of life, after which disease won't be observed, and older animals may not shed virus or even seroconvert (88). Even in a study evaluating a wild-type macaque rotavirus in 14-42 day old macaques, they remained clinically normal despite shedding large amounts of virus (88).

Mice are attractive animal models due to their size, ease of maintenance compared to Gn pigs, and availability of numerous strains and genetic knockouts. The major downside of the murine rotavirus model is that mice are only susceptible to disease for approximately 15 days after birth (89). Adult mice can be used to study rotavirus infection, however infections are subclinical and often do not predict protective efficacy of interventions against clinical infection (81, 89).

Research on norovirus infection and immunology has been limited by lack of easily accessible animal models. Although mouse models using murine norovirus exist, lack of clinical signs such as vomiting and diarrhea, limit the usefulness (90)

Murine norovirus can be studied in mice and cell culture. However, immunocompetent mice may not be infected or show clinical signs (91). A study using human norovirus GII.4 showed inability to infect wild-type BALB/c mice (91). BALB/c Rag-γc-deficient mice did have replication of GII.4 as indicated by increased viral loads over time, and infection was confirmed by detection of structural and nonstructural proteins in cells with macrophage-like morphology in spleens and livers of the rag-γc-deficient mice (91).

Gnotobiotic pigs can be used to study human norovirus (HuNoV). Porcine norovirus in wild type pigs, are typically without clinical signs (92). Gn pigs can be infected with genogroup II genotype 4 2006b variant. The median infectious dose is lower for neonatal pigs (4-5 days of age) than older pigs (33-34 days) (93). Pigs developed diarrhea and increased viral loads in intestinal contents and detection of viral antigen in duodenal villous were evidence of infection (93). Another study using GII.4 in gnotobiotic pigs showed many developed diarrhea and were positive for the virus via rtPCR on rectal swabs (94). These animals also seroconverted and had IFA positivity for HuNoV capsid in duodenal and jejunal enterocytes (94). Similar to humans, pigs share A and H HBGAs (93) and the genetically determined difference in susceptability to HuNoV infection A study showed that non-A+ or H+ gnotobiotic pigs are significantly more resistance to HuNoV GII.4 infection than A+/H+ pigs (98).

Gnotobiotic calves infected with HuNoV train GII.4-HS66 developed diarrhea and intestinal lesions in the proximal small intestine (95). All infected calves shed virus, developed HuNoV specific fecal IgA and/or IgG, and some developed viremia, and /or had detectable viral capsid antigen in the jejunum via IHC (95). The facilities required for

Gn calf studies, availability of calves, and expense limit large scale studies using gnotobiotic calves.

Chimpanzees inoculated intravenously with HuNoV strain, Norwalk virus did not develop clinical signs but had onset and duration of viral shedding and a serum antibody response similar to what were seen in human infections (96). A subset of infected animals were not reinfected when challenged at multiple time points up to two years after initial exposure and the presence of norovirus specific serum antibodies correlated with protection (96). Aside from the expense and regulations involved with nonhuman primate usage, this model is not an option in the United States due to a moratorium on chimpanzee research.

In vitro studies have been hampered by reproducible in vitro cultivation systems, until recently. Multiple strains of HuNoV have been grown in enterocytes from stem cell derived nontransformed human intestinal enteroid monolayer cultures (97). Bile is required for replication of some strains (97). One study demonstrated infection of human B cell line by HuNoV in the presence of HBGA expressing bacteria (65), however; the system has difficulties in being repeated in other labs.

References

1. Jandhyala SM, Talukdar R, Subramanyam C, Vuyyuru H, Sasikala M, Nageshwar Reddy D. Role of the normal gut microbiota. World J Gastroenterol. 2015;21(29):8787-803.
2. O'Hara AM, Shanahan F. The gut flora as a forgotten organ. EMBO Rep. 2006;7(7):688-93.
3. Hollister EB, Gao C, Versalovic J. Compositional and functional features of the gastrointestinal microbiome and their effects on human health. Gastroenterology. 2014;146(6):1449-58.
4. Arumugam M, Raes J, Pelletier E, Le Paslier D, Yamada T, Mende DR, et al. Enterotypes of the human gut microbiome. Nature. 2011;473(7346):174-80.
5. Magwira CA, Taylor MB. Composition of gut microbiota and its influence on the immunogenicity of oral rotavirus vaccines. Vaccine. 2018;36(24):3427-33.
6. Dominguez-Bello MG, Costello EK, Contreras M, Magris M, Hidalgo G, Fierer N, et al. Delivery mode shapes the acquisition and structure of the initial microbiota across multiple body habitats in newborns. Proc Natl Acad Sci U S A. 2010;107(26):11971-5.
7. Arrieta MC, Stiemsma LT, Amenyogbe N, Brown EM, Finlay B. The intestinal microbiome in early life: health and disease. Front Immunol. 2014;5:427.
8. Bezirtzoglou E, Tsiotsias A, Welling GW. Microbiota profile in feces of breast- and formula-fed newborns by using fluorescence in situ hybridization (FISH). Anaerobe. 2011;17(6):478-82.
9. Zivkovic AM, German JB, Lebrilla CB, Mills DA. Human milk glycobiome and its impact on the infant gastrointestinal microbiota. Proc Natl Acad Sci U S A. 2011;108 Suppl 1:4653-8.
10. Karlsson F, Tremaroli V, Nielsen J, Backhed F. Assessing the human gut microbiota in metabolic diseases. Diabetes. 2013;62(10):3341-9.
11. Xu Z, Knight R. Dietary effects on human gut microbiome diversity. Br J Nutr. 2015;113 Suppl:S1-5.
12. Purchiaroni F, Tortora A, Gabrielli M, Bertucci F, Gigante G, Ianiro G, et al. The role of intestinal microbiota and the immune system. Eur Rev Med Pharmacol Sci. 2013;17(3):323-33.
13. Tomkovich S, Jobin C. Microbiota and host immune responses: a love-hate relationship. Immunology. 2016;147(1):1-10.
14. Wieland Brown LC, Penaranda C, Kashyap PC, Williams BB, Clardy J, Kronenberg M, et al. Production of alpha-galactosylceramide by a prominent member of the human gut microbiota. PLoS Biol. 2013;11(7):e1001610.
15. Alakomi HL, Skytta E, Saarela M, Mattila-Sandholm T, Latva-Kala K, Helander IM. Lactic acid permeabilizes gram-negative bacteria by disrupting the outer membrane. Appl Environ Microbiol. 2000;66(5):2001-5.

16. Mirpuri J, Raetz M, Sturge CR, Wilhelm CL, Benson A, Savani RC, et al. Proteobacteria-specific IgA regulates maturation of the intestinal microbiota. Gut Microbes. 2014;5(1):28-39.
17. Sjogren YM, Tomicic S, Lundberg A, Bottcher MF, Bjorksten B, Sverremark-Ekstrom E, et al. Influence of early gut microbiota on the maturation of childhood mucosal and systemic immune responses. Clin Exp Allergy. 2009;39(12):1842-51.
18. Salas JT, Chang TL. Microbiome in human immunodeficiency virus infection. Clin Lab Med. 2014;34(4):733-45.
19. Lundell AC, Bjornsson V, Ljung A, Ceder M, Johansen S, Lindhagen G, et al. Infant B cell memory differentiation and early gut bacterial colonization. J Immunol. 2012;188(9):4315-22.
20. Mazmanian SK, Liu CH, Tzianabos AO, Kasper DL. An immunomodulatory molecule of symbiotic bacteria directs maturation of the host immune system. Cell. 2005;122(1):107-18.
21. Crawford SE, Ramani S, Tate JE, Parashar UD, Svensson L, Hagbom M, et al. Rotavirus infection. Nat Rev Dis Primers. 2017;3:17083.
22. Banyai K, Estes MK, Martella V, Parashar UD. Viral gastroenteritis. Lancet. 2018;392(10142):175-86.
23. Lundgren O, Svensson L. Pathogenesis of rotavirus diarrhea. Microbes Infect. 2001;3(13):1145-56.
24. Arias CF, Silva-Ayala D, Lopez S. Rotavirus entry: a deep journey into the cell with several exits. J Virol. 2015;89(2):890-3.
25. Cheung W, Gill M, Esposito A, Kaminski CF, Courousse N, Chwetzoff S, et al. Rotaviruses associate with cellular lipid droplet components to replicate in viroplasms, and compounds disrupting or blocking lipid droplets inhibit viroplasm formation and viral replication. J Virol. 2010;84(13):6782-98.
26. Richardson S, Grimwood K, Gorrell R, Palombo E, Barnes G, Bishop R. Extended excretion of rotavirus after severe diarrhoea in young children. Lancet. 1998;351(9119):1844-8.
27. Desselberger U. Rotaviruses. Virus research. 2014;190:75-96.
28. Desselberger U, Huppertz HI. Immune responses to rotavirus infection and vaccination and associated correlates of protection. J Infect Dis. 2011;203(2):188-95.
29. Tate JE, Burton AH, Boschi-Pinto C, Parashar UD, World Health Organization-Coordinated Global Rotavirus Surveillance N. Global, Regional, and National Estimates of Rotavirus Mortality in Children <5 Years of Age, 2000-2013. Clin Infect Dis. 2016;62 Suppl 2:S96-S105.
30. Bialowas S, Hagbom M, Nordgren J, Karlsson T, Sharma S, Magnusson KE, et al. Rotavirus and Serotonin Cross-Talk in Diarrhoea. PLoS One. 2016;11(7):e0159660.
31. Franco MA, Angel J, Greenberg HB. Immunity and correlates of protection for rotavirus vaccines. Vaccine. 2006;24(15):2718-31.
32. Robilotti E, Deresinski S, Pinsky BA. Norovirus. Clin Microbiol Rev. 2015;28(1):134-64.
33. Wilen CB, Lee S, Hsieh LL, Orchard RC, Desai C, Hykes BL, Jr., et al. Tropism for tuft cells determines immune promotion of norovirus pathogenesis. Science. 2018;360(6385):204-8.

34. Nelson CA, Wilen CB, Dai YN, Orchard RC, Kim AS, Stegeman RA, et al. Structural basis for murine norovirus engagement of bile acids and the CD300lf receptor. Proc Natl Acad Sci U S A. 2018;115(39):E9201-E10.
35. Orchard RC, Wilen CB, Virgin HW. Sphingolipid biosynthesis induces a conformational change in the murine norovirus receptor and facilitates viral infection. Nat Microbiol. 2018;3(10):1109-14.
36. Rockx B, De Wit M, Vennema H, Vinje J, De Bruin E, Van Duynhoven Y, et al. Natural history of human calicivirus infection: a prospective cohort study. Clin Infect Dis. 2002;35(3):246-53.
37. Rha B, Burrer S, Park S, Trivedi T, Parashar UD, Lopman BA. Emergency department visit data for rapid detection and monitoring of norovirus activity, United States. Emerg Infect Dis. 2013;19(8):1214-21.
38. Phillips G, Tam CC, Rodrigues LC, Lopman B. Prevalence and characteristics of asymptomatic norovirus infection in the community in England. Epidemiol Infect. 2010;138(10):1454-8.
39. Marionneau S, Ruvoen N, Le Moullac-Vaidye B, Clement M, Cailleau-Thomas A, Ruiz-Palacois G, et al. Norwalk virus binds to histo-blood group antigens present on gastroduodenal epithelial cells of secretor individuals. Gastroenterology. 2002;122(7):1967-77.
40. Lindesmith L, Moe C, Marionneau S, Ruvoen N, Jiang X, Lindblad L, et al. Human susceptibility and resistance to Norwalk virus infection. Nat Med. 2003;9(5):548-53.
41. Rydell GE, Kindberg E, Larson G, Svensson L. Susceptibility to winter vomiting disease: a sweet matter. Rev Med Virol. 2011;21(6):370-82.
42. Kambhampati A, Payne DC, Costantini V, Lopman BA. Host Genetic Susceptibility to Enteric Viruses: A Systematic Review and Metaanalysis. Clin Infect Dis. 2016;62(1):11-8.
43. Burnett E, Jonesteller CL, Tate JE, Yen C, Parashar UD. Global Impact of Rotavirus Vaccination on Childhood Hospitalizations and Mortality From Diarrhea. J Infect Dis. 2017;215(11):1666-72.
44. Vesikari T, Matson DO, Dennehy P, Van Damme P, Santosham M, Rodriguez Z, et al. Safety and efficacy of a pentavalent human-bovine (WC3) reassortant rotavirus vaccine. N Engl J Med. 2006;354(1):23-33.
45. Leshem E, Lopman B, Glass R, Gentsch J, Banyai K, Parashar U, et al. Distribution of rotavirus strains and strain-specific effectiveness of the rotavirus vaccine after its introduction: a systematic review and meta-analysis. Lancet Infect Dis. 2014;14(9):847-56.
46. Leshem E, Moritz RE, Curns AT, Zhou F, Tate JE, Lopman BA, et al. Rotavirus vaccines and health care utilization for diarrhea in the United States (2007-2011). Pediatrics. 2014;134(1):15-23.
47. Doro R, Laszlo B, Martella V, Leshem E, Gentsch J, Parashar U, et al. Review of global rotavirus strain prevalence data from six years post vaccine licensure surveillance: is there evidence of strain selection from vaccine pressure? Infect Genet Evol. 2014;28:446-61.

48. Parker EP, Ramani S, Lopman BA, Church JA, Iturriza-Gomara M, Prendergast AJ, et al. Causes of impaired oral vaccine efficacy in developing countries. Future Microbiol. 2018;13:97-118.
49. Zimmermann P, Curtis N. The influence of the intestinal microbiome on vaccine responses. Vaccine. 2018;36(30):4433-9.
50. Marie C, Ali A, Chandwe K, Petri WA, Jr., Kelly P. Pathophysiology of environmental enteric dysfunction and its impact on oral vaccine efficacy. Mucosal Immunol. 2018;11(5):1290-8.
51. Naylor C, Lu M, Haque R, Mondal D, Buonomo E, Nayak U, et al. Environmental Enteropathy, Oral Vaccine Failure and Growth Faltering in Infants in Bangladesh. EBioMedicine. 2015;2(11):1759-66.
52. Becker-Dreps S, Vilchez S, Bucardo F, Twitchell E, Choi WS, Hudgens MG, et al. The Association Between Fecal Biomarkers of Environmental Enteropathy and Rotavirus Vaccine Response in Nicaraguan Infants. Pediatr Infect Dis J. 2017;36(4):412-6.
53. Harris V, Ali A, Fuentes S, Korpela K, Kazi M, Tate J, et al. Rotavirus vaccine response correlates with the infant gut microbiota composition in Pakistan. Gut Microbes. 2018;9(2):93-101.
54. Harris VC, Armah G, Fuentes S, Korpela KE, Parashar U, Victor JC, et al. The infant gut microbiome correlates significantly with rotavirus vaccine response in rural Ghana. J Infect Dis. 2016.
55. Parker EPK, Praharaj I, Zekavati A, Lazarus RP, Giri S, Operario DJ, et al. Influence of the intestinal microbiota on the immunogenicity of oral rotavirus vaccine given to infants in south India. Vaccine. 2018;36(2):264-72.
56. Taniuchi M, Platts-Mills JA, Begum S, Uddin MJ, Sobuz SU, Liu J, et al. Impact of enterovirus and other enteric pathogens on oral polio and rotavirus vaccine performance in Bangladeshi infants. Vaccine. 2016;34(27):3068-75.
57. Mwila-Kazimbaya K, Garcia MP, Bosomprah S, Laban NM, Chisenga CC, Permar SR, et al. Effect of innate antiviral glycoproteins in breast milk on seroconversion to rotavirus vaccine (Rotarix) in children in Lusaka, Zambia. PLoS One. 2017;12(12):e0189351.
58. Becker-Dreps S, Choi WS, Stamper L, Vilchez S, Velasquez DE, Moon SS, et al. Innate Immune Factors in Mothers' Breast Milk and Their Lack of Association With Rotavirus Vaccine Immunogenicity in Nicaraguan Infants. J Pediatric Infect Dis Soc. 2017;6(1):87-90.
59. Chilengi R, Simuyandi M, Beach L, Mwila K, Becker-Dreps S, Emperador DM, et al. Association of Maternal Immunity with Rotavirus Vaccine Immunogenicity in Zambian Infants. PLoS One. 2016;11(3):e0150100.
60. Wilks J, Golovkina T. Influence of microbiota on viral infections. PLoS Pathog. 2012;8(5):e1002681.
61. Pfeiffer JK, Virgin HW. Viral immunity. Transkingdom control of viral infection and immunity in the mammalian intestine. Science. 2016;351(6270).
62. Robinson CM, Pfeiffer JK. Viruses and the Microbiota. Annu Rev Virol. 2014;1:55-69.
63. Wilks J, Beilinson H, Golovkina TV. Dual role of commensal bacteria in viral infections. Immunol Rev. 2013;255(1):222-9.

64. Kuss SK, Best GT, Etheredge CA, Pruijssers AJ, Frierson JM, Hooper LV, et al. Intestinal microbiota promote enteric virus replication and systemic pathogenesis. Science. 2011;334(6053):249-52.
65. Jones MK, Watanabe M, Zhu S, Graves CL, Keyes LR, Grau KR, et al. Enteric bacteria promote human and mouse norovirus infection of B cells. Science. 2014;346(6210):755-9.
66. Lynch SV. Viruses and microbiome alterations. Ann Am Thorac Soc. 2014;11 Suppl 1:S57-60.
67. Kane M, Case LK, Kopaskie K, Kozlova A, MacDearmid C, Chervonsky AV, et al. Successful transmission of a retrovirus depends on the commensal microbiota. Science. 2011;334(6053):245-9.
68. Grzybowski MM, Dlugonska H. Natural microbiota in viral and helminth infections. Addendum to: Personalized vaccination. II. The role of natural microbiota in a vaccine-induced immunity. Ann Parasitol. 2012;58(3):157-60.
69. Heyman M, Corthier G, Petit A, Meslin JC, Moreau C, Desjeux JF. Intestinal absorption of macromolecules during viral enteritis: an experimental study on rotavirus-infected conventional and germ-free mice. Pediatr Res. 1987;22(1):72-8.
70. Uchiyama R, Chassaing B, Zhang B, Gewirtz AT. Antibiotic treatment suppresses rotavirus infection and enhances specific humoral immunity. J Infect Dis. 2014;210(2):171-82.
71. Zhang H, Wang H, Shepherd M, Wen K, Li G, Yang X, et al. Probiotics and virulent human rotavirus modulate the transplanted human gut microbiota in gnotobiotic pigs. Gut pathogens. 2014;6:39.
72. Wen K, Tin C, Wang H, Yang X, Li G, Giri-Rachman E, et al. Probiotic Lactobacillus rhamnosus GG enhanced Th1 cellular immunity but did not affect antibody responses in a human gut microbiota transplanted neonatal gnotobiotic pig model. PLoS ONE. 2014;9(4):e94504.
73. Twitchell EL, Tin C, Wen K, Zhang H, Becker-Dreps S, Azcarate-Peril MA, et al. Modeling human enteric dysbiosis and rotavirus immunity in gnotobiotic pigs. Gut pathogens. 2016;8:51.
74. Varyukhina S, Freitas M, Bardin S, Robillard E, Tavan E, Sapin C, et al. Glycan-modifying bacteria-derived soluble factors from Bacteroides thetaiotaomicron and Lactobacillus casei inhibit rotavirus infection in human intestinal cells. Microbes Infect. 2012;14(3):273-8.
75. Wang M, Donovan SM. Human microbiota-associated swine: current progress and future opportunities. ILAR J. 2015;56(1):63-73.
76. Saif LJ, Ward LA, Yuan L, Rosen BI, To TL. The gnotobiotic piglet as a model for studies of disease pathogenesis and immunity to human rotaviruses. Archives of virology Supplementum. 1996;12:153-61.
77. Yuan L, Kang SY, Ward LA, To TL, Saif LJ. Antibody-secreting cell responses and protective immunity assessed in gnotobiotic pigs inoculated orally or intramuscularly with inactivated human rotavirus. J Virol. 1998;72(1):330-8.
78. Barnes GL, Townley RR. Duodenal mucosal damage in 31 infants with gastroenteritis. Archives of disease in childhood. 1973;48(5):343-9.

79. Davidson GP, Barnes GL. Structural and functional abnormalities of the small intestine in infants and young children with rotavirus enteritis. Acta paediatrica Scandinavica. 1979;68(2):181-6.
80. Ward LA, Rosen BI, Yuan L, Saif LJ. Pathogenesis of an attenuated and a virulent strain of group A human rotavirus in neonatal gnotobiotic pigs. The Journal of general virology. 1996;77 (Pt 7):1431-41.
81. Yuan L, Saif LJ. Induction of mucosal immune responses and protection against enteric viruses: rotavirus infection of gnotobiotic pigs as a model. Veterinary immunology and immunopathology. 2002;87(3-4):147-60.
82. Saif L, Yuan L, Ward L, To T. Comparative studies of the pathogenesis, antibody immune responses, and homologous protection to porcine and human rotaviruses in gnotobiotic piglets. Adv Exp Med Biol. 1997;412:397-403.
83. Yuan L, Ward LA, Rosen BI, To TL, Saif LJ. Systematic and intestinal antibody-secreting cell responses and correlates of protective immunity to human rotavirus in a gnotobiotic pig model of disease. J Virol. 1996;70(5):3075-83.
84. Ward LA, Yuan L, Rosen BI, To TL, Saif LJ. Development of mucosal and systemic lymphoproliferative responses and protective immunity to human group A rotaviruses in a gnotobiotic pig model. Clinical and diagnostic laboratory immunology. 1996;3(3):342-50.
85. Iosef C, Chang KO, Azevedo MS, Saif LJ. Systemic and intestinal antibody responses to NSP4 enterotoxin of Wa human rotavirus in a gnotobiotic pig model of human rotavirus disease. Journal of medical virology. 2002;68(1):119-28.
86. Tzipori SR, Makin TJ, Smith ML. The clinical response of gnotobiotic calves, pigs and lambs to inoculation with human, calf, pig and foal rotavirus isolates. The Australian journal of experimental biology and medical science. 1980;58(3):309-18.
87. Mebus CA, Wyatt RG, Kapikian AZ. Intestinal lesions induced in gnotobiotic calves by the virus of human infantile gastroenteritis. Vet Pathol. 1977;14(3):273-82.
88. McNeal MM, Sestak K, Choi AH, Basu M, Cole MJ, Aye PP, et al. Development of a rotavirus-shedding model in rhesus macaques, using a homologous wild-type rotavirus of a new P genotype. J Virol. 2005;79(2):944-54.
89. Ward RL, McNeal MM, Sheridan JF. Development of an adult mouse model for studies on protection against rotavirus. J Virol. 1990;64(10):5070-5.
90. Ha S, Choi IS, Choi C, Myoung J. Infection models of human norovirus: challenges and recent progress. Arch Virol. 2016;161(4):779-88.
91. Taube S, Kolawole AO, Hohne M, Wilkinson JE, Handley SA, Perry JW, et al. A mouse model for human norovirus. MBio. 2013;4(4):e00450-13.
92. Wang QH, Costantini V, Saif LJ. Porcine enteric caliciviruses: genetic and antigenic relatedness to human caliciviruses, diagnosis and epidemiology. Vaccine. 2007;25(30):5453-66.
93. Bui T, Kocher J, Li Y, Wen K, Li G, Liu F, et al. Median infectious dose of human norovirus GII.4 in gnotobiotic pigs is decreased by simvastatin treatment and increased by age. The Journal of general virology. 2013;94(Pt 9):2005-16.
94. Cheetham S, Souza M, Meulia T, Grimes S, Han MG, Saif LJ. Pathogenesis of a genogroup II human norovirus in gnotobiotic pigs. J Virol. 2006;80(21):10372-81.

95. Souza M, Azevedo MS, Jung K, Cheetham S, Saif LJ. Pathogenesis and immune responses in gnotobiotic calves after infection with the genogroup II.4-HS66 strain of human norovirus. J Virol. 2008;82(4):1777-86.
96. Bok K, Parra GI, Mitra T, Abente E, Shaver CK, Boon D, et al. Chimpanzees as an animal model for human norovirus infection and vaccine development. Proc Natl Acad Sci U S A. 2011;108(1):325-30.
97. Ettayebi K, Crawford SE, Murakami K, Broughman JR, Karandikar U, Tenge VR, et al. Replication of human noroviruses in stem cell-derived human enteroids. Science. 2016;353(6306):1387-93.
98. Cheetham S, Souza M, McGregor R, Meulia T, Wang Q, Saif LJ. Binding patterns of human norovirus-like particles to buccal and intestinal tissues of gnotobiotic pigs in relation to A/H histo-blood group antigen expression. J Virol. 2007;81(7):3535-44.

Chapter 2 Modeling human enteric dysbiosis and rotavirus immunity in gnotobiotic pigs

Erica L. Twitchell[1], Christine Tin[1], Ke Wen[1], Husen Zhang[2], Sylvia Becker-Dreps[3], M. Andrea Azcarate-Peril[4], Samuel Vilchez[5], Guohua Li[1], Ashwin Ramesh[1], Mariah Weiss[1], Shaohua Lei[1], Tammy Bui[1], Xingdong Yang[1], Stacey Schultz-Cherry[6], Lijuan Yuan[1]*

1. Department of Biomedical Sciences and Pathobiology, Virginia-Maryland College of Veterinary Medicine, Virginia Polytechnic Institute and State University, Blacksburg, Virginia, USA
2. Microbiome Core, Cancer Inflammation Program, National Cancer Institute, Bethesda, Maryland, USA
3. Department of Family Medicine, University of North Carolina School of Medicine, Chapel Hill, North Carolina, USA
4. Department of Cell Biology and Physiology, School of Medicine and Microbiome Core Facility, Center for Gastrointestinal Biology and Disease, University of North Carolina, Chapel Hill, North Carolina, USA
5. Department of Microbiology and Parasitology, Faculty of Medical Sciences, National Autonomous University of Nicaragua, León, Nicaragua
6. Department of Infectious Diseases, St. Jude Children's Research Hospital, Memphis, Tennessee, USA

*Correspondence and request for materials should be addressed to L.Y. (email: lyuan@vt.edu)

Published in *Gut Pathogens* 2016 **8**:51. Open access.

Abstract

Background: Rotavirus vaccines have poor efficacy in infants from low- and middle-income countries. Gut microbiota is thought to influence the immune response to oral vaccines. Thus, we developed a gnotobiotic (Gn) pig model of enteric dysbiosis to study the effects of human gut microbiota (HGM) on immune responses to rotavirus vaccination, and the effects of rotavirus challenge on the HGM by colonizing Gn pigs with healthy HGM (HHGM) or unhealthy HGM (UHGM). The UHGM was from a Nicaraguan infant with a high enteropathy score (ES) and no seroconversion following administration of oral rotavirus vaccine, while the converse was characteristic of the HHGM. Pigs were vaccinated, a subset was challenged, and immune responses and gut microbiota were evaluated.

Results: Significantly more rotavirus-specific IFN-γ producing T cells were in the ileum, spleen, and blood of HHGM than those in UHGM pigs after three vaccine doses, suggesting HHGM induces stronger cell-mediated immunity than UHGM. There were significant correlations between multiple Operational Taxonomic Units (OTUs) and frequencies of IFN-γ producing T cells at the time of challenge. There were significant positive correlations between *Collinsella* and CD8+ T cells in blood and ileum, as well as CD4+ T cells in blood, whereas significant negative correlations between *Clostridium* and *Anaerococcus*, and ileal CD8+ and CD4+ T cells. Differences in alpha diversity and relative abundances of OTUs were detected between the groups both before and after rotavirus challenge.

Conclusion: Alterations in microbiome diversity and composition along with correlations between certain microbial taxa and T cell responses warrant further investigation into the role of the gut microbiota and certain microbial species on enteric immunity. Our results support the use of HGM transplanted Gn pigs as a model of human dysbiosis during enteric infection, and oral vaccine responses.

Keywords: enteric dysbiosis, gnotobiotic pig, rotavirus, vaccine, enteric immunity

Introduction

Rotavirus gastroenteritis accounted for approximately 37% of all diarrhea-related deaths and 5% of all deaths in children less than 5 years of age; in all, rotavirus killed approximately 453,000 children in 2008, mostly from low-middle income countries (LMICs) (1, 2). Oral vaccines for rotavirus, poliovirus, cholera and shigellosis are less efficacious in children from LMICs than in children from higher income countries (3, 4). Specifically regarding oral rotavirus vaccination, the two commercially available vaccines (RotaTeq® and Rotarix®) only have 39-70% efficacy, with an average of 50-60% efficacy in LMICs; whereas rotavirus vaccines are 80-90% effective in high-income countries (3, 5-7). Differences in rotavirus vaccine efficacy may be due to a combination of factors including environmental enteric dysfunction (EED), variations in the gut microbiome, an altered gut microbiota composition (dysbiosis), high maternal antibody titers transferred through the placenta or breast milk, malnutrition, or influence of concurrent enteropathogens (3, 4, 6-8).

EED, also known as environmental enteropathy is a structural and functional disorder of the small intestine that is most frequently seen in children from low income

settings (9). EED leads to gut barrier disruption, nutrient malabsorption, impaired gut immune function, and ultimately, oral vaccine failure, growth stunting, and delayed cognitive development (9-11). However, children with EED do not always have diarrhea (10). Histologic features include villous blunting, crypt hyperplasia, and lymphocytic infiltration of the epithelium and lamina propria in the small intestine (9). The cause of this condition is unknown, but theories include constant exposure to enteropathogens in food, water, or the environment, imbalance of gut microbiota, and an altered immune response triggered by intestinal microbes (4, 9, 10).

The gastrointestinal microbiota is important for the development of enteric immunity, prevention of enteropathogen colonization, and utilization of dietary energy (4, 12). The composition of the gut microbiota in children is influenced by the method of delivery (vaginal or C-section), environmental hygiene, and nutritional status (4). Studies have shown that the composition of gut microbiota is significantly different between African and northern European infants, and between malnourished and well-nourished children (10, 12, 13).

The goal of this study was to create a gnotobiotic (Gn) pig model of human enteric dysbiosis to evaluate the influence of the gut microbiota on immune responses to an attenuated human rotavirus vaccine (AttHRV). Since pigs and humans share high genomic and protein sequence homologies, an omnivorous diet, colonic fermentation, and similar immune systems, pigs serve as valuable models in biomedical research (14). To this effect, the neonatal Gn pig model is a proven model of human rotavirus disease and immunity (15). Protection against rotavirus diarrhea in the Gn pig model is positively correlated with frequencies of intestinal IFN-γ producing T cells, rotavirus- specific

serum IgA, intestinal IgA and intestinal IgG antibody titers, and IgA antibody secreting cells in the intestine (16-18).

The study of microbiota on virus life cycle is facilitated by the germ-free condition in Gn pigs (19-22). In addition, our previous studies of human gut microbiota (HGM) transplanted Gn pigs, demonstrated that HGM from a healthy C-section delivered infant was able to colonize newborn Gn pig intestine and similar microbiota was observed between HGM from the infant and colonized Gn pigs (20, 21). In this study we attempted to develop a Gn pig model of human enteric dysbiosis by colonizing Gn pigs with unhealthy HGM (UHGM). UHGM designates the HGM samples from children with evidence of gut inflammation and permeability (based on enteropathy scores (ES) and an impaired immune response to the rotavirus vaccine RV5 (RotaTeq®), suggesting an unhealthy gut. HGM from children with low ES and a robust immune response to RV5, suggesting a normal gut, was designated as healthy HGM (HHGM). We hypothesized that HHGM in Gn pigs would induce a stronger immune response after vaccination than the dysbiosis pigs, and that certain components of the HGM may be correlated with impaired immune responses.

Results

Antibody response in HHGM and UHGM pigs

HHGM and UHGM samples were orally inoculated into a subset of newborn Gn pigs, respectively. After AttHRV inoculation and virulent HRV (VirHRV) challenge, antibody titers were measured in small intestinal contents (SIC), large intestinal contents (LIC), and serum. Rotavirus-specific immunoglobulin titers in intestinal contents from HHGM pigs consistently trended higher than titers from the UHGM pigs, before and after

VirHRV challenge, including IgG and IgA in SIC and IgA in LIC (Fig 1A). However, rotavirus-specific IgA, IgG, and virus neutralizing antibody responses in serum did not differ between the two groups at any time point (Fig 1B). These data suggest that HHGM could have an influence toward a stronger mucosal immune response to oral rotavirus vaccine than UHGM.

Virus specific effector T cell response

Frequencies of IFN-γ+CD8+T cells among total CD8+ T cells in the ileum, spleen, and blood of HHGM pigs were significantly higher than those in UHGM pigs at the time of VirHRV challenge (Fig 2). Frequencies of IFN-γ+CD4+ T cells among total CD4+ T cells in the ileum and blood were also significantly higher in HHGM pigs than in UHGM pigs at the time of VirHRV challenge. After challenge, IFN-γ+CD8+ and IFN-γ+CD4+ T cell responses did not differ significantly between the two groups in any tissue. The data demonstrate that the AttHRV vaccine induced significantly stronger anti-viral effector T cell immune responses in pigs colonized with HHGM than those with UHGM. The significantly higher virus-specific effector T cell responses at the time of challenge were associated with increased protection against rotavirus shedding and clinical signs (Fig 2 and Table 1).

Clinical signs and virus shedding

After challenge with VirHRV, HHGM pigs had significantly reduced incidence and shorter duration of viral shedding, and lower mean peak virus titer than UHGM pigs (Table 1). HHGM pigs had a slightly lower incidence, delayed onset, shorter duration of diarrhea, and lower cumulative diarrhea score compared to the UHGM pigs. These results suggest that HHGM is associated with less severe clinical signs and viral shedding than

UHGM in vaccinated pigs subsequently challenged with VirHRV, indicating that HHGM facilitates the development of a stronger protective immunity.

Microbiome analysis

Alpha diversity, measured by Shannon index, phylogenic diversity, observed species, and Chao 1 were compared between HHGM and UHGM pig groups (Table 2). Measurements of alpha diversity in HHGM pigs were significantly lower than those in UHGM pigs at post-inoculation day (PID) 28 and post-challenge day (PCD) 7. In addition, alpha diversity measurements decreased in HHGM pigs from PID28 to PCD7. There were no significant differences before or after challenge for the UHGM pigs. These results suggest that VirHRV challenge caused a greater disruption to the microbiota in HHGM pigs than in UHGM pigs. Beta diversity analysis was visualized with a PCoA plot based on unweighted UniFrac. Regardless of the time point, the microbiota from pigs with HHGM clustered in one group while samples from UHGM pigs formed another group (Fig 3).

In HGM transplanted pigs, phyla represented in UHGM pigs were similar to those in the human infant samples, with Firmicutes being the most abundant. Firmicutes was also the most abundant phylum in the healthy human infant stool sample. Conversely, Proteobacteria or Bacteroidetes was the most abundant phyla in HHGM pigs with Firmicutes being second or third in mean relative abundance (Fig 4). There were significantly more Firmicutes in UHGM pigs than in HHGM pigs at PID28. After VirHRV challenge on PCD7, the phyla, Firmicutes, Proteobacteria and Tenericutes had significantly higher mean relative abundance in the UHGM pigs while mean relative abundance of Bacteroidetes was significantly higher in HHGM pigs. When evaluating

microbiome shifts in HHGM pigs before and after VirHRV, Firmicutes, Proteobacteria and Verrucomicrobia were shown to be significantly decreased while Bacteroidetes significantly increased in mean relative abundance. There were no significant changes in gut phyla composition in UHGM between pre- and post-VirHRV challenge samples (Fig 5).

Differences at the genera level were also evaluated between the two groups. On PID28, the mean relative abundance was significantly higher for the following OTUs in the HHGM group compared to the UHGM group; *Enterococcus*, *Collinsella*, *Stenotrophomonas*, *Pseudomonas*, and unclassified members of Lactobacillales and Enterococcaceae. The mean relative abundance of the following OTUs were significantly higher in UHGM pigs compared to HHGM pigs on PID28; *Clostridium*, *Streptococcus*, *Ruminococcus*, *Anaerococcus*, *Propionibacterium*, *Blautia*, and unclassified members of Clostridiales, Bacillales, and Lachnospiraceae (Figs. 6 and 7).

At PCD7, mean relative abundance was significantly higher for *Bacteroides*, *Collinsella*, and unclassified members of Clostridiaceae and Erysipelothichaceae in HHGM pigs compared to that in UHGM pigs. UHGM pigs had a significantly higher mean relative abundance of *Ruminococcus*, *Streptococcus*, *Clostridium*, *Bifidobacterium*, *Staphylococcus*, *Turicibacter*, *Propriobacterium*, *Haemophilus*, *Moraxella*, *Blautia*, *Prevotella*, *Granulicatella*, and unclassified members of Enterobacteriaceae, Bacillales, Lachnospiraceae, and Clostridiales than the HHGM pigs (Figs. 6 and 7).

Spearman's correlation coefficients were determined for frequencies of rotavirus-specific IFN-γ producing T cells in ileum, spleen, and blood, and OTUs at the genus level on PID28 (PCD0) and PCD7 (Table 3). There were significant positive correlations

between *Collinsella* and CD8+ T cells in blood and ileum, as well as CD4+ T cells in blood at PCD0. At PCD0, significant negative correlations existed between *Clostridium* and *Anaerococcus,* and ileal CD8+ and CD4+ T cells. At this time point, CD8+ T cells in blood were negatively correlated with *Propionibacterium*, *Blautia,* and an unclassified member of Bacillales, while CD4+ T cells in blood were negatively correlated with 2 unclassified members of Clostridiales.

At PCD7, there were significant positive correlations between unclassified members of Clostridiales and Mycoplasmataceae and ileal CD8+ T cells. Splenic CD8+ and CD4+ T cells and ileal CD8+ T cells were negatively correlated with *Anaerococcus*. A negative correlation also existed between splenic CD4+ T cells and Staphylococcus.

These data suggest the influence of specific bacterial OTUs on the vaccine-induced T cell responses, as well as the selective impact of IFN-γ producing T cell responses on the gut microbiome. Further investigations are needed to determine which OTUs are most important for influencing the immune response and the mechanism by which they do so.

Enteropathy biomarkers, histopathology, pig weights

Concentrations of α-1-antitrypsin, myeloperoxidase and regenerating islet derived protein 1 beta (REG1B) in SIC and LIC were measured using porcine specific ELISAs. Alpha-1-antitrypsin is a serum protein that is not present in stool unless there increased gut permeability(9). Myeloperoxidase is released from activated neutrophils and is an indicator of inflammation (9). REG1B is a proporliferative antiapoptotic protein secreted by damaged enterocyte and is involved in tissue repair, cell growth and regeneration (23, 24). There were no significant differences between the two pig groups at PID28 or PCD7

(S2 Table). When compared to those of the two human infants (Table 4), the α-1-antitrypsin and myeloperoxidase concentrations were even lower than the HHGM, suggesting that no enteropathy developed in the pigs.

Histopathologic evaluation of villus length, crypt depth, villus to crypt ratio, villus width, and mitotic index in duodenum, jejunum, and ileum did not reveal any significant differences between the two groups at the two time points (S3 Table and S1-S3 Fig.). Thus, the enteropathy status of the UHGM infant donor, as indicated by the higher ES of the UHGM samples, was not recapitulated in the UHGM-colonized Gn pigs.

Weights of pigs did not differ between the groups at any of the time points (S4 Table). This suggests the microbiota did not differentially affect nutrient assimilation or growth. The lack of significant differences between the groups in regards to enteropathy biomarkers, histopathology, or weight indicates enteropathy did not develop in this Gn model within the timeframe of this experiment.

Discussion

In this study we demonstrated that Gn pigs colonized by UHGM can serve as a model system for enteric dysbiosis and impaired immunity. We used this neonatal pig model system to evaluate the effects of gut microbiota on immune responses to oral rotavirus vaccination. We also evaluated the impact of rotavirus challenge on the gut microbiota. In this model system, the only variable was the different HGM; thus any observed difference in the results could be attributed to differences in the gut microbiota. We demonstrated that pigs colonized with HHGM had a significantly stronger effector T cell immune response to vaccination compared to UHGM pigs. Additionally, we found significant correlations between some bacterial OTUs and frequencies of effector T cells,

and we also observed differences in the gut microbiome composition and diversity both before and after VirHRV challenge.

When the two groups were compared, UHGM had weaker virus-specific T cell immune responses to AttHRV and trended lower rotavirus-specific antibody titers in intestinal contents. These data indicate that HHGM facilitated a stronger adaptive immune response to oral rotavirus vaccine than did UHGM. Evidently, UHGM pigs had higher viral shedding and more severe clinical signs compared to HHGM pigs after challenge with VirHRV.

The rotavirus challenge caused significant decreases in alpha diversity indices in the HHGM pigs, while no significant changes were detected in UHGM pigs. The decreased alpha diversity in HHGM pigs after VirHRV challenge was expected. A study evaluating microbiome and diarrhea found that diarrhea was associated with decreased phylogenetic diversity (25). Although no samples were available for time points after PCD7, it is expected, given our data on enteropathy biomarkers, that diversity of HHGM pigs would return to normal levels. The lack of significant differences in alpha diversity parameters in UHGM pigs from PID28 to PCD7 may be due to an already abnormal microbiome and/or previous exposure to rotavirus based on pre-vaccination serum IgA titer in the infant donor.

The mean relative abundance of phyla between UHGM pig LIC samples and infant stool sample (PM25) was similar, which was as expected. However, HHGM pig samples differed from their infant donor (SV14). Community structure may have been different between the human and pigs because of influence of different environments, differences in diet, lack of natural microbial succession in the pigs, or differences in host

genetics (26). The phylum and genus level differences between HHGM and UHGM pigs at both time points warrant further study to assess the influences of these OTUs on the host immune response. In HHGM pigs, after VirHRV challenge, there was a decrease in the relative abundance of Firmicutes, similar to previous observations (21). Although we did not sample pigs without AttHRV vaccination, human studies have shown that rotavirus vaccination does not have any major effects on the gut microbiota of children (27, 28). Similar to a human study, HHGM pigs had an increased mean relative abundance of *Bacteroides* after rotavirus infection (29). *Bacteroides* and *Lactobacillus* species have been shown to modify cell-surface glycans in human intestinal cultured cells, effectively blocking rotavirus infection (30). This may partially explain why HHGM pigs had decreased viral shedding when compared to UHGM pigs. In agreement with a previous study, we also observed a decrease in levels of *Streptococcus* in HHGM pigs after the rotavirus challenge (21). There is limited data on mechanisms by which microbiota directly influences enteric virus infectivity. Microbiota may modify the cell surface or bind to pathogens. *In vitro* experiments have demonstrated soluble factors from *Bacteroides thetaiotaomicron* and *Lactobacillus casei* can increase cell surface galactose and block rotavirus infection (30). Poliovirus binds bacterial surface polysaccharides, which enhances virion stability and cell attachment, and may enhance transmission (31). Gnotobiotic pigs colonized with *E. coli* Nissle1917 (EcN) had lower viral shedding titers, which the authors speculated was because EcN bound to HRV particles (32).

There were significant positive and negative correlations between OTUs and IFN-γ producing T cell responses in the ileum, blood, and spleen. The biological relevance of

these findings needs to be explored further. Previous studies have shown that the HGM promotes development of the neonatal immune system as evidenced by the significantly enhanced IFN-γ producing T cell response and decreased regulatory T cells in AttHRV-vaccinated pigs when comparing HGM colonized Gn pigs to non-HGM colonized Gn pigs (20). Human studies have shown correlations between microbiome components and response to vaccination. In Bangladeshi infants, Actinobacteria, Coriobacteriaceae, and *Bifidobacterium* abundance were positively correlated with T cell responses to oral polio vaccine, while Pseuodmonadales, Clostridiales, and Enterobacteriales had a negative correlation (33). Concurring with the human study, in this present study *Collinsella,* a member of the Coriobacteriaceae, was strongly and positively correlated with intestinal and circulating rotavirus specific IFN-γ producing CD8+ T cell responses, which are known to correlate with protection against rotavirus diarrhea (18).

We successfully generated a model of dysbiosis, but not enteropathy. There were no differences between the pig groups in regards to gut permeability, assessed by α-1-antitrypsin, gut inflammation, assessed by myeloperoxidase or epithelial regeneration assessed by REG1B. Histopathologic parameters did not differ between the groups. Our Gn pig model did not exhibit small intestinal villous blunting, crypt hyperplasia, or lymphocytic infiltration, which are the histologic lesions of EED. The pigs also did not have microscopic lesions of rotavirus infection, the lack of which may be partially due to timing. At PCD7, the small intestine has recovered from rotavirus infection and there are no histopathologic lesions in Gn pigs (15). Although the nutritional status of the pigs was not assessed in this study, the lack of significant differences in body weights between the groups suggests that nutrient assimilation was not altered. We can speculate that other

factors such as malnutrition or concurrent enteropathogen infections are needed to induce the EED phenotype. Additionally, 6 weeks may not have provided sufficient time to develop EED; however it is logistically difficult to keep Gn pigs for extended periods of time.

A recent paper describing a Gn mouse model of EED demonstrated that both malnutrition and gut microbiome were key to developing the model (34). Our pigs received a nutritionally adequate diet. Thus, we suspect incorporation of malnutrition, and potentially enteropathogens into our dysbiosis model will be required to establish a Gn pig model of EED. A mouse study demonstrated that protein-energy malnutrition alone does not impair vaccine efficacy or increase the severity of infection (35). Another recent paper showed that EED, systemic inflammation, and poor maternal health were associated with underperformance of oral rotavirus vaccine (Rotarix®) and oral poliovirus vaccine but not parenteral vaccines in Bangladeshi children (11). Systemic inflammation and poor maternal health were also predictive of malnutrition (11). In the future, we can use the Gn pig model to address effects of malnutrition and systemic inflammation on gut immunity.

In future studies, if we succeed in creating histologic changes and altered biomarker concentrations in our attempt to create an enteropathy pig model, additional assays can be utilized to further characterize the model. Tight junction and adherens junction proteins such as occludin, claudins, E-cadherin, and catenins can provide further insight into intestinal permeability. Systemic inflammation can be assessed with cytokines and acute phase proteins such as IL-1β, IL-4, IL-5, TNFα, C reactive protein (CRP), ferritin, and soluble CD14 (sCD14) (11). Endotoxin core antibody IgG (Endocab)

in serum can be used to evaluate bacterial translocation as well as systemic inflammation (9). The lactulose to mannitol ratio assay is a standard test used in children to assess intestinal permeability and impaired tight junctions (9). We did not utilize this test as the requirement for 2 to 5 hour urine collection and the need to use a closed urinary collection system in the pigs is not technically feasible with gnotobiotic pig isolators or behavior of pigs (9).

There are limitations to this study. Due to the size and weight constraints of the pig isolators, long-term studies are not feasible. This limitation did not allow us to determine if structural or functional changes occur after a longer time period. Regarding the HGM, we used one HHGM and one UHGM sample, both from breastfed, vaginally delivered, Nicaraguan children living in homes with piped water and indoor toilets. As stated previously, numerous factors contribute to gut microbiome composition and environmental enteropathy. We do not know if the same results would be obtained with different HHGM and UHGM samples. Ideally, future studies will evaluate multiple HHGM and UHGM from children exposed to different variables such as diet, access to clean water, method of delivery and country of habitation with equal numbers of male and female samples. Despite the limitations, the Gn pig model of dysbiosis provides a valuable tool for future studies to investigate the immunomodulating mechanisms of the gut microbiota on the immune system and disease pathogenesis.

Further studies are needed to characterize the roles of specific bacterial species on enteric immunity and rotavirus infectivity. Additionally, by adding malnutrition and enteropathogens to this model, we may be able to recapitulate EED. A pig model of EED and rotavirus vaccination will be valuable since mouse models of subclinical enteric viral

infections often do not predict vaccine efficacy against disease in humans. Rotavirus pathogenesis and immunity are similar in pigs and humans, but different in mice (36).

Conclusions

We established a HGM transplanted Gn pig model of dysbiosis and evaluated the influence of the gut microbiota on vaccine immunogenicity and microbiota response to VirHRV challenge. We demonstrated that impaired enteric immunity in human infants can be recapitulated in the Gn pig model with UHGM transplantation. Our findings indicate that the gut microbiota has a major impact on vaccine immunogenicity. This animal model will be valuable in the evaluation of various strategies (i.e. probiotics, prebiotics, nutritional supplementation) to modulate the intestinal microbiome in order to enhance the immune responses to rotavirus vaccine as well as other vaccines, and enteropathogens such as norovirus, enterotoxigenic *E.coli* and *Shigella*. Results from this study provide a stepping stone for further research involving influence of specific bacterial species on enteric immunity and interaction with rotavirus. Additionally, by adding additional factors to this model such as malnutrition, it may be possible to emulate EED. Enteric dysbiosis, malnutrition, and EED interact in a complex and ill-defined way to negatively impact the health and immunity of young children in the developing world, leading to widespread morbidity and likely increased mortality.

Materials and Methods

Stool samples for HGM transplantation

Stool samples were obtained and analyzed from infants as described in a previous manuscript (37). Briefly, infants from León, Nicaragua were recruited one day prior to

their first pentavalent rotavirus (RV5) immunization, had blood drawn and a stool sample collected from a soiled diaper. A second blood sample was collected 1 month after the first dose of vaccine. Stool specimens were diluted 20-fold and homogenized in sterile pre-reduced anaerobic saline-0.1M potassium phosphate buffer (pH 7.2) containing 15% glycerol (v/v). The samples were snap frozen in liquid nitrogen in the field, immediately transferred to -80°C, shipped on dry ice to our lab, and stored at -80°C until assayed. All stool samples underwent 16S rRNA amplicon sequencing for characterization of the gut microbiome, as previously described (25). ELISAs for 4 biomarkers of enteropathy (α-1 antitrypsin, neopterin, myeloperoxidase and calprotectin) were run on the samples (38, 39). Results from each marker were divided into quantiles with 1 assigned to first quantile, 2 for second quantile, 3 for third quantile and 4 for fourth quantile. The numbers were then added to create a combined enteropathy score (ES) for these 4 biomarkers ranging from 4-16. Rotavirus-specific serum IgA titers were measured on all blood samples. Results of the infant studies were detailed in a previous publication (37). Compared to infants who seroconverted, infants who did not seroconvert had higher concentrations of both myeloperoxidase and calprotectin in stool samples, and higher mean ES. The UHGM sample (ID PM25) was collected from a 9-week old female child with poor seroconversion to the RV5 vaccine, high ES and low alpha diversity (AD). Conversely, the HHGM sample (ID SV14) was collected from an 8-week old male child with a strong IgA response to the RV5 vaccine, low ES, and high AD. The parameters for each variable in the two samples are listed in Table 4. The composition of the microbiome for each sample is shown in Fig 8. Both children were delivered vaginally

and breastfed. They came from different homes; both homes had municipal indoor piped water and indoor toilets.

Studies were approved by the Office of Human Research Ethics at the University of North Carolina (UNC) at Chapel Hill (#14-1136) and the Universidad Nacional Autónoma de Nicaragua, León (#110). Parents or legal guardians of the infants provided written consent.

Selection and preparation of infant samples for HGM Gn pig transplantation

The UHGM stool sample was selected from an infant who did not seroconvert following receipt of the first dose of RV5 (seroconversion defined as > 4-fold increase in rotavirus-specific serum IgA titers 1 month after RV5 immunization), low phylogenetic diversity of the gut microbiome, and high ES. The HHGM stool sample was selected from a child with high RV5 immunogenicity (experienced a > 4-fold increase in rotavirus-specific serum IgA titers after RV5 immunization), high phylogenetic diversity of the gut microbiome, and low ES.

The selected HGM were screened and confirmed negative for rotavirus, astrovirus, norovirus, sapovirus, adenovirus, and *Klebsiella* spp. via PCR prior to oral transplantation into the Gn pigs. *Klebsiella* spp. were specifically targeted because previous studies have lost HGM transplanted pigs to *Klebsiella* infection from the inocula (20, 40). Primers for the *Klebsiella* spp. PCR targeted the *gyr*A gene and were based on previous publications (41, 42). The universal 16S rRNA primers, 27F and 1492R were included in the PCR protocol to confirm the presence of amplifiable DNA. DNA was extracted with ZR Fecal DNA MiniPrep (Zymo, Irvine, CA) from 150 µl of sample per manufacturer's instructions. *Klebsiella pneumoniae*, obtained from the Virginia Tech

Animal Laboratory Services bacteriology laboratory was used as a positive control sample. The master mix contained 5 µl PFX 50 PCR mix, 1 µl PFX 50 DNA polymerase (ThermoFisher Scientific, Waltham, MA), 1.5 µl 10mM dNTPs, 1.5 µl of each primer (10uM), 4-30 µl of DNA and water added to a final volume of 50 µl. After a 2-min incubation at 94°C, 35 cycles of 94°C 15 sec, 60°C 20 sec, and 68°C 1 min were performed, followed by a final extension at 68°C for 5 min.

PCR for norovirus genogroups I and II, adenovirus, sapovirus, and astrovirus were carried out at St. Jude Children's Research Hospital. DNA and RNA were extracted from 175 µl of sample using the MagMax Total Nucleic Acid isolation kit (ThermoFisher Scientific). PCR buffer for the RNA samples was Taqman fast virus 1-step (ThermoFisher Scientific). Taq core kit (Qiagen, Valencia, CA.) was used for DNA samples. Norovirus I and II, sapovirus, adenovirus, and astrovirus real-time PCR primers, as well as, probes and conditions, were based on previous publications (43-46).

RT-PCR for rotavirus gene segment 6 was used to screen samples for rotavirus. RNA was extracted from samples using TRIZOL LS (ThermoFisher Scientific) per manufacturer's instructions. The mixture for cDNA synthesis included 2 µmol of primer 1581, and 11 µl of RNA. RNA was denatured at 95°C for 5 min then cooled to 4°C. The mixture for reverse transcription contained 4 µl of 5X buffer, 1µl 0.1 M DTT, 1 µl Superscript III reverse transcriptase (ThermoFisher Scientific) and 1 µl of RNase free water. The cDNA sample was combined with the mixture for reverse transcription and incubated at 50°C for 60 min then 70°C for 15 min and held at 4°C. One µl of RNaseH (New England Biolabs, Ipswich, MA) was added and the sample was incubated at 37°C for 20 min. The PCR mix contained 10 µl of buffer, 1 µl of MyTaq DNA polymerase

(Bioline, Taunton, MA), 27 µl of ddH2O, 1µl of each 20 µM primer (158 (forward) and 15 (reverse), and 10 µl of DNA. The sequence for primer 158 was GGC TTT AAA ACG AAG TCT TCG AC and that for primer 15 was GGT CAC ATC CTC TCA CTA. The sample was incubated at 95°C for 3 min followed by 35 cycles of 95°C 20 sec, 47.5°C 30 sec, and 72°C 90 sec. Final extension was at 72°C for 7 minutes. AttHRV was used as a positive control.

HGM was prepared for oral inoculation into the Gn pigs as described previously (20). The sample was washed with 10-fold volume of sterile PBS to remove glycerol, and then centrifuged at 2000 rpm for 10 min at 4°C. The pellet was resuspended to the original volume with sterile PBS. Pigs received 400-700 µl of HGM sample at 5, 6 and 7 days of age.

Pig studies

Near-term pigs (Yorkshire crossbred) were derived by hysterectomy and maintained in sterile isolator units as described previously (47). The estimated sample size to obtain greater than 0.9 power is n≥6 based on a power analysis using an ANOVA or ANCOVA model by the Virginia Tech Department of Statistics. Sterility was confirmed by culturing isolator swabs and porcine rectal swabs on blood agar plates and in thioglycollate media 3 days after derivation. Commercial ultra-high temperature-treated sterile cow milk was used throughout the study. The pigs were housed with a 12-hour light-dark cycle at 80-93°F (based on age) and provided with a toy for environmental enrichment. The animal experimental protocol is outlined in S1 Table. These pigs and data generated from them have not been used in previous publications. In total, 24 pigs were randomly assigned to the 4 groups (HHGM-PID28/PCD0 *n*=5,

HHGM PCD7 *n*=7, UHGM PID28/PCD0 *n*=6 and UHGM PCD7 *n*=6). Intraperitoneal (IP) injections of gamma-irradiated, commercially available porcine serum (Rocky Mountain Biologicals Inc., Missoula, MT) were given to the pigs in an attempt to provide immunoprotection against potentially pathogenic bacteria in the HGM transplants. A total volume of 60 ml was given at 3 time points, 6 hours apart, starting on the day of or day after derivation. In the commercial serum, rotavirus-specific virus neutralization titer was measured at 64, rotavirus-specific IgG titer at 65,536, and rotavirus-specific IgA titer at 64. At PCD 0, the geometric mean titers for rotavirus-specific antibodies among all pigs were 16.7 for virus neutralizing antibodies, 10,935 for IgG, and 75.9 for IgA. These titers mimic normal maternally acquired rotavirus antibody titers in conventionally derived suckling pigs or human infants (48). The cell culture-adapted HRV Wa strain (G1P1A[8]), derived from the 35^{th} passage in African green monkey kidney cells (MA104), was used as the AttHRV vaccine for oral inoculation at a dose of 5 X 10^7 focus-forming units (FFU) on PID 0 (7 days of age), PID10 and PID20 (17). A subset of pigs (*n*=5-6) from each group was euthanized before challenge PID28/PCD0 for evaluation of immune responses induced by AttHRV vaccination. The remaining pigs (*n*= 6-7) were orally challenged with 10^5 FFU of VirHRV Wa strain (G1P1A [8]) and monitored from PCD0-PCD7 to evaluate virus shedding and diarrhea before euthanasia on PCD7. The 50% infectious dose (ID50) of VirHRV in neonatal Gn pigs is approximately 1 FFU (15). Rectal swabs were collected daily to monitor virus shedding by ELISA and CCIF from PCD0-PCD7. Daily diarrhea scoring was defined as 0) solid, 1) pasty, 2) semi-liquid, or 3) liquid. Scores of 2 or higher represented diarrhea.

All animal protocols were approved by the Institutional Animal Care and Use Committee at Virginia Tech (protocol #13-187-CVM) and performed in accordance with federal and university guidelines, as well as with recommendations in the American Veterinary Medical Association Guidelines for the Euthanasia of Animals. All sow surgeries were performed under ketamine and tiletamine-zolazepam anesthesia, and immediately followed by euthanasia. A lidocaine epidural was administered preoperatively.

Rotavirus-specific serum and intestinal antibody titers

Pigs were bled and weighed weekly starting at 7 days of age (PID 0). The LIC and SIC were collected at necropsy. Determination of rotavirus-specific IgA and IgG antibody titers in serum and SIC, and IgA in LIC, were based on previously described methods (16, 49). Briefly, 96-well microtiter plates were coated with semi-purified AttHRV antigen at 1:60 or mock-infected MA104 cell culture control lysate at 1:60 in 0.05M carbonate buffer pH 9.6 overnight at room temperature. The plate was washed with TBS pH 8.0 with 0.05% Tween (TBST) five times. Plates were blocked with TBS containing 1% BSA for 1 hour at room temperature. Four-fold serial dilutions of each sample in TBST containing 1% BSA were performed on a separate plate. The samples were then transferred to the antigen-coated plate and incubated for 2 hours at room temperature followed by five washes with TBST. Plates were then incubated for 1 hour at room temperature with the detection antibody. The IgA assay used goat anti-porcine IgA polyclonal HRP-conjugated antibody (A100-102P, Montgomery, TX; AB_67219) and the IgG assay used goat anti-porcine IgG-Fc fragment polyclonal HRP-conjugated antibody (A100-104P, Bethyl Laboratories, Inc.; AB_67225). Both antibodies were

diluted 1:35000 in TBST containing 1% BSA. Plates were washed five times with TBST and developed with ABTS (2,2'-azino-di(3-ethylbenzothiazoline-6-sulfonate) HRP substrate (KPL, Inc., Gaithersburg, MD) for 15-30 min at room temperature. The reaction was stopped with ABST peroxidase stop solution (KPL, Inc.) diluted 1:5 in water. Optical density was measured at 405 nm.

Rotavirus-specific serum virus neutralizing antibody titer

African green monkey kidney cells, MA104 (ATCC, Manassas, VA, # CRL-2378.1, purchased from ATCC in January 2008) were grown in 96-well plates for 3-4 days. Monolayers were washed once with Eagle's minimum essential medium (EMEM) (ATCC), and 100 µl of EMEM was added to each well. The plate was incubated at 37°C for 2h. In a separate 96-well plate, serum samples were diluted four-fold in duplicate. One set of each sample was inoculated with AttHRV (4 X 10^3 FFU) and the other set with EMEM. This plate was incubated at 37°C for 1h. After the 2h incubation, EMEM in the MA104 plates was discarded and the cells were incubated with 50 µl/well of the serum with AttHRV or EMEM in duplicate at 37°C for 1h. Fifty µl of EMEM with trypsin (0.5 ug/ml) was added to each well and the plate was incubated at 37°C with 5% CO_2 for 18-24h. Liquid in the wells was discarded and the plates were fixed with 80% acetone at room temperature for 10 min. Acetone was discarded and plates were air-dried. Fixed plates were stored at –20°C or stained immediately. For immunofluorescence staining, plates were initially rinsed with PBS containing 0.05% Tween 20 (PBST) pH7.4 once for 2 min. Each well received 50 µl of goat anti-bovine rotavirus polyclonal unconjugated antibody (PA1-7241, ThermoFisher Scientific; AB_561090) diluted 1:250 in PBST containing 2% nonfat dry milk then incubated at

37°C for 1h. Plates were rinsed 3 times with PBST. Fifty µl of rabbit anti-goat IgG whole molecule polyclonal FITC-conjugated antibody (F7367, Sigma-Aldrich, St. Louis, MO; AB_259726) diluted 1:400 in PBST containing 2% nonfat dry milk was added to each well and incubated at 37°C for 1h. Plates were rinsed 3 times with PBS pH 7.4 and once with PBS pH8.0. Mounting media (60% glycerol, 40% PBS pH 8.0) was added to each well. Fluorescing cells were enumerated by fluorescent microscopy. The virus neutralizing antibody titer was defined as the reciprocal of the serum dilution which reduced the number of fluorescent cell forming units by >80% (50).

CCIF and rotavirus antigen ELISA

Rectal swabs were processed as reported in a previous study (51). Briefly, two rectal swabs per pig were rinsed in 8 ml diluent #5 (minimal essential media (MEM, ThermoFisher Scientific) 1% penicillin and streptomycin, 1% HEPES) and then centrifuged at 2100 rpm for 15 min at 4 °C. Viral antigen and infectious virus in the rectal swabs were measured using ELISA or cell culture immunofluorescence (CCIF), respectively, as previously described (52).

The CCIF was performed in MA104 cells grown in 96-well plates for 3-4 days. Plates were washed with PBS. One hundred µl of EMEM was added to each well and the plate was incubated for 2 hours at 37 °C with 5% CO_2. In separate 96-well plates, ten-fold serial dilutions of the samples were made in EMEM. After the plate with cells was removed from the incubator, media was discarded. Fifty µl from each well on the dilution plate was added to the cells in duplicate. The plate was centrifuged at 2000 rpm for 1 hour at 21°C with slow deceleration. EMEM containing trypsin was then added to each well for a final trypsin concentration of 0.5 µg/ml. The cells were incubated at 37°C for

18-24 hours in a CO_2 incubator. The protocol for acetone fixation and immunofluorescence staining of the plates was the same as described for the neutralizing antibody titer assay.

Using ELISA to detect rotavirus antigen, a 96-well microtiter plate was coated with 100 µl/well goat anti-bovine rotavirus polyclonal unconjugated antibody (PA1-7241, ThermoFisher Scientific; AB_561090) in 0.05M carbonate buffer pH 9.6 at a dilution of 1:250. The plates were incubated overnight at 4 °C. Plates were then washed twice with PBST, blocked with 300 µl/well of PBS pH 7.4 containing 5% nonfat dry milk then incubated for 1h at 37 °C. Plates were washed 3 times with PBST. One hundred µl/well of diluted sample (in PBS with 0.1%BSA) was added in duplicate. Semi-purified AttHRV antigen or supernatant of mock-infected MA104 cells were used as a positive and negative control respectively. Plates were incubated for 1h at 37 °C then washed 3 times with PBST. One hundred µl/well of goat anti-bovine rotavirus polyclonal HRP-conjugated antibody (PA1-73015, ThermoFisher Scientific; AB_1018382) diluted 1:200 in PBS containing 1% BSA was then added to each well and incubated for 1h at 37 °C, followed by 3 washes with PBST. One hundred µl/well of ABST peroxidase substrate solution was added and the plate was incubated for 15-30 min at room temperature. The reaction was stopped with 100 µl/well of ABST stop solution diluted 1:5. The optical density values were measured at 405 nm.

Mononuclear cell isolation

Mononuclear cells (MNC) were isolated from the ileum, spleen, and blood as described in previous publications (17, 18, 53). Briefly, after rinsing the ileum samples with HBSS without Ca^{2+} and Mg^{2+} (GE Healthcare, Logan, UT), they were manually

minced with scissors, resuspended in 40 ml solution A (HBSS without Ca2+, Mg2+ with 200 ug/ml gentamicin, 20 ug/ml ampicillin, 40mM HEPES, 5mM EDTA, 0.29 mg/ml DTT, and 7% NaHCO3) then placed on a shaker at 37°C for 30 minutes. Tissue fragments were further minced and solution C (RPMI-1640 (ThermoFisher Scientific) with 8% FBS, 200 ug/ml gentamicin, 20 ug/ml ampicillin, 20 mM HEPES, 5mM EDTA, 0.29 mg/ml DTT, and 400 U/ml collagenase type II (Worthington Biochemical Co, Lakewood, NJ) was added to 40 ml and digested at 37 °C for 30 min with shaking. Supernatants were collected and remaining tissue was ground on an 80-mesh screen. The cell suspension was collected and the remaining tissue underwent another digestion step with repeated grinding on the screen. Cell suspensions were divided equally between three 50 ml conical vials and wash media (RPMI-1640 with 200 ug/ml gentamicin, 20 ug/ml ampicillin, and 10mM HEPES) was added to a volume of 35 ml. Percoll (GE Healthcare) was added to each tube to bring the final Percoll concentration to 30% and then centrifuged at 1800*g* for 20 min at 4 °C without the brake. Cell pellets were resuspended in 15 ml conical vials with 10 ml of 43% Percoll, underlaid with 5 ml of 70% Percoll, and centrifuged at 1800*g* for 30 min at 4 °C without brake. MNC were collected from the 43% to 70% Percoll interface into 50 ml conical vials with 50 ml of wash buffer and centrifuged at 800*g* for 15 min at 4°C.

Blood was mixed with 30% (vol/vol) of acid citrate dextrose at the time of necropsy, divided equally between three 50 ml conical vials with HBSS added to bring the volume to 50 ml, and then centrifuged for 30 min at 1200*g* with no brake at room temperature. The buffy coat was transferred to a 50 ml conical vial with HBSS added to a volume of 30 ml. The buffy coat mixture is then divided equally among three 15 ml

centrifuge tubes, underlaid with 5 ml of Ficoll-Paque PREMIUM® (GE Healthcare Bio-Sciences, Pittsburgh, PA) and centrifuged at 1200*g* for 30 min at room temperature with no break. MNC were collected from the interface, placed in a 50 ml vial, HBSS added to bring the volume to 30 ml, and then centrifuged for 15 min at 800*g* 4°C. Remaining erythrocytes were lysed by mixing 5 ml of sterile distilled water with the cell pellet, after which HBSS was added to a final volume of 50 ml. The samples were centrifuged for 15 min at 400*g* 4°C, after which the HBSS wash and centrifugation step was repeated.

The spleens were minced and ground as described for the ileum without the solution C step. Cells were suspended in 50 ml of wash media then centrifuged for 30 min 1000*g* 4°C. The cell pellet was resuspended in 20 ml of wash buffer and then Percoll was added to bring the final Percoll concentration to 30%. Samples were centrifuged for 1200*g* 4°C without brake. Cells were resuspended with 30 ml of 43% Percoll, divided into three 15 ml tubes, underlaid with 5 ml of 90% Percoll and then centrifuged for 30 min at 1900*g* for 30 min 4°C without the brake. MNC were collected at the 43%-70% Percoll interface into a 50 ml conical vile with wash buffer, centrifuged for 15 min at 504*g* for 15 min 4°C twice, changing the wash buffer between steps. MNC from all tissues were resuspended with 2-10 ml of enriched-RPMI (RPMI-1640 with 20 mM HEPES, 100 ug/ml gentamicin, 10 ug/ml ampicillin, 8% FBS, 2mM L-glutamine, 0.1 mM nonessential amino acids, 1mM sodium pyruvate, and 50mM 2-mercaptoethanol.

Flow cytometry for rotavirus-specific IFN-γ producing T cells

Frequencies of HRV-specific IFN-γ producing CD4+ and CD8+ T cells among the lymphocytes of the ileum, spleen, and blood were determined with flow cytometry. MNC were stimulated in 12-well culture plates with 12 μg/ml of semi-purified AttHRV

antigen for 17h at 37°C in a CO_2 incubator. Brefeldin A (Sigma-Aldrich) at 5mg/ml, and mouse anti-human CD49d monoclonal APC-conjugated antibody (561892, BD Biosciences, San Jose, CA; AB_10896134) at 1µg/ml were added at hour 12 of the incubation. MNC were washed with staining buffer (3%FBS and 0.09% sodium azide in DPBS (0.2 mg/ml KCl, 0.2 mg/ml KH_2PO_4, 8 mg/ml NaCl and 2.16 mg/ml $Na_2HPO_4 \cdot 7H2O$, pH 7.2–7.4) and centrifuged at 500*g* for 5min 4°C. The MNC (2×10^6 cells/tube in 100µl staining buffer) were stained at 4°C for 15 min using the following monoclonal antibodies: 1) One µl mouse anti-porcine CD4a monoclonal FITC-conjugated antibody, clone 74-12-4 (559585, BD Biosciences; AB_397279), 2) 0.5 µl mouse anti-pig CD8α monoclonal SPRD-conjugated antibody, clone 76-2-11 (4520-13, SouthernBiotech, Birmingham, AL) and 3) 2 µl of mouse anti-pig CD3ε monoclonal UNLB-conjugated antibody, clone PPT3 (4510-01, Southern Biotech) and then washed with staining buffer. Next the MNC were centrifuged at 500*g* for 5 min, followed by the addition of 1 µl of rat anti-mouse IgG_1 monoclonal APC-conjugated antibody, clone X56 (550874, BD Biosciences; AB_398470) to the samples and stained for 15 min at 4°C, and then washed with staining buffer. Samples were centrifuged at 500*g* for 5 min. One hundred µl of Cytofix/Cytoperm (BD Biosciences) was added to the samples, which were then incubated for 30 min at 4°C and washed once with Perm/Wash buffer (BD Biosciences). Next, 1 µl of mouse anti-pig IFN-γ monoclonal PE-conjugated antibody, clone P2G10 (559812, BD Biosciences; AB_397341) was added and the samples were incubated at 4°C for 30 min. The samples were washed with Perm/Wash buffer solution, centrifuged at 500*g* for 5 min and then had 0.25 ml of staining buffer added. A minimum

of 100,000 events were acquired using a FACSAria sorter. Flow cytometry data were analyzed using FlowJo 7.2.2 software (Tree Star, Ashland, OR).

DNA isolation and 16S rRNA amplicon sequencing

LIC were collected at necropsy, snap frozen in liquid nitrogen and shipped on dry ice to the UNC Microbiome Core Facility where 16S rRNA amplicon sequencing DNA isolation was carried out as described (25). Briefly, samples (200 mg) were transferred to sterile 2 ml tubes containing 200 mg of 212-300 μm glass beads (Sigma-Aldrich) and 1.4 ml of Qiagen ASL buffer for bead beating and subsequently incubated at 95°C for 5 minutes. Supernatants were treated with InhibiEx inhibitor adsorption tablets (Qiagen) to remove PCR inhibitors. After a brief centrifugation, supernatants were transferred to a new tube with Qiagen AL buffer containing Proteinase K (600IU/ μl) and incubated at 70°C for 10 minutes. DNA was purified using Zymo-spin columns (Genesee Scientific, Morrisville, NC) and Qiagen buffers AW1 and AW2 as washing agents, and eluted in 10mM Tris (pH 8.0).

Sequencing libraries were prepared from total DNA (12.5 ng) amplified using a combination (4:1) of Universal and *Bifidobacterium*-specific primers targeting the V1-V2 region of the bacterial 16S rRNA gene (54-56). Primers contained overhang adapters for compatibility with the Illumina sequencing platform and sequencing adapters. Master mixes contained 12.5 ng of total DNA, 0.2 μM of each primer and 2x KAPA HiFi HotStart ReadyMix (KAPA Biosystems, Wilmington, MA). Amplicons were purified using the AMPure XP reagent (Beckman Coulter, Indianapolis, IN) and then amplified using a limited cycle PCR program, adding Illumina sequencing adapters and dual-index barcodes (index 1(i7) and index 2(i5)) (Illumina, San Diego, CA) to the amplicon target.

Final libraries were purified, quantified and normalized prior to pooling. The DNA library pool was then denatured with NaOH, diluted with hybridization buffer, and heat denatured before loading on the MiSeq reagent cartridge (Illumina) and on the MiSeq instrument (Illumina). Automated cluster generation and paired–end sequencing with dual reads were performed according to the manufacturer's instructions.

Sequencing data analysis

Multiplexed paired-end fastq files were generated from sequencing data using the Illumina software configureBclToFastq. The paired-end fastqs were then joined into a single multiplexed, single-end fastq using the software tool fastq-join. Demultiplexing and quality filtering was performed on the joined results and quality analysis reports were produced using the FastQC software. Subsequent analyses were performed using the Quantitative Insights Into Microbial Ecology (QIIME v.1.8.0) (57) as described (25, 58). Sequences were clustered into operational taxonomic units (OTU) at 97% similarity threshold using UCLUST (59), and they were aligned in order to build a phylogenetic tree (60). A random selection of 1118 sequences from each sample was used for rarefaction analysis to determine diversity using observed species (S) and phylogenetic diversity (PD) metrics on rarefied OTU tables. Beta diversity and principal coordinates analysis (PCoA) were calculated using unweighted UniFac distances between samples at a depth of 1118 sequences per sample. Taxa of the L6 OTU (genus level) table with a relative abundance of 0.5% or greater and all taxa of the L2 OTU (phylum level) table were compared between groups at PCD0 and PCD7. Alpha diversity was compared in a similar fashion. Spearman's rank correlation coefficients were determined between the

frequencies of T cells in the ileum, blood and spleen of all pigs and taxa of the L6 and L2 OTU tables at PCD0 and PCD7.

Histopathology

Sections of duodenum, jejunum, and ileum were collected, routinely processed, and analyzed as previously described (51). The pathologist, blinded to the animal identification, evaluated villus length, crypt depth, villus-to-crypt ratio, crypt mitotic index, and lamina propria width.

Enteropathy biomarkers

Large intestinal contents collected at necropsy were used for biomarker evaluation using commercial porcine ELISA kits (α-1-antitrypsin, TSZ ELISA, BIOTANG Inc. Lexington, MA; Reg1B, Elabsceince, Wuhan, Hubei, China; myeloperoxidase, MyBioSource, San Diego, CA). Assays were run per manufacturer's instructions.

Statistical analysis

Kruskal-Wallis rank sum test was used for comparisons of rotavirus-specific antibody titers in serum, LIC and SIC, frequencies of IFN-γ producing T cells, enteropathy biomarkers measured in pigs, histopathology, diarrhea duration and score, virus shedding duration and titer, and comparisons of microbiome composition between HGM groups. Fisher's exact test was used for comparisons of percentages of virus shedding and diarrhea. The correlations between T cell frequencies in the ileum, blood and spleen of all pigs, and taxa of the L6 OTU table at PCD0 and PCD7 were determined by Spearman's rank correlation analysis with the Benjamini-Hochberg method for false detection rate. Correlations were considered strongly negative or positive if $\rho<-0.8$ or $\rho>0.8$, respectively. Statistical significance was assessed at $p<0.05$.

Declarations

Ethics approval and consent to participate: Studies were approved by the Office of Human Research Ethics at the University of North Carolina (UNC) at Chapel Hill (#14-1136) and the Universidad Nacional Autónoma de Nicaragua, León (#110). Parents or legal guardians of the infants provided written consent. All animal protocols were approved by the Institutional Animal Care and Use Committee at Virginia Tech (protocol #13-187-CVM).

Consent for publication: not applicable

Availability of data and materials: All data generated or analyzed in this study are included in the published article and its supplementary information files.

Competing interest: The authors declare that they have no competing interests.

Funding: This work was supported by the Bill and Melinda Gates Foundation (www.gatesfoundation.org) Grant # OPP1108188 to LY. A Virginia Tech Graduate Student Assembly Graduate Research and Development Fund Award (Spring 2015) provided financial support for the porcine enteropathy ELISA kits. Erica Twitchell is supported by a Ruth L. Kirschstein Institutional National Research Service Award from the National Institutes of Health. The funding body had no role in the design of the study, or collection, analysis, or interpretation of data, or writing the manuscript.

Author's contributions: LY, ET, CT, KW, HZ, SBD, MAAP, SV, GL, AR, MW, SL, TB, XY, and SSC contributed to the design of the experiment, acquisition of data or analysis and interpretation of data. ET and LY drafted the manuscript. All authors critically reviewed the manuscript. All authors read and approved the final manuscript perform experiments.

Acknowledgements: We thank Dr. Kevin Pelzer, Dr. Sherrie Clark-Deener and all of the other veterinarians who provided veterinary services, and TRACCS staff members for their care of the pigs. Wansuk Choi performed the Benjamini-Hochberg analysis.

References

1. Rotavirus vaccines. WHO position paper - January 2013. Wkly Epidemiol Rec. 2013;88(5):49-64.
2. Tate JE, Burton AH, Boschi-Pinto C, Steele AD, Duque J, Parashar UD, et al. 2008 estimate of worldwide rotavirus-associated mortality in children younger than 5 years before the introduction of universal rotavirus vaccination programmes: a systematic review and meta-analysis. Lancet Infect Dis. 2012;12(2):136-41.
3. Gilmartin AA, Petri WA, Jr. Exploring the role of environmental enteropathy in malnutrition, infant development and oral vaccine response. Philos Trans R Soc Lond B Biol Sci. 2015;370(1671).
4. Valdez Y, Brown EM, Finlay BB. Influence of the microbiota on vaccine effectiveness. Trends Immunol. 2014;35(11):526-37.
5. Armah GE, Sow SO, Breiman RF, Dallas MJ, Tapia MD, Feikin DR, et al. Efficacy of pentavalent rotavirus vaccine against severe rotavirus gastroenteritis in infants in developing countries in sub-Saharan Africa: a randomised, double-blind, placebo-controlled trial. Lancet. 2010;376(9741):606-14.
6. Leshem E, Lopman B, Glass R, Gentsch J, Banyai K, Parashar U, et al. Distribution of rotavirus strains and strain-specific effectiveness of the rotavirus vaccine after its introduction: a systematic review and meta-analysis. Lancet Infect Dis. 2014;14(9):847-56.
7. Zaman K, Dang DA, Victor JC, Shin S, Yunus M, Dallas MJ, et al. Efficacy of pentavalent rotavirus vaccine against severe rotavirus gastroenteritis in infants in developing countries in Asia: a randomised, double-blind, placebo-controlled trial. Lancet. 2010;376(9741):615-23.
8. Becker-Dreps S, Vilchez S, Velasquez D, Moon SS, Hudgens MG, Zambrana LE, et al. Rotavirus-specific IgG antibodies from mothers' serum may inhibit infant immune responses to the pentavalent rotavirus vaccine. Pediatr Infect Dis J. 2015;34(1):115-6.
9. Ali A, Iqbal NT, Sadiq K. Environmental enteropathy. Curr Opin Gastroenterol. 2016;32(1):12-7.
10. Crane RJ, Jones KD, Berkley JA. Environmental enteric dysfunction: an overview. Food Nutr Bull. 2015;36(1 Suppl):S76-87.
11. Naylor C, Lu M, Haque R, Mondal D, Buonomo E, Nayak U, et al. Environmental Enteropathy, Oral Vaccine Failure and Growth Faltering in Infants in Bangladesh. EBioMedicine. 2015;2(11):1759-66.
12. Grzeskowiak L, Collado MC, Mangani C, Maleta K, Laitinen K, Ashorn P, et al. Distinct gut microbiota in southeastern African and northern European infants. J Pediatr Gastroenterol Nutr. 2012;54(6):812-6.
13. Monira S, Nakamura S, Gotoh K, Izutsu K, Watanabe H, Alam NH, et al. Gut microbiota of healthy and malnourished children in bangladesh. Front Microbiol. 2011;2:228.
14. Wang M, Donovan SM. Human microbiota-associated swine: current progress and future opportunities. ILAR J. 2015;56(1):63-73.
15. Ward LA, Rosen BI, Yuan L, Saif LJ. Pathogenesis of an attenuated and a virulent strain of group A human rotavirus in neonatal gnotobiotic pigs. The Journal of general virology. 1996;77 (Pt 7):1431-41.

16. To TL, Ward LA, Yuan L, Saif LJ. Serum and intestinal isotype antibody responses and correlates of protective immunity to human rotavirus in a gnotobiotic pig model of disease. J Gen Virol. 1998;79 (Pt 11):2661-72.
17. Yuan L, Ward LA, Rosen BI, To TL, Saif LJ. Systematic and intestinal antibody-secreting cell responses and correlates of protective immunity to human rotavirus in a gnotobiotic pig model of disease. J Virol. 1996;70(5):3075-83.
18. Yuan L, Wen K, Azevedo MS, Gonzalez AM, Zhang W, Saif LJ. Virus-specific intestinal IFN-gamma producing T cell responses induced by human rotavirus infection and vaccines are correlated with protection against rotavirus diarrhea in gnotobiotic pigs. Vaccine. 2008;26(26):3322-31.
19. Lei S, Samuel H, Twitchell E, Bui T, Ramesh A, Wen K, et al. Enterobacter cloacae inhibits human norovirus infectivity in gnotobiotic pigs. Sci Rep. 2016;6:25017.
20. Wen K, Tin C, Wang H, Yang X, Li G, Giri-Rachman E, et al. Probiotic Lactobacillus rhamnosus GG enhanced Th1 cellular immunity but did not affect antibody responses in a human gut microbiota transplanted neonatal gnotobiotic pig model. PLoS ONE. 2014;9(4):e94504.
21. Zhang H, Wang H, Shepherd M, Wen K, Li G, Yang X, et al. Probiotics and virulent human rotavirus modulate the transplanted human gut microbiota in gnotobiotic pigs. Gut pathogens. 2014;6:39.
22. Wen K, Liu F, Li G, Bai M, Kocher J, Yang X, et al. Lactobacillus rhamnosus GG Dosage Affects the Adjuvanticity and Protection Against Rotavirus Diarrhea in Gnotobiotic Pigs. Journal of pediatric gastroenterology and nutrition. 2015;60(6):834-43.
23. Donowitz JR, Haque R, Kirkpatrick BD, Alam M, Lu M, Kabir M, et al. Small Intestine Bacterial Overgrowth and Environmental Enteropathy in Bangladeshi Children. MBio. 2016;7(1):e02102-15.
24. Peterson KM, Buss J, Easley R, Yang Z, Korpe PS, Niu F, et al. REG1B as a predictor of childhood stunting in Bangladesh and Peru. Am J Clin Nutr. 2013;97(5):1129-33.
25. Becker-Dreps S, Allali I, Monteagudo A, Vilchez S, Hudgens MG, Rogawski ET, et al. Gut Microbiome Composition in Young Nicaraguan Children During Diarrhea Episodes and Recovery. Am J Trop Med Hyg. 2015;93(6):1187-93.
26. Schmidt B, Mulder IE, Musk CC, Aminov RI, Lewis M, Stokes CR, et al. Establishment of normal gut microbiota is compromised under excessive hygiene conditions. PLoS One. 2011;6(12):e28284.
27. Ang L, Arboleya S, Lihua G, Chuihui Y, Nan Q, Suarez M, et al. The establishment of the infant intestinal microbiome is not affected by rotavirus vaccination. Sci Rep. 2014;4:7417.
28. Garcia-Lopez R, Perez-Brocal V, Diez-Domingo J, Moya A. Gut microbiota in children vaccinated with rotavirus vaccine. Pediatr Infect Dis J. 2012;31(12):1300-2.
29. Zhang M, Zhang M, Zhang C, Du H, Wei G, Pang X, et al. Pattern extraction of structural responses of gut microbiota to rotavirus infection via multivariate statistical analysis of clone library data. FEMS Microbiol Ecol. 2009;70(2):21-9.
30. Varyukhina S, Freitas M, Bardin S, Robillard E, Tavan E, Sapin C, et al. Glycan-modifying bacteria-derived soluble factors from Bacteroides thetaiotaomicron and Lactobacillus casei inhibit rotavirus infection in human intestinal cells. Microbes Infect. 2012;14(3):273-8.

31. Robinson CM, Jesudhasan PR, Pfeiffer JK. Bacterial lipopolysaccharide binding enhances virion stability and promotes environmental fitness of an enteric virus. Cell Host Microbe. 2014;15(1):36-46.
32. Kandasamy S, Vlasova AN, Fischer D, Kumar A, Chattha KS, Rauf A, et al. Differential Effects of Escherichia coli Nissle and Lactobacillus rhamnosus Strain GG on Human Rotavirus Binding, Infection, and B Cell Immunity. J Immunol. 2016;196(4):1780-9.
33. Huda MN, Lewis Z, Kalanetra KM, Rashid M, Ahmad SM, Raqib R, et al. Stool microbiota and vaccine responses of infants. Pediatrics. 2014;134(2):e362-72.
34. Brown EM, Wlodarska M, Willing BP, Vonaesch P, Han J, Reynolds LA, et al. Diet and specific microbial exposure trigger features of environmental enteropathy in a novel murine model. Nat Commun. 2015;6:7806.
35. Maier EA, Weage KJ, Guedes MM, Denson LA, McNeal MM, Bernstein DI, et al. Protein-energy malnutrition alters IgA responses to rotavirus vaccination and infection but does not impair vaccine efficacy in mice. Vaccine. 2013;32(1):48-53.
36. Yuan L, Saif LJ. Induction of mucosal immune responses and protection against enteric viruses: rotavirus infection of gnotobiotic pigs as a model. Veterinary immunology and immunopathology. 2002;87(3-4):147-60.
37. Becker-Dreps SV, S.; Bucardo, F.; Twitchell, E.; Choi, W.S.; Hudgens, M.G.; Perez, J., Yuan, L. The association between fecal biomarkers of environmental enteropathy and rotavirus vaccine response in Nicaraguan infants. submitted for publication.
38. George CM, Oldja L, Biswas S, Perin J, Lee GO, Kosek M, et al. Geophagy is associated with environmental enteropathy and stunting in children in rural Bangladesh. Am J Trop Med Hyg. 2015;92(6):1117-24.
39. Kosek M, Haque R, Lima A, Babji S, Shrestha S, Qureshi S, et al. Fecal markers of intestinal inflammation and permeability associated with the subsequent acquisition of linear growth deficits in infants. Am J Trop Med Hyg. 2013;88(2):390-6.
40. Wei H, Shen J, Pang X, Ding D, Zhang Y, Zhang B, et al. Fatal infection in human flora-associated piglets caused by the opportunistic pathogen Klebsiella pneumoniae from an apparently healthy human donor. J Vet Med Sci. 2008;70(7):715-7.
41. Brisse S, Verhoef J. Phylogenetic diversity of Klebsiella pneumoniae and Klebsiella oxytoca clinical isolates revealed by randomly amplified polymorphic DNA, gyrA and parC genes sequencing and automated ribotyping. Int J Syst Evol Microbiol. 2001;51(Pt 3):915-24.
42. Chander Y, Ramakrishnan MA, Jindal N, Hanson K, Goyal S. Differentiation of Klebsiella pneumoniae and K. oxytoca by multiplex polymerase chain reaction. Intern J Appl Res Vet Med. 2011;9(2):138-42.
43. Gu Z, Zhu H, Rodriguez A, Mhaissen M, Schultz-Cherry S, Adderson E, et al. Comparative Evaluation of Broad-Panel PCR Assays for the Detection of Gastrointestinal Pathogens in Pediatric Oncology Patients. J Mol Diagn. 2015;17(6):715-21.
44. Jothikumar N, Cromeans TL, Hill VR, Lu X, Sobsey MD, Erdman DD. Quantitative real-time PCR assays for detection of human adenoviruses and identification of serotypes 40 and 41. Appl Environ Microbiol. 2005;71(6):3131-6.

45. Oka T, Katayama K, Hansman GS, Kageyama T, Ogawa S, Wu FT, et al. Detection of human sapovirus by real-time reverse transcription-polymerase chain reaction. J Med Virol. 2006;78(10):1347-53.
46. Stals A, Baert L, Botteldoorn N, Werbrouck H, Herman L, Uyttendaele M, et al. Multiplex real-time RT-PCR for simultaneous detection of GI/GII noroviruses and murine norovirus 1. J Virol Methods. 2009;161(2):247-53.
47. Meyer RC, Bohl EH, Kohler EM. Procurement and Maintenance of Germ-Free Seine for Microbiological Investigations. Appl Microbiol. 1964;12:295-300.
48. Nguyen TV, Yuan L, Azevedo MS, Jeong KI, Gonzalez AM, Iosef C, et al. Low titer maternal antibodies can both enhance and suppress B cell responses to a combined live attenuated human rotavirus and VLP-ISCOM vaccine. Vaccine. 2006;24(13):2302-16.
49. Parreno V, Hodgins DC, de Arriba L, Kang SY, Yuan L, Ward LA, et al. Serum and intestinal isotype antibody responses to Wa human rotavirus in gnotobiotic pigs are modulated by maternal antibodies. J Gen Virol. 1999;80 (Pt 6):1417-28.
50. Hodgins DC, Kang SY, deArriba L, Parreno V, Ward LA, Yuan L, et al. Effects of maternal antibodies on protection and development of antibody responses to human rotavirus in gnotobiotic pigs. J Virol. 1999;73(1):186-97.
51. Yang X, Twitchell E, Li G, Wen K, Weiss M, Kocher J, et al. High protective efficacy of rice bran against human rotavirus diarrhea via enhancing probiotic growth, gut barrier function, and innate immunity. Sci Rep. 2015;5:15004.
52. Liu F, Li G, Wen K, Bui T, Cao D, Zhang Y, et al. Porcine small intestinal epithelial cell line (IPEC-J2) of rotavirus infection as a new model for the study of innate immune responses to rotaviruses and probiotics. Viral Immunol. 2010;23(2):135-49.
53. Lei S, Ryu J, Wen K, Twitchell E, Bui T, Ramesh A, et al. Increased and prolonged human norovirus infection in RAG2/IL2RG deficient gnotobiotic pigs with severe combined immunodeficiency. Sci Rep. 2016;6:25222.
54. Edwards U, Rogall T, Blocker H, Emde M, Bottger EC. Isolation and direct complete nucleotide determination of entire genes. Characterization of a gene coding for 16S ribosomal RNA. Nucleic Acids Res. 1989;17(19):7843-53.
55. Fierer N, Hamady M, Lauber CL, Knight R. The influence of sex, handedness, and washing on the diversity of hand surface bacteria. Proc Natl Acad Sci U S A. 2008;105(46):17994-9.
56. Martinez I, Kim J, Duffy PR, Schlegel VL, Walter J. Resistant starches types 2 and 4 have differential effects on the composition of the fecal microbiota in human subjects. PLoS One. 2010;5(11):e15046.
57. Caporaso JG, Kuczynski J, Stombaugh J, Bittinger K, Bushman FD, Costello EK, et al. QIIME allows analysis of high-throughput community sequencing data. Nat Methods. 2010;7(5):335-6.
58. Allali I, Delgado S, Marron PI, Astudillo A, Yeh JJ, Ghazal H, et al. Gut microbiome compositional and functional differences between tumor and non-tumor adjacent tissues from cohorts from the US and Spain. Gut Microbes. 2015;6(3):161-72.
59. Edgar RC. Search and clustering orders of magnitude faster than BLAST. Bioinformatics. 2010;26(19):2460-1.
60. Price MN, Dehal PS, Arkin AP. FastTree 2--approximately maximum-likelihood trees for large alignments. PLoS One. 2010;5(3):e9490.

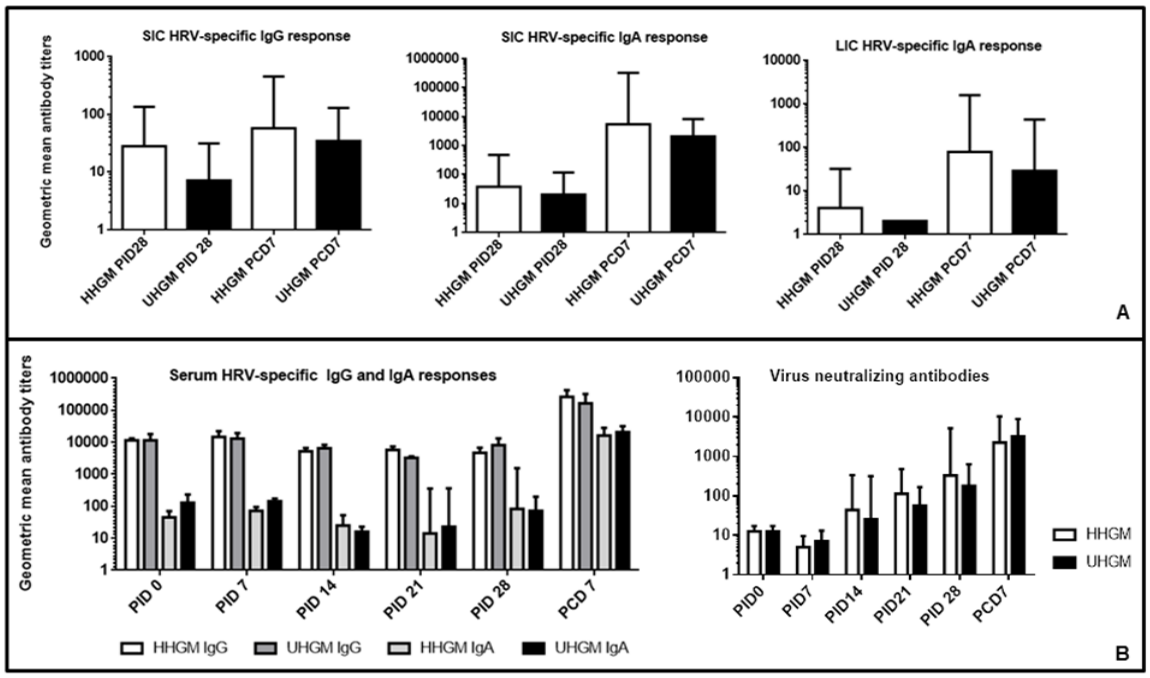

Figure 1. Rotavirus-specific antibody responses.

Rotavirus-specific antibody responses. Rotavirus-specific IgG and IgA antibody responses in small and large intestinal contents (A) and IgG, IgA and virus neutralizing antibody response in serum (B). Error bars are represented as standard error of mean. Kruskal-Wallis rank sum test was used for comparisons. There are no significant differences between the groups. SIC, small intestinal contents; LIC, large intestinal contents; PID, post-inoculation day; PCD, post-challenge day.

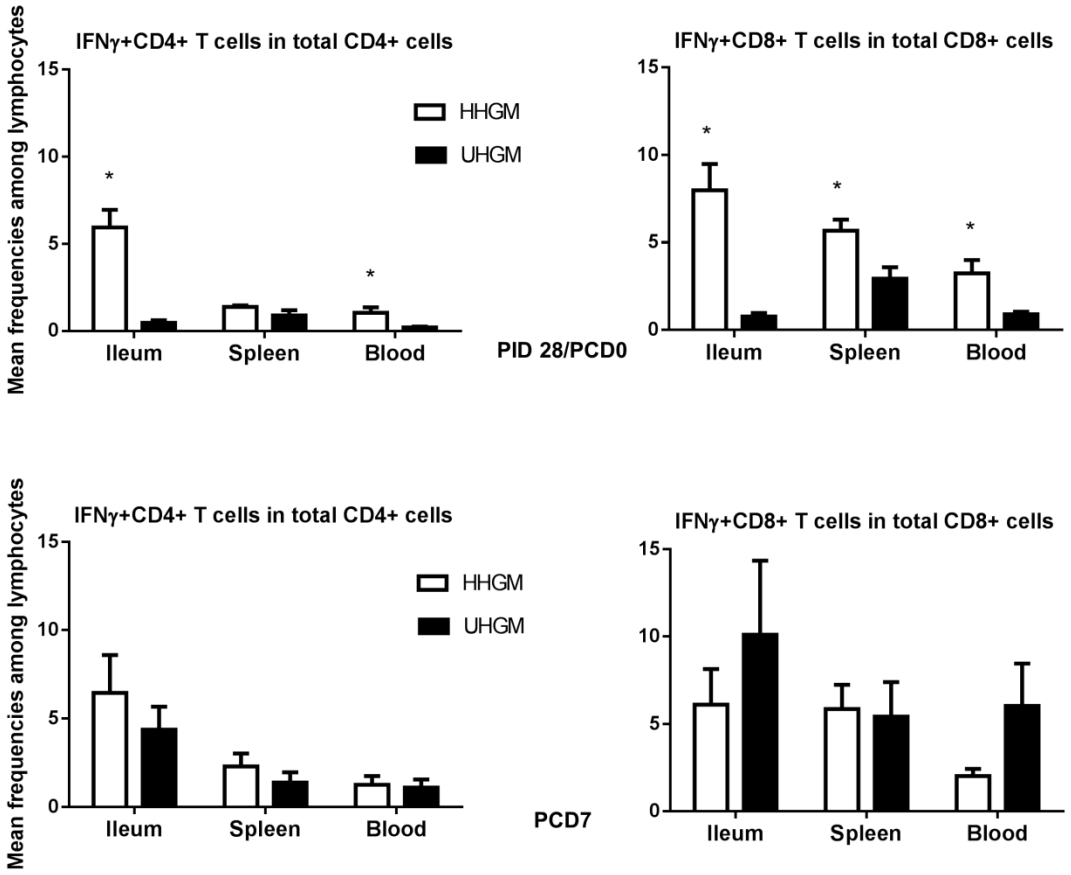

Figure 2. Frequencies of IFN-γ producing CD8+ and CD4+ T cells.

Frequencies of IFN-γ producing CD8+ and CD4+ T cells among total CD3+CD8+ and CD3+CD4+ cells on PID28/PCD0 (upper panel) and PCD7 (lower panel) in ileum, spleen and blood of HHGM verses UHGM colonized pigs. Error bars indicate standard errors of the mean. Asterisks indicate significant differences when compared to PM25 pigs (Kruskal-Wallis rank sum test, $P<0.05$; $n=5$-7).

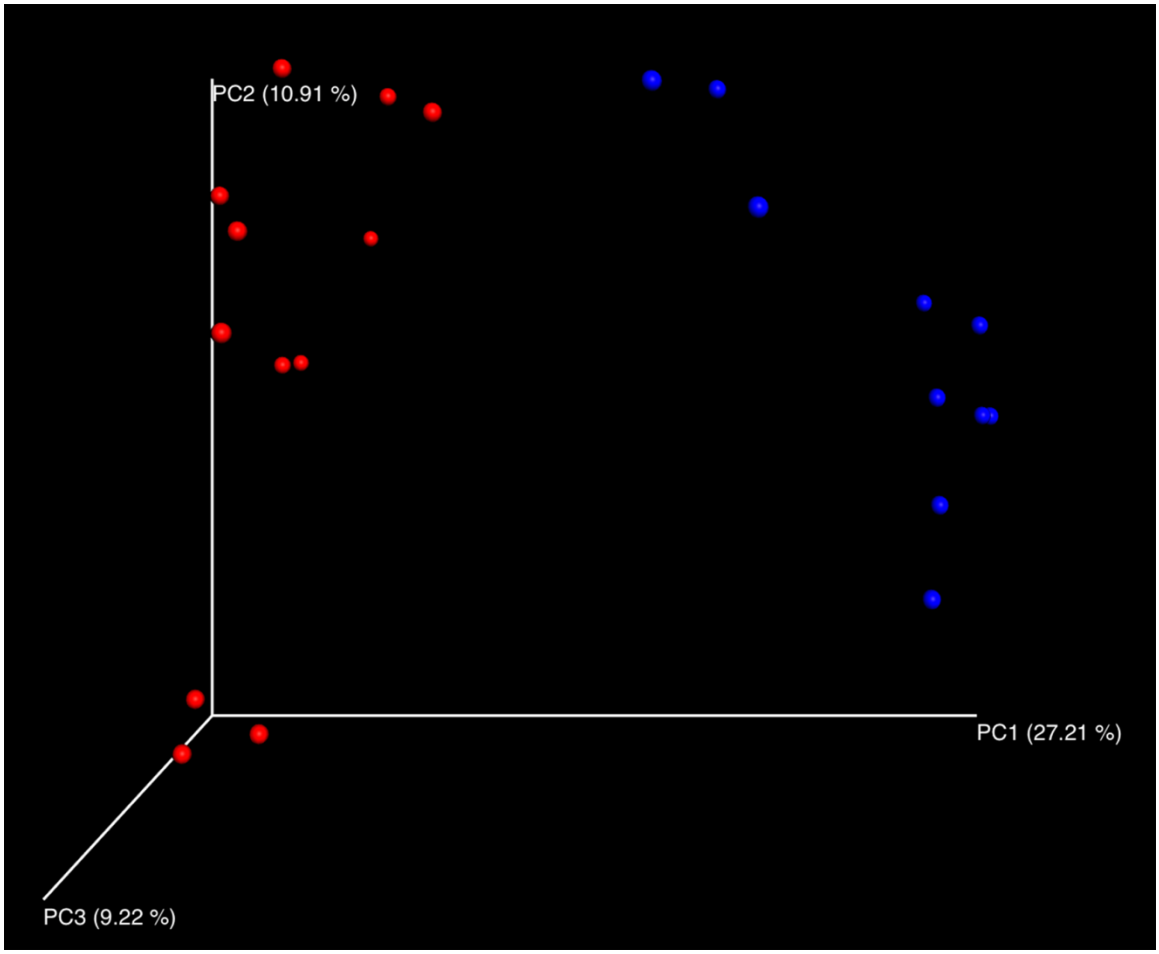

Figure 3. PCoA plot of the microbial communities in the large intestinal contents of Gn pigs.

PCoA plot of the microbial communities in the large intestinal contents of Gn pigs. Communities were plotted based on unweighted UniFrac. Blue dots represent HHGM and red dots represent UHGM.

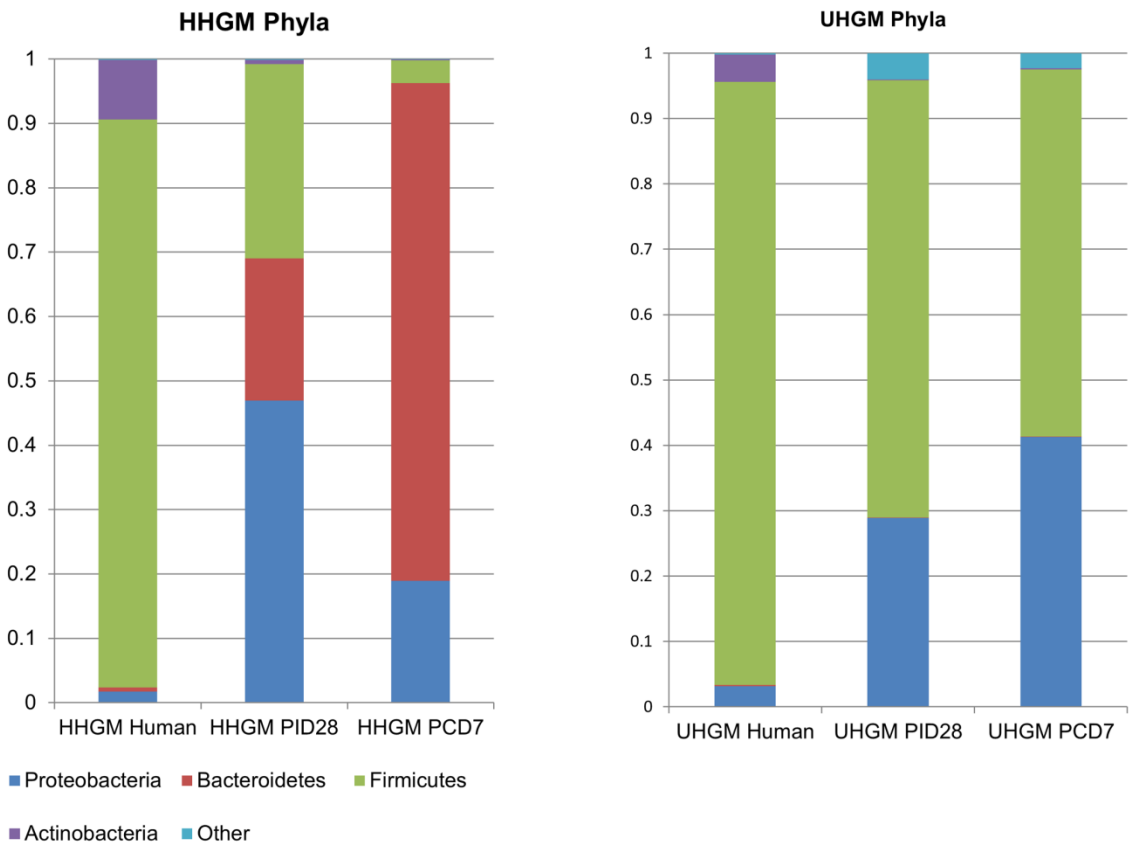

Figure 4. Mean relative abundance of phyla in the microbial community of large intestinal contents.

Mean relative abundance of phyla in the microbial community of large intestinal contents of HGM-colonized Gn pigs before HRV challenge (PID28/PCD0) and postchallenge (PCD7) compared to infant HGM. Numbers represent the single stool sample from infant HGM and averages for the pig groups (n=5-6).

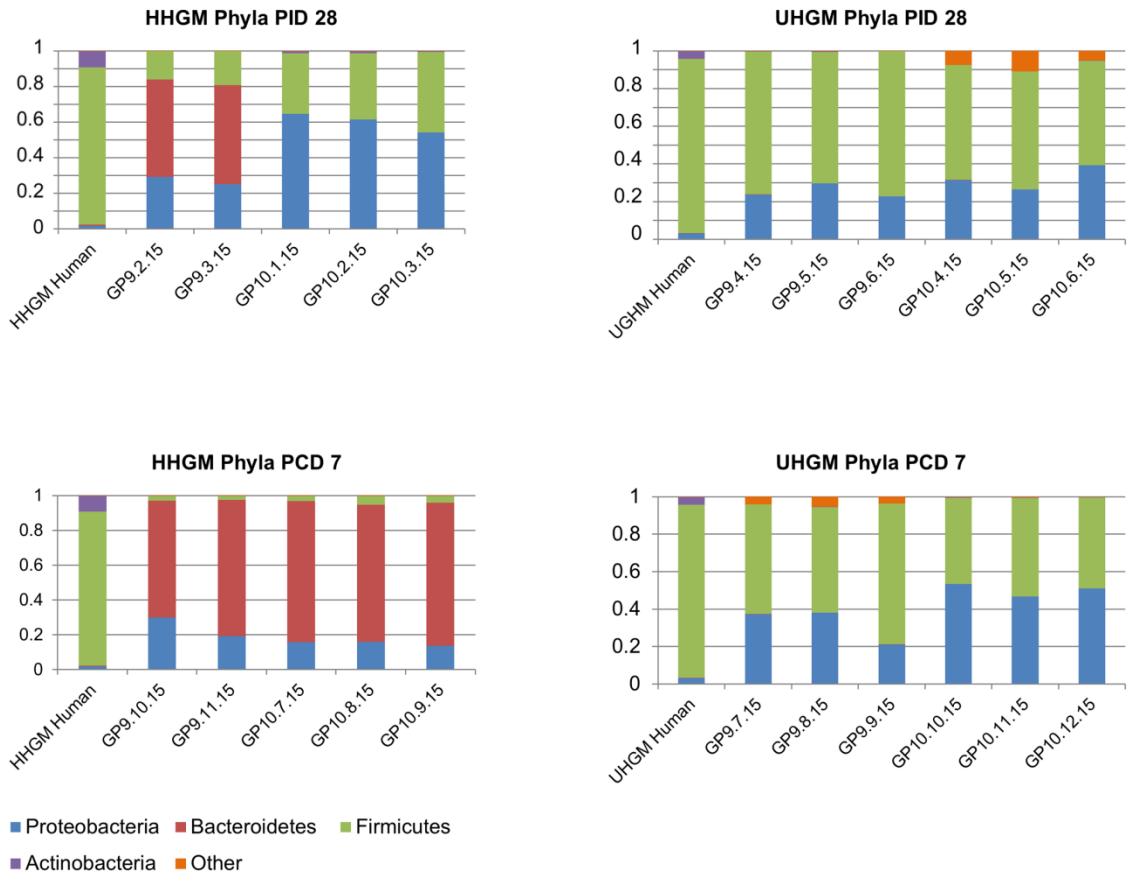

Figure 5. Relative abundance of phyla in the microbial community of large intestinal contents of individual pigs.

Relative abundance of phyla in the microbial community of large intestinal contents of individual HGM-colonized Gn pigs before VirHRV challenge (PID28/PCD0) and postchallenge (PCD7). The HHGM human sample is included for reference in each panel. HHGM human is the sample from child SV14 and UHGM human is the sample from child PM25.

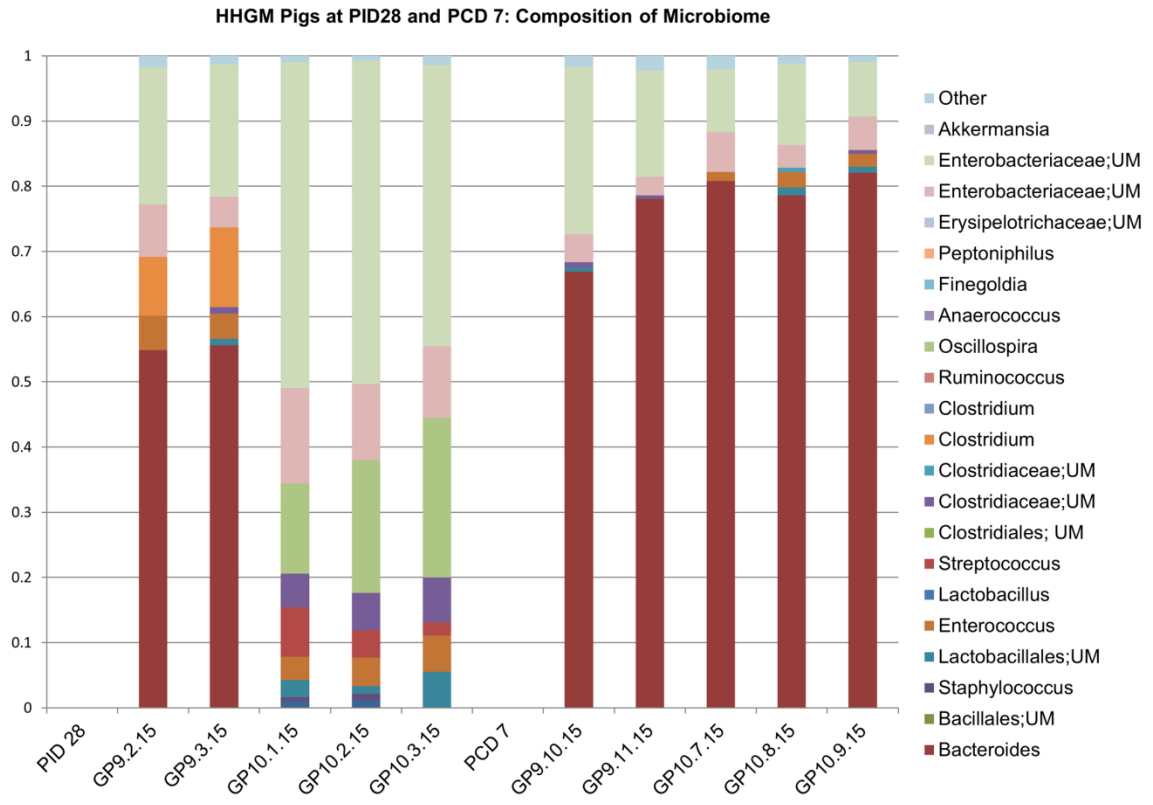

Figure 6. Relative abundance of specified bacterial taxa in the microbial community of large intestinal contents in HHGM pigs.

Relative abundance of order, family, or genera of bacteria in the large intestinal contents at specified time points in HHGM pigs. Bars to the right of PID 28 are pigs euthanized on PID 28. Bars to the right of PCD 7 are pigs euthanized on PCD 7.

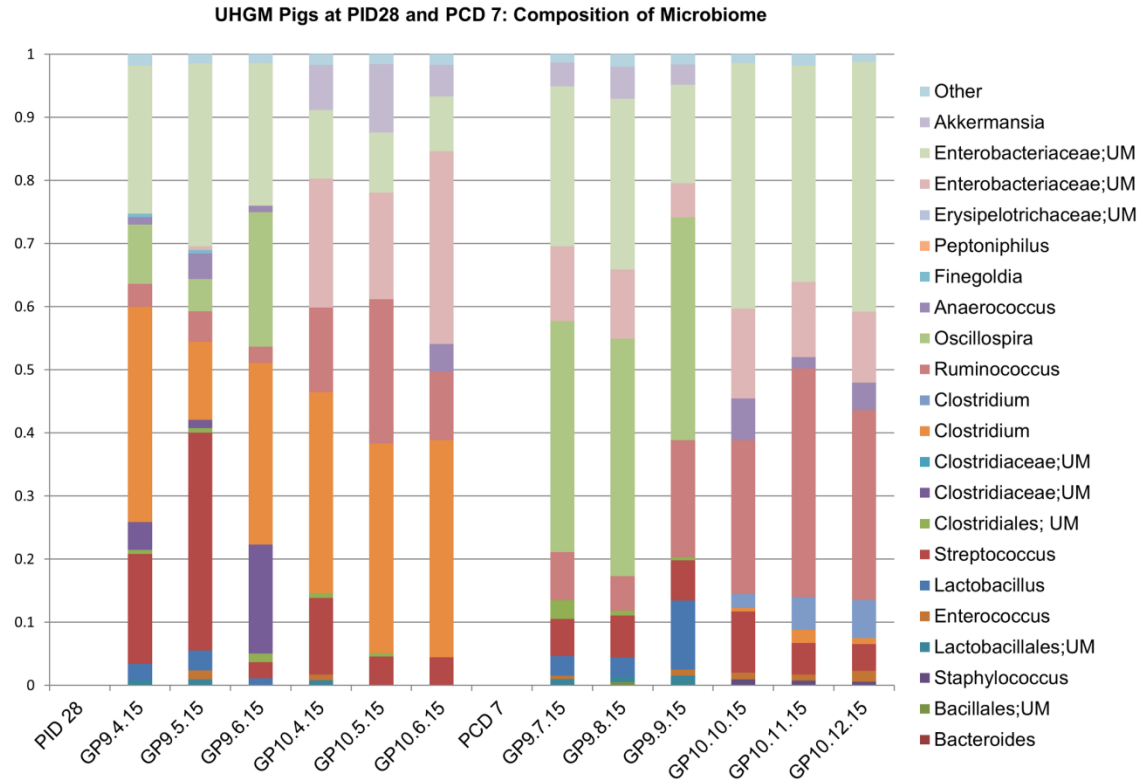

Figure 7. Relative abundance of specified bacterial taxa in the microbial community of large intestinal contents in UHGM pigs.

Relative abundance of order, family, or genera of bacteria in the large intestinal contents at specified time points in UHGM pigs. Bars to the right of PID 28 are pigs euthanized on PID 28. Bars to the right of PCD 7 are pigs euthanized on PCD 7.

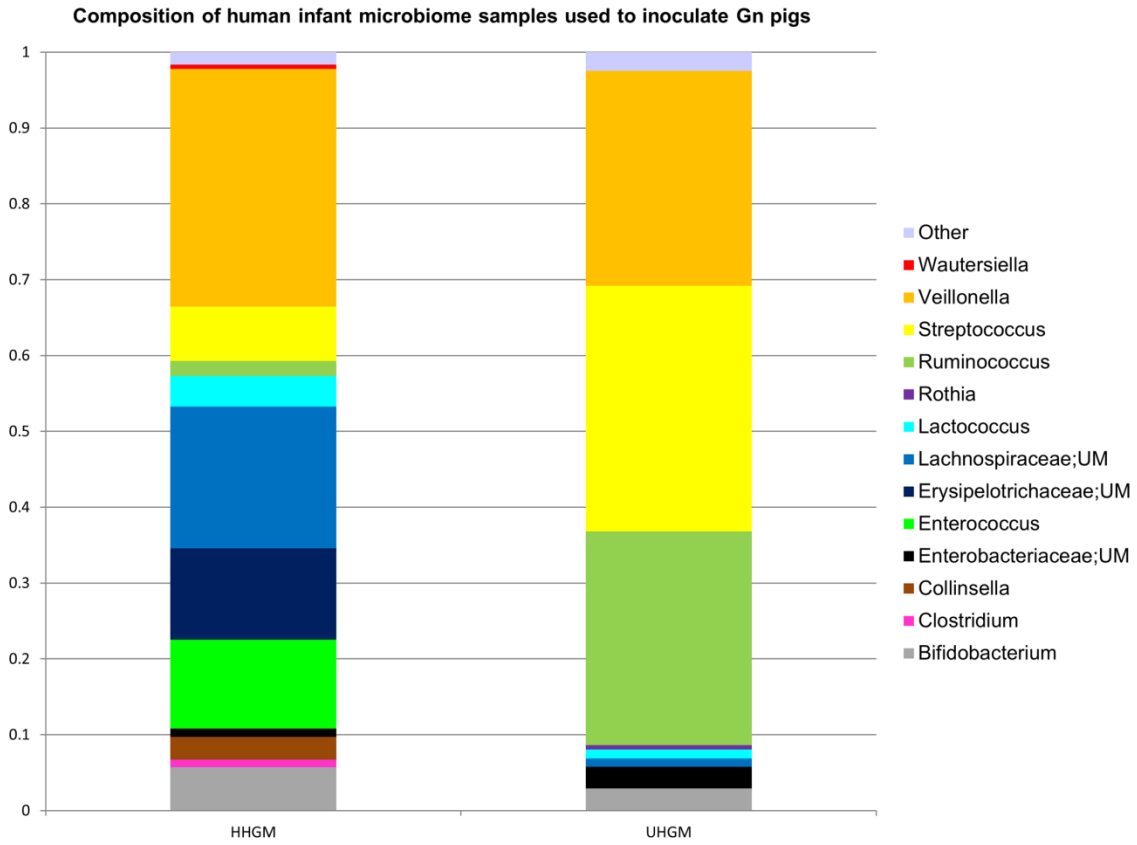

Figure 8. Composition of human infant microbiome samples used to inoculate Gn pigs.

UM indicates unclassified member. Relative abundance is on the y-axis.

Table 1. Clinical signs and rotavirus fecal shedding in Gn pigs after VirHRV challenge

Group	N	Clinical signs				Fecal virus shedding (by CCIF and/or ELISA)			
		% with diarrhea [a*]	Mean days to onset [d**]	Mean duration days [**]	Mean cumulative score [c**]	% shedding virus [*]	Mean days to onset [d**]	Mean duration days [**]	Mean peak titer (FFU/ml)
HHGM	7	57.1	4.3 (0.23[b])	1.3 (0.57[b])	7.7 (0.77[b])	42.85*	1.7 (0.2[b])	1.6 (0.7[b])	657.4
UHGM	6	83.3	2.3 (1.1)	2.0 (0.89)	11.2(1.2)	100*	2.4 (0.3)	3.0 (0.63)	1683.7

[a] Pigs with daily fecal scores of ≥2 were considered diarrheic. Fecal consistency was scored as follows: 0, normal; 1, pasty; 2, semiliquid; and 3, liquid.

[b] Standard error of the mean.

[c] Mean cumulative score calculation included all the pigs in each groups.

[d] In the groups where some but not all pigs had diarrhea or shedding, the onset of diarrhea or shedding for non-diarrheic/shedding pigs was designated as 8 for calculating the mean days to onset

[e] For days of diarrhea and virus shedding, if no diarrhea or virus shedding until the euthanasia day (PCD7), the duration days were recorded as 0.

[*] Fisher's exact test was used for comparisons. Asterisk indicate significant differences among groups (n=6-7; $p<0.05$)

**Kruskal-Wallis rank sum test was used for comparisons. No statistically significant differences were observed between the groups.

ELISA, enzyme-linked immunosorbent assay; CCIF, cell culture immunofluorescent assay; FFU, fluorescence forming unit

Table 2. Mean alpha diversity parameters in gut microbiome of HGM colonized Gn pigs

	Comparison between time points				Comparison between groups		
HHGM	PID28	PCD7	p**	PID28	HHGM	UHGM	p
Shannon Index	2.366	1.236	0.009	Shannon Index	2.366	2.743	0.006
Phylogenetic Diversity	6.806	6.108	0.016	Phylogenetic Diversity	6.806	6.580	0.855
Observed Species	92.460	65.180	0.009	Observed Species	92.460	90.550	0.855
Chao 1	168.399	125.946	0.009	Chao 1	168.399	189.092	0.201
UHGM	PID28	PCD7	p	PCD7	HHGM	UHGM	p
Shannon Index	2.743	2.780	0.749	Shannon Index	1.236	2.780	0.006
Phylogenetic Diversity	6.580	6.988	0.262	Phylogenetic Diversity	6.108	6.988	0.045
Observed Species	90.550	102.583	0.173	Observed Species	65.180	102.583	0.006
Chao 1	189.092	206.175	0.631	Chao 1	125.946	206.175	0.006

**Kruskal-Wallis rank sum test was used for comparisons. $P < 0.05$ is considered significant

Table 3. Spearman's rank correlation coefficients between specified OTUs and rotavirus-specific IFN-γ+CD8+ or IFN-γ+CD4+ T cells among all Gn pigs

Positive Correlations	OTU	Tissue	T cell type	ρ	p-value	adj. p-value
PCD0	*Collinsella*	Ileum	CD8+	0.91	<0.01	0.001
	Collinsella	Blood	CD8+	0.83	<0.01	0.016
	Collinsella	Blood	CD4+	0.89	<0.01	0.002
PCD7	Clostridiales (unclassified)	Ileum	CD8+	0.89	<0.01	0.002
	Mycoplasmataceae (unclassified)	Ileum	CD8+	0.80	0.01	0.021
Negative Correlations	**OTU**	**Tissue**	**T cell type**	**ρ**	**p-value**	**adj. p-value**
PCD0	*Clostridium*	Ileum	CD8+	-0.90	<0.01	0.002
	Anaerococcus	Ileum	CD8+	-0.88	<0.01	0.002
	Propionibacterium	Blood	CD8+	-0.88	<0.01	0.002
	Bacillales (unclassified)	Blood	CD8+	-0.87	<0.01	0.003
	Blautia	Blood	CD8+	-0.81	<0.01	0.009
	Clostridium	Ileum	CD4+	-0.83	<0.01	0.013
	Anaerococcus	Ileum	CD4+	-0.86	<0.01	0.006
	Clostridiales (unclassified)	Blood	CD4+	-0.89	<0.01	<0.01
	Clostridiales (unclassified)	Blood	CD4+	-0.82	<0.01	0.014
PCD7	*Anaerococcus*	Ileum	CD8+	-0.84	<0.01	0.010
	Anaerococcus	Spleen	CD8+	-0.83	<0.01	0.016
	Anaerococcus	Spleen	CD4+	-0.87	<0.01	0.005
	Staphylococcus	Spleen	CD4+	-0.81	<0.01	0.020

Table 4. Characterization of HGM samples used for oral inoculation of Gn pigs

	SV14 (healthy gut)	PM25 (unhealthy gut)
Enteropathy Score	4	11
Myeloperoxidase	0.37 ug/ml	2.08 ug/ml
α-1-antitrypsin	22.9 ug/ml	141.4 ug/ml
Neopterin	74.7 nmol/l	412.4 nmol/l
Calprotectin	148.5 ug/g	220.6 ug/g
Pre-vaccination IgA titer	1:20	1:50
Post-vaccination IgA titer	1:3200	1:100
Fold increase in IgA titer	160	2
Phylogenetic diversity	7.8	5.7
Shannon Index	4	3.3
Observed Species	107.4	67.3

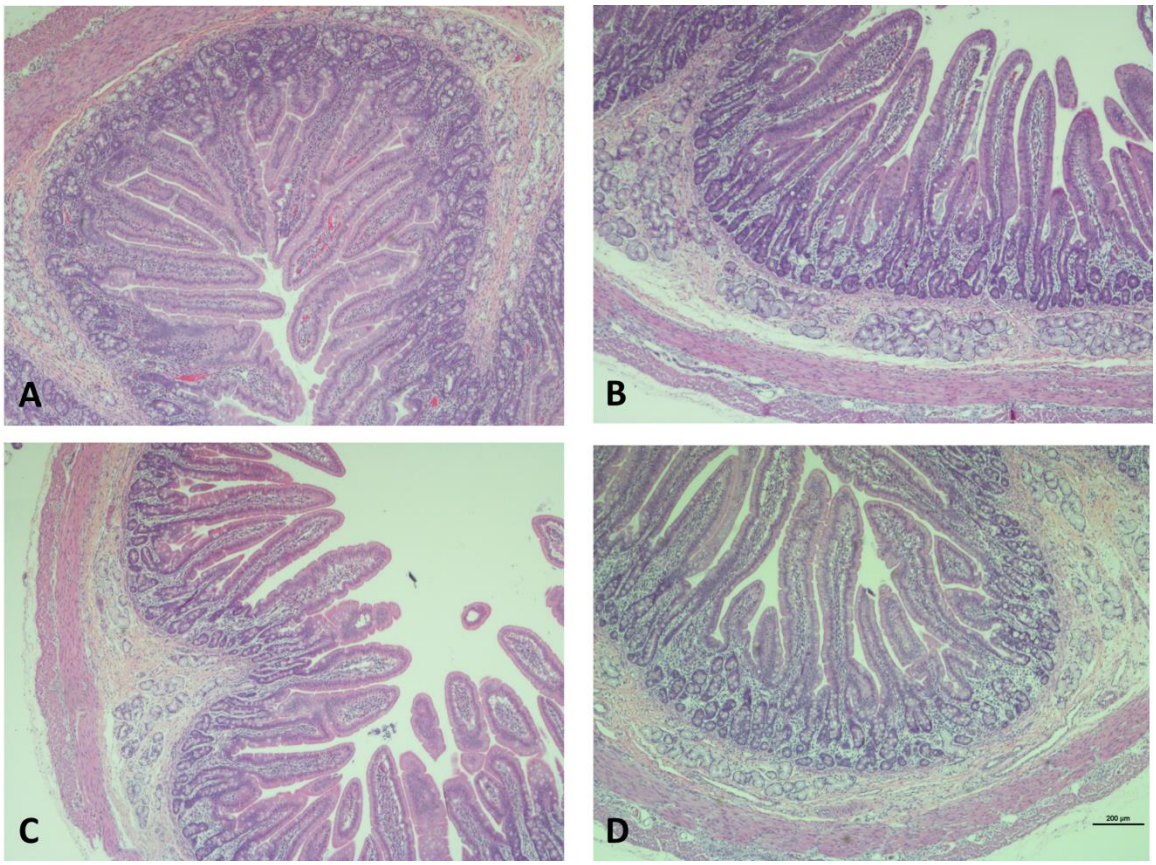

Supplemental Figure 1. Duodenum Histopathology

Representative photomicrographs of duodenum sections from a pig in each group at each time point. A. HHGM PID 28, B. HHGM PCD 7, C. UHGM PID28, D. UHGM PCD7. There are no significant histologic differences between the groups. Scale bar is 200 um.

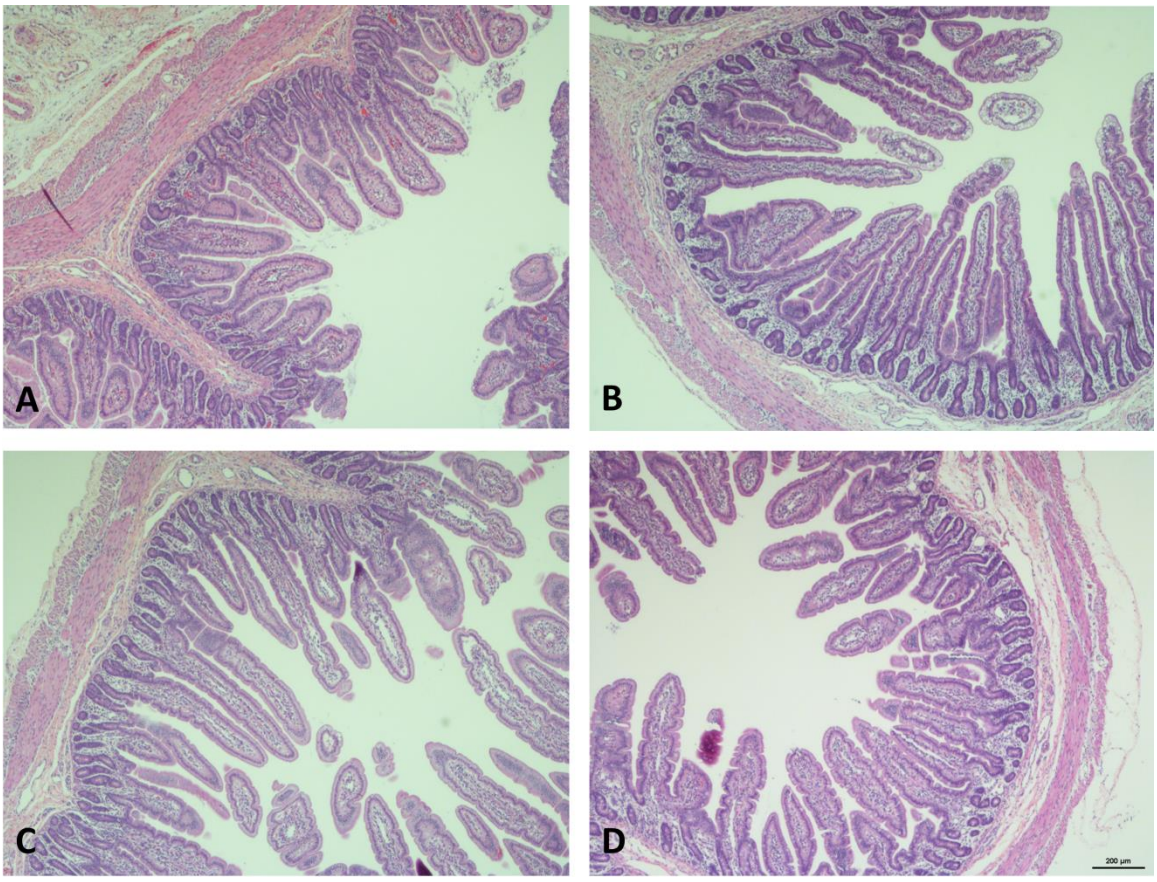

Supplemental Figure 2. Jejunum Histology

Representative photomicrographs of jejunum sections from a pig in each group at each time point. A. HHGM PID 28, B. HHGM PCD 7, C. UHGM PID28, D. UHGM PCD7. There are no significant histologic differences between the groups. Scale bar is 200 um.

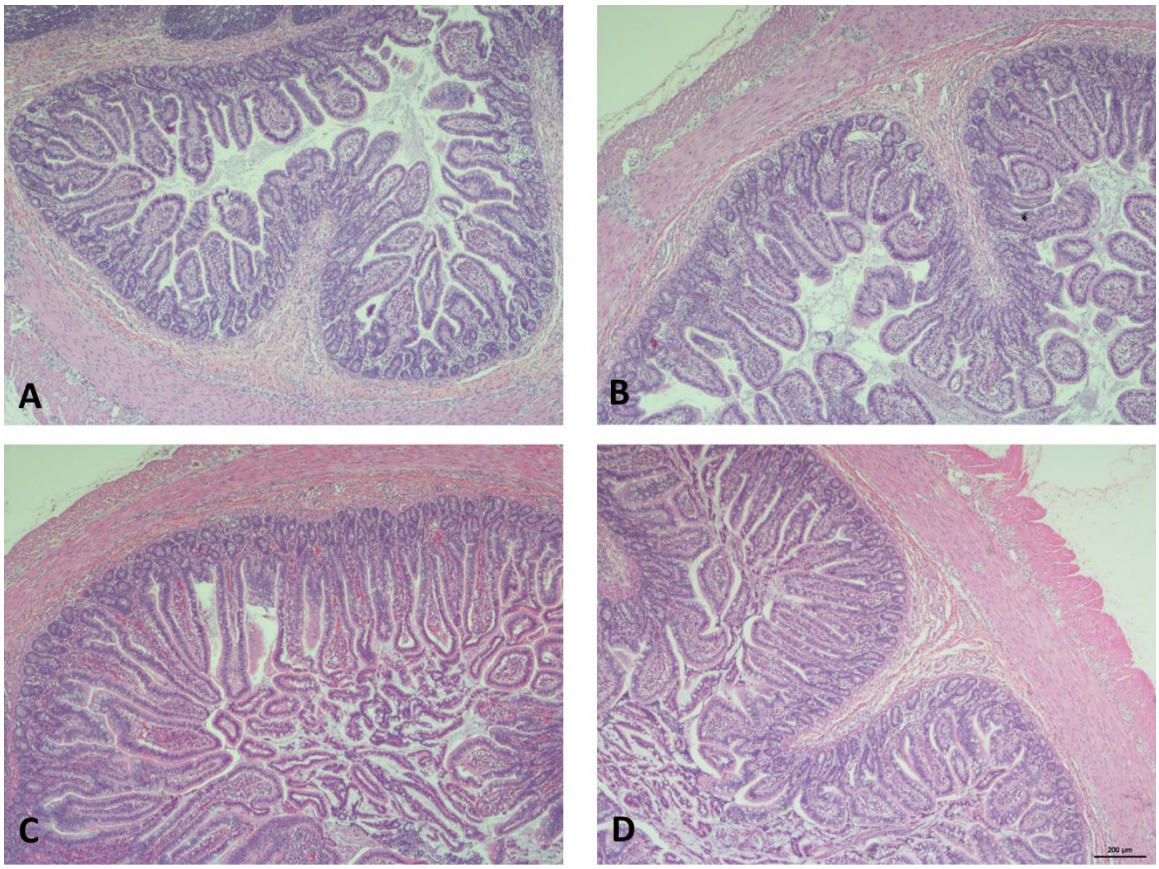

Supplemental Figure 3. Ileum Histopathology

Representative photomicrographs of ileum sections from a pig in each group at each time point. There are no significant histologic differences between the groups. A. HHGM PID 28, B. HHGM PCD 7, C. UHGM PID28, D. UHGM PCD7. Scale bar is 200 um.

Supplemental Table 1: Experimental design for Gn pig study

Experimental design for Gn pig study	
Activity	**Date**
Derivation of Gn pigs	PPD0*
Intraperitoneal injection of normal swine serum to provide baseline passive protection (60ml/pig)	PPD0 or PPD1
Sterility test	PPD3
Oral inoculation with HGM SV14 or PM25	PPD5,6,7
Bleeding for detection of serum antibody by ELISA	Weekly, starting PID0
Oral vaccination with attenuated HRV Wa vaccine (AttHRV 5X10^7 fluorescence forming unit [FFU])	PID0, PID10, PID20**
Oral challenge with virulent HRV Wa (G1P1A[8], 1X10^5 FFU)	PID 28 (PCD0)
Record daily fecal consistency scores	PCD0-7***
Rectal swabs for virus shedding (CCIF, ELISA)	PCD0-7
Euthanasia (with one day variation around the specified dates)	PID28 or PCD7

*Postpartum day (PPD), **Post-inoculation day (PID), ***Post-challenge day (PCD)

Supplemental Table 2: Mean concentration of specified enteropathy biomarkers in large intestinal contents on PID28 and PCD7.

Group	α-1-antitrypsin ug/ml	Myeloperoxidase ug/ml	REG1B ng/ml
HHGM PID28	18.01	0.173	3.61
HHGM PCD7	11.57	0.117	2.32
UHGM PID28	18.89	0.13	3.78
UHGM PCD7	14.97	0.117	3.00

Supplemental Table 3. Small intestinal histopathology. Mean measurements per group for specified parameter and tissue. V:C is the villous to crypt ratio. Mitotic index was determined by counting mitotic figures in 50 crypts. Measurements are in mm.

Group	Tissue	Villus length	Crypt depth	V:C	Lamina propria width	Mitotic index
PID28						
HHGM	duodenum	0.56	0.23	2.45	0.05	0.36
UHGM	duodenum	0.51	0.26	2.03	0.04	0.25
HHGM	jejunum	0.54	0.24	2.24	0.04	0.54
UHGM	jejunum	0.5	0.17	2.98	0.06	0.41
HHGM	ileum	0.3	0.15	2.02	0.05	0.37
UHGM	ileum	0.3	0.16	1.95	0.05	0.42
PCD7						
HHGM	duodenum	0.54	0.27	2.03	0.04	0.27
UHGM	duodenum	0.64	0.24	2.7	0.04	0.3
HHGM	jejunum	0.54	0.18	2.98	0.06	0.44
UHGM	jejunum	0.52	0.18	2.34	0.07	0.53
HHGM	ileum	0.35	0.16	2.15	0.05	0.27
UHGM	ileum	0.35	0.18	2.07	0.05	0.29

Supplemental Table 4. Weights (in kg) of Gn pigs during the study.

Inoculum	Pig ID	PID0	PID7	PID14	PID21	PID 28	PCD 7
HHGM	Gp 9-2-15	2	2.2	3	4	5	.
	Gp 9-3-15	1.5	1.9	2.6	3.1	4	.
	Gp 10-1-15	2	2.2	3	3.8	4.9	.
	Gp 10-2-15	1.8	2	2.8	3.7	5	.
	Gp 10-3-15	1.9	2.1	2.9	3.8	5.2	.
	Gp 6-1-15	1.6	1.8	2.5	3.4	4.1	5
	Gp 6-2-15	1.5	1.8	2.2	3	4	4.4
	Gp 9-10-15	1.4	2	2.6	3.2	4	5.4
	Gp 9-11-15	1.7	2.2	3	3.9	4.9	5.9
	Gp 10-7-15	1.9	2.2	3	3.6	4.4	5.1
	Gp 10-8-15	2	2.1	3	3.8	4.8	5.4
	Gp 10-9-15	1.9	2	2.9	3.6	5	5.2
	Ave	1.7667	2.0417	2.7917	3.575	4.6083	5.2
	SD	0.2188	0.1505	0.261	0.3279	0.4699	0.4583
	SEM	0.0632	0.0434	0.0753	0.0946	0.1357	0.1732
UHGM	Gp 9-4-15	1.8	1.8	2.5	3.2	4.2	.
	Gp 9-5-15	1.8	1.8	2.5	3.1	4	.
	Gp 9-6-15	1.5	2.1	2.7	3.2	4	.
	Gp 10-4-15	1.9	2.1	2.8	3.8	4.4	.
	Gp 10-5-15	1.9	2	2.4	3.6	4.6	.
	Gp 10-6-15	2.1	2.4	3	4	5.1	.
	Gp 9-7-15	1.2	1.7	2.4	3.4	4	4.8
	Gp 9-8-15	1.2	1.8	2.4	3.2	4.2	4.5
	Gp 9-9-15	1	1.6	2.3	3	4	4.3
	Gp 10-10-15	2	2.5	3.2	4.2	5.1	5.5
	Gp 10-11-15	2	2.2	2.9	3.8	5	5.3
	Gp 10-12-15	2.2	3	3.3	4.2	5.3	5.8
	Ave	1.717	2.083	4.95	3.558	4.492	5.033
	SD	0.395	0.4	7.895	0.434	0.505	0.592
	SEM	0.114	0.115	2.279	0.125	0.146	0.242

Chapter 3 Human gut microbiota enhances human norovirus infection

Shaohua Lei1,+, Erica L Twitchell1,+, Jiyoung Lee2, Ashwin Ramesh1, Tammy Bui1, Elizabeth Majette1, Christine M Tin1,3, Sylvia Becker-Dreps4, Roger Avery1, Xi Jiang5, Song Li2, Lijuan Yuan1*

1 Department of Biomedical Sciences and Pathobiology, Virginia-Maryland College of Veterinary Medicine, Virginia Tech, Blacksburg, VA 24061, USA.
2 Department of Crop & Soil Environmental Sciences, College of Agriculture and Life Sciences, Virginia Tech, Blacksburg, VA 24061, USA.
3 Caliciviruses Section, Laboratory of Infectious Diseases, National Institute of Allergy and Infectious Diseases, National Institutes of Health, Bethesda, MD 20894, USA
4 Department of Family Medicine, School of Medicine, University of North Carolina at Chapel Hill, Chapel Hill, NC 27599, USA.
5 Division of Infectious Diseases, Cincinnati Children's Hospital Medical Center, Cincinnati, OH 45229, USA

¶ ǂThese authors contributed equally to this work.
* Correspondence and requests for materials should be addressed to L.Y. (email: lyuan@vt.edu).

Manuscript in preparation for submission.

Abstract

Human noroviruses are a leading cause of gastroenteritis worldwide in all age groups. In this study gnotobiotic pigs were used to demonstrate the influence of human gut microbiota on human norovirus infection. Clinical signs, viral shedding, viral distribution, and transcriptome were analyzed. Viral shedding and duration were greater in HGM+HuNoV pigs compared to HuNoVpigs. HGM+HuNoV pigs had more severe and longer mean duration of diarrhea compared to the HuNoV pigs on PID4-10. Viral titers were higher in the duodenum and distal ileum of HGM+HuNoV pigs compared to HuNoV pigs on PID3. There was no significant difference in viral genome level in plasma and whole blood cells of HGM+HuNoV or HuNoV pigs. On PID3, 27 genes related to "immune system process" were consistently and highly upregulated in HGM+HuNoV pigs compared to HuNoV pigs. Additionally, immunoglobulin constant chain and immunoglobulin variable chain genes were significantly upregulated in the HGM+HuNoV pigs. As a whole, these results show that HGM enhances infectivity of HuNoV in the gnotobiotic pig model and alters host gene expression, especially genes related to the immune system.

Introduction

Human noroviruses (HuNoVs), non-enveloped RNA viruses with a positive-sense single-stranded genome in the *Caliciviridae* family, are the leading cause of epidemic acute gastroenteritis around the world (1). Annually, HuNoV infections cause 685 million illnesses and over 212,000 deaths worldwide, in which 30% of illnesses and 25% of deaths are in children under 5 years old (2). HuNoV gastroenteritis has an economic cost of approximately $4 billion in direct healthcare costs and approximately $60 billion in loss of productivity globally (3). Despite the tremendous burden of disease and financial cost, no vaccines or antivirals are currently available to prevent or control HuNoV infections, primarily resulting from the long absence of a readily reproducible cultivation system and a suitable small animal model (4).

The ability of commensal microbiota to enhance enteric viral infections was first demonstrated by two studies using poliovirus, reovirus, and mouse mammary tumor virus (5,6). The microbiota-driven enhancement of murine rotavirus infection was evidenced by the reduced rotavirus infectivity and diarrhea in antibiotics treated suckling mice (7). Similarly, antibiotic treatment reduced acute murine norovirus (MNV) infection and prevented persistent MNV infection in mice (8,9). Persistent infection could be restored by microbial colonization (9). However, it is also known that gut microbiota can protect against enteropathogens due to their colonization resistance and immunomodulatory functions (10). The existence of contradictory reports suggests that the role of microbiota in viral infections varies in regard to the individual virus and host. For example, human rotavirus challenge in the gnotobiotic (Gn) pig model resulted in significantly more viral shedding and more severe diarrhea in germ-free pigs compared to human gut microbiota

(HGM) transplanted pigs (11). After antibiotic depletion of the gut microbiota, mice were more susceptible to flaviviruses such as West Nile, Dengue, and Zika virus (12).

While commensal bacteria have been found to promote MNV infections in mice (13), the effects of HGM on HuNoV infectivity remain unknown. Disruption of HGM due to HuNoV infection has been reported in human patients. Seven out of thirty-eight HuNoV-infected patients showed significantly decreased abundance of *Bacteroidetes* and increased abundance of *Proteobacteria* (14). One study evaluating healthy human volunteers found lower salivary anti-HuNoV IgA titers were correlated with higher abundance of certain bacterial groups such as *Ruminococcus* spp. and *Faecalibacterium*, demonstrating a potential link between the susceptibility to HuNoV infection and HGM composition (15). Human B lymphocytes (BJAB cell line) supported moderate *in vitro* HuNoV replication using unfiltered HuNoV-positive stool sample as inoculum, whereas the filtered inoculum failed to establish HuNoV infection (8). In efforts to dissect such microbiota-dependent infection, synthetic histo-blood group antigen (HBGA) or HBGA-expressing bacteria such as *Enterobacter cloacae* were identified as a cofactor for HuNoV infection of B cells (8). However, our previous study using a Gn pig model showed that *E. cloacae* inhibited HuNoV infection *in vivo*, and viral infection of B cells was not observed with or without the presence of *E. cloacae* (17). In addition, bacteria were not required for efficient viral infection of human intestinal enteroids, which have been established as a novel HuNoV cultivation system for multiple GII.3 and GII.4 strains (18, 19). These conflicting results raise new questions about the role and importance of HGM on HuNoV infection.

Neonatal Gn pigs share high similarity of gastrointestinal physiology and immune system with infants and young children, and have been widely used for the studies of pathogenesis, host immunity, and the role of microbiome/bacteria in enteric virus infections (20). The evaluations of vaccine candidates and therapeutic agents against enteric viruses in Gn pigs have high translational implications (21-24). In addition, Gn pigs are the only animal model that recapitulates the hallmark features of HuNoV biology, such as natural oral route of infection, fecal viral shedding, transient viremia, and increased and prolonged infection in immunodeficient host (20). Additionally, the germ-free environment is ideal for the reconstruction of HGM in animal models. Studies have shown by microbiome analysis that HGM-transplanted Gn pigs were colonized by microbiota similar to that of infant donors (11, 25). The HGM-transplanted Gn pig model has enabled research into the effects of enteric dysbiosis and protein malnutrition on rotavirus vaccine efficacy (26, 27).

In this study, with the aim of determining the influence of HGM on HuNoV infection *in vivo*, we first established the HGM-transplanted Gn pig model of HuNoV infection and disease. Subsequently, HuNoV-induced disease, virus shedding in feces, and virus distribution in tissues were evaluated and compared between HGM-transplanted Gn pigs and control groups. Finally, the influence and mechanisms of altered HuNoV infectivity in the presence of HGM were explored by intestinal transcriptome analysis, with emphasis on immune response related genes.

Results

HGM-transplanted pig model of HuNoV infection and disease

To establish and validate the HGM-transplanted pig model in this study, a heathy infant stool sample was used for transplantation in Gn pigs. The characteristics of "healthy" stool samples were described in Chapter 2. HuNoV infection and/or HGM colonization was tested using four treatment groups: (i) Mock (n = 5), naïve Gn pigs; (ii) HuNoV (n = 19), Gn pigs were inoculated with HuNoV; (iii) HGM (n = 7), Gn pigs were colonized with HGM only; (iv) HGM+HuNoV (n = 11), Gn pigs were colonized with HGM prior to HuNoV inoculation (**Fig 1A**). To confirm the colonization of HGM in Gn pigs, fecal bacteria shedding was monitored after HGM feeding. Bacteria shedding was detected in all pigs in HGM group and HGM+HuNoV group, whereas pigs in Mock group and HuNoV group remained sterile during the entire study (**Fig 1B**).

HGM promoted HuNoV shedding and diarrhea

HuNoV shedding in Gn pigs peaked on PID4 with or without HGM colonization (**Fig 2A**). Daily fecal virus shedding increased in the HGM+HuNoV group, and statistical significance was observed on PID 3, 4, 6, 8, and 9 (**Fig 2A**). Compared to the HuNoV group, the peak shedding in the HGM+HuNoV group was significantly higher during PID 1-3 (**Fig 2B**), and the cumulative shedding in the HGM+HuNoV group was significantly higher during PID 1-3 and PID 4-10 (**Fig 2C**). In addition, HGM+HuNoV pigs had a significantly longer mean duration of virus shedding during PID 1-3 and PID 4-10 (2.4 versus 1.5 days and 6.8 versus 4.9 days, respectively) (**Table 1**). Taken together, these data demonstrated higher HuNoV shedding in HGM-transplanted pigs, indicating that the presence of HGM promoted HuNoV infectivity in Gn pigs.

The fecal consistency was evaluated daily for all groups, HGM colonization did not induced diarrhea (**Table 1**), as the pigs shared comparable fecal consistency scores in

the mock and HGM groups (**Fig 3**). Consistent with the higher virus shedding, more severe HuNoV-induced diarrhea was observed in the HGM+HuNoV group, characterized by significantly higher cumulative fecal consistency scores and mean duration of diarrhea (3.8 versus 2.0 days) during PID 4-10 than those of the HuNoV group (**Fig 3B and Table 1**). Pigs in the HGM+HuNoV group experienced lower incidence and mean duration of diarrhea during PID 1-3 (**Table 1**), indicating intestinal protection due to the pre-colonization of HGM, which might delay the occurrence of HuNoV-induced diarrhea.

HuNoV distribution in gut tissues, blood, and mononuclear cells

After HuNoV inoculation, pigs were euthanized at PID3 or PID10 for the collection of gut tissues and blood. Compared to the HuNoV group, on PID3, virus titers were significantly higher in duodenum and distal ileum of the HGM+HuNoV group (**Fig 4A**), indicating that HGM played a favorable role in HuNoV infection of Gn pigs. Consistent with the virus shedding, virus titers in all sections of intestine were comparable between the two groups on PID10 (**Fig 4B**). Viral genomes were detected in plasma and whole blood cells of both groups, although statistical significance was not observed (**Fig 4C and 4D**), suggesting unaltered and transient HuNoV viremia in Gn pigs colonized with HGM.

Previous studies indicated that enterocytes are the only target of HuNoV in different types of Gn pig models, including naïve Gn pigs (28, 29)[9], *E. cloacae* colonized Gn pigs (17), and RAG2/IL2RG immunodeficient Gn pigs (30). To examine whether HuNoV could infect other cell types, particularly immune cells, in the presence of HGM in Gn pigs, we performed qRT-PCR to detect viral genomes in mononuclear cells (MNC) from ileum, duodenum, spleen, and blood. Although a small portion of pigs in both

groups had detectable virus in MNC, the titers were generally as low (200 genomic copies per 10^7 MNC) (**Fig 4E**). Furthermore, immunohistochemistry targeting viral capsid was performed on sections of duodenum and jejunum from both groups, and our results showed that the only HuNoV-positive cells were enterocytes, whereas all cells in the lamina propria from both groups remained negative (**Fig 5**). In all, these data suggest that HGM might promote HuNoV infectivity in Gn pigs via enhancement of HuNoV infection and/or replication in enterocytes.

HGM enhanced intestinal immunity upon HuNoV infection

To determine the influence of HGM colonization on host responses during HuNoV infection, RNA sequencing (RNA-seq) was performed using distal ileum from pigs euthanized on PID3 in Mock, HuNoV, and HGM+HuNoV groups. These distal ileum samples were selected due to the observed higher HuNoV titers in the HGM+HuNoV group than that of HuNoV group (**Fig 4A**), as well as the higher abundance of bacteria and lymphoid tissue in ileum compared to the duodenum (31). For transcriptome analysis, an average of 92.0% of sequencing reads from 11 RNA-seq libraries were uniquely mapped to the genome, and 53.7% of mapped reads were assigned to annotated genomic features, which were consisted mainly of exons of coding genes. There were 517 significantly differentially expressed genes were identified from differentially expressed gene (DEGs) analysis. Among these DEGs, 242 genes were up-regulated in the HuNoV group and 275 genes were up-regulated in the HGM+HuNoV.

For functional analysis of DEGs, upregulated genes in the HuNoV and HMG+HuNoV groups were compared to the Mock group. In the HuNoV group, the enrichment was observed with 232 upregulated protein coding genes, which belonged to

five gene ontology (GO) and KEGG categories such as “Cell projection” and “Ion binding”. In the HGM+HuNoV group, the enrichment was observed with 254 upregulated genes, which belonged to 30 functional categories, suggesting activated host responses. In addition, “Immune system process” was a major induced category in the HGM+HuNoV group, and it encompassed multiple sub-functional categories such as “Regulation of immune system process”, “Cellular response to lipopolysaccharide”, and “Cellular response to molecule of bacterial origin”. DEGs related to “Immune system process” were plotted, and the result showed that 27 out of 32 genes were highly and consistently upregulated in the HGM+HuNoV group compared to the Mock and HuNoV groups, whereas only inconsistent moderate upregulations were observed in the HuNoV group (**Fig 6**). These genes included those involved in adaptive and innate immunity. Two genes, DHX58 and OAS2 are known components of the innate antiviral response (61, 61) Taken as a whole, these transcriptome enrichment data indicate that the presence of HGM promoted host responses, including HuNoV-induced immune responses.

Bile acid and glycosphingolipid metabolism were investigated as mechanisms underlying the HGM-promoted HuNoV infection because of previous studies (1). In the current pig genome annotation, there are 44 genes related to either bile acid metabolic process or transportation of bile acid across membrane, and 9 genes related to glycosphingolipid metabolic processes. However, differentially expressions were not observed for those genes in the HGM+HuNoV group, suggesting that bile acid and glycosphingolipid pathways were unaffected by the presence of HGM. Intriguingly, ten IG_C genes (immunoglobulin constant chain,) and three IG_V genes (immunoglobulin variable chain) were significantly upregulated in the HGM+HuNoV group, whereas no

IG_C or IG_V genes were upregulated in the HuNoV group. Since secretory immunoglobulins play an important role in MNV infection (32), one potential mechanisms of HGM in enhancing HuNoV infection might be inducing the production of immunoglobulins, which warrants further investigation.

Discussion

Microbiota are indispensable for the development and maintenance of a healthy enteric nervous system (33,34), immune system (10), and gastrointestinal physiology (35). The lack of maternal antibodies and gut microbiota in neonatal Gn pigs contributes to their underdeveloped mucosal immunity, predisposing these pigs to enteric pathogens (36). Unlike the reduced human rotavirus infection and disease in HGM colonized Gn (11), HGM enhanced HuNoV infection and disease in HGM-transplanted Gn pigs compared to noncolonized Gn pigs in this study. HuNoV has not been able to infect conventional pigs; the resistance presumably results from the well-developed mucosal immunity due to the naturally acquired porcine gut microbiota. Therefore, it is likely that HGM has a unique component that facilitates HuNoV infection in pigs, and such component could be illuminated by further studies evaluating microbiome dynamics, transcriptome analysis of viral target cells, and metabolome profiling and pathway analysis of intestinal contents.

Previous studies have demonstrated enhancement of poliovirus infection in mice by commensal bacteria was attributed to virus binding to the bacterial outer-membrane component polysaccharides, resulting in virion thermostability and attachment to host cells (37). HuNoV has also been shown to bind to a bacteria, including a commensal bacterial species, *E. cloacae* (38), the representatives in HGM (39), and multiple

probiotic strains (40, 41). One mechanism of HuNoV-bacterial binding is the direct interaction between the viral capsid and HBGA-like carbohydrates on bacterial surface, which might also enhance HuNoV thermostability (38, 42). Both enhancement and inhibition of HuNoV P particle cell attachment have been observed *in vitro* in the presence of HuNoV-binding probiotics, such as *Escherichia coli* Nissle 1917 and *Lactobacillus casei* BL23 (40). HBGA-expressing *E. cloacae* has been suggested as a helper in HuNoV infection of human B cells, which is a novel HuNoV cell culture system, despite the inconsistent results in other laboratories (8, 43). Previous studies in Gn pigs showed that *E. cloacae*, *Lactobacillus rhamnosus* GG, and *Escherichia coli* Nissle 1917 exhibited inhibitory effects on HuNoV infection *in vivo* (17, 41), presumably resulting from bacteria-and-virus interaction and/or bacterial immunomodulatory functions. Therefore, the impact of HuNoV-binding bacteria on viral infections differs in different studies. There are likely certain bacterial strains in HGM that inhibit HuNoV infection, such as *E. cloacae,* and other species which enhance infection. Further investigation are needed to determine the influence and interaction of different bacterial strains on HuNoV infection.

Although most enteric pathogens target intestinal epithelial cells, the presence of HuNoV antigens or virions has not been reported in clinical biopsy samples from immunocompetent humans, and the cellular tropism of HuNoV is uncertain (44-48). In intestinal biopsies from an immunocompromised patient cohort, HuNoV replication was observed only in enterocytes from sections of duodenum and jejunum, and the HuNoV-associated histopathological features in enterocytes were present as well (48). Additionally, enterocytes in the stem cell-derived and nontransformed human intestinal

enteroids supported the cultivation of multiple HuNoV strains (18), altogether indicating enterocytes as the primary target for HuNoV infection *in vivo* and *in vitro*. Consistent with previous findings in different Gn models for HuNoV challenge study (17, 28-30), enterocytes were the only detectable HuNoV-positive cell type in HGM-transplanted pigs in this study. Recently, tuft cells, a rare type of intestinal cell, have been recognized as a target of MNV strain CR6 (49). Notably, approximately 1.4% of intestinal tuft cells or an estimated 100 cells per mouse were infected by MNV-CR6 (49). Given the rarity of infected tuft cell, and lack of reliable pig-specific molecular reagents, the identification of HuNoV-positive tuft cells is challenging in the current study.

Next-generation sequencing (NGS) technologies such as RNA-seq have promoted the systematic and unbiased host transcriptome analysis, and RNA-seq has been widely employed to explore an organism's response to infectious pathogens. In particular, transcriptome profiling of MNV-infected mouse macrophages has illustrated changes in innate immune response, MHC maturation, and viral recognition processes (51, 52). To gain insight into a global view of host response upon HGM colonization and HuNoV infection, we performed transcriptome analysis using distal ileum tissue. The capacity of transcriptome analysis has been largely limited by the low quality of genome and gene annotation in many species compared with model species such as human and mouse. The previous version of pig reference genome (Sscrofa 10.2) has the shortest scaffold N50 length (576,008 bp) and the longest total gap length compared with six other domesticated species [*Transcriptome Analysis in Domesticated Species: Challenges and Strategies*]. With the development of NGS technology, the latest version of pig reference genome (Sscrofa 11.1) has improved assembly efficiency with higher scaffold N50 length

(88,231,837 bp) than those of human (GRCh38.p12, 59,364,414 bp). Even though the total number of coding genes from both species are similar (20, 418 for human, and 22,452 for pig), the number of gene transcripts of human (206,762) is fourfold more than those of pig (49,448). To further improve the efficiency and accuracy of transcriptome analysis in pigs, porcine gene transcripts databases need to be expanded in terms of various tissue types and different experimental conditions, as wells as establishing comprehensive annotation for gene functional studies.

Recent work, including this study, implies that antibiotics could be used to treat enteric viral infections, but this is clearly not a feasible option because of the multivariate health benefits offered by the bacterial microbiota (10, 33-35), and the fact that microbiota's role in viral infections varies for different viral species. In addition, it is well known that antibiotic overuse contributes to antibiotic resistance, which is an urgent and growing public health threat (53). Thus, the side effects and public health implications of broad-spectrum antibiotic usage as mentioned in some studies would far outweigh the potential positive effects of treating certain enteric virus infections with antibiotics. While HGM promoted HuNoV infection in Gn pigs, the HGM colonization might also provide protection for the host, as lower incidence and mean duration of diarrhea were observed in the HGM+HuNoV group in the initial stage (**Table 1**). Therefore, the beneficial effects of microbiota exist even in the scenarios that increased pathogenic infections occur.

In this study we proved that HGM transplanted pigs can be used as a model of HuNoV infection and disease. Using this model we demonstrated that viral shedding was

greater in HGM+HuNoV pigs compared to HuNoV pigs, and longer in duration. The HGM+HuNoV group also had more severe and longer duration of diarrhea than the HuNoV group pigs on PID 4-10. Viral titers in the duodenal and distal ileal tissues were greater in HGM+HuNoV pigs compared to HuNoV pigs on PID3. These results show that HGM promoted norovirus infectivity and worsened clinical signs. HGM may have provided short term protection from diarrhea, as the HGM+HuNoV group had lower incidence and mean duration of diarrhea on PID1-3. The main finding from RNA-seq analysis was that 27 genes related to "immune system process" were consistently and highly upregulated in HGM+HuNoV pigs compared to Mock and HuNoV pigs. These genes were involved in both adaptive and innate immunity, suggesting direct modulation of host immunity by HGM.

Materials and methods

Virus and stool samples

The HuNoV inoculum containing the GII.4/2006b variant 092895 (GenBank accession number KC990829) was prepared from a stool sample obtained from a child with norovirus gastroenteritis at the Cincinnati Children's Hospital Medical Center in 2008 (29). The stool for HGM transplantation (SV5) was collected from a vaginally delivered, breast-fed, male infant in León, Nicaragua as described previously (26, 54). The stool samples underwent 16S rRNA amplicon sequencing for characterization of the gut microbiome, as previously described (Shannon index, 3.92; observed species 95.4; phylogenetic diversity, 7.46; Chao1, 207) (55). ELISAs for 4 biomarkers of enteropathy were run (calprotectin, 146.22 ug/g; alpha-1-antitrypsin, 12.99 ug/ml; neopterin, 126.71 nmol/l; and myeloperoxidase, 0.22 ug/ml) (54). The samples was previously confirmed negative for rotavirus, astrovirus, norovirus, sapovirus, adenovirus, and *Klebsiella* spp. via PCR prior to oral transplantation into the Gn pigs (26).

Gnotobiotic pigs and treatments

Near-term Yorkshire pigs were derived via hysterectomy, maintained in Gn isolator units, and fed with sterile cow milk (36). Neonatal Gn pigs were randomly assigned to the four treatment groups: Mock (n = 5), HuNoV (n = 19), HGM (n = 7), HGM+HuNoV (n = 11). Due to the lack of maternal antibody transfer across the porcine placenta and the deprivation of sow colostrum/milk in our Gn system, naïve Gn pigs have no maternal antibodies and thus are susceptible to enteric pathogens. Intraperitoneal (IP) injections of gamma-irradiated, commercially available porcine serum were given to the pigs in an attempt to provide immunoprotection against potentially pathogenic bacteria in the HGM transplants (26). The porcine serum was screened using a luciferase immunoprecipitation system assay (56) and no antibodies against a broad range of HuNoV genotypes,, including GI.5, GI.6, GII.1, GII.2, GII.3, GII.4/MD145, GII.6, GIV.1, or GII.4/2006b were detected. All piglets received 60 ml gamma-irradiated, non-heat treated porcine serum (Rocky Mountain Biologicals Inc) divided over three intraperitoneal injections at 24, 30, and 36 hours post derivation. Prior to the oral transplantation of HGM into Gn pigs, the 5% stool sample (SV5) was washed with 10-fold volume of sterile PBS to

remove glycerol, centrifuged at 2000 rpm for 10 min at 4 °C to pellet bacteria, and then resuspended to the original volume with sterile PBS as HGM inoculum. Pigs in the HGM group and HGM+HuNoV group received 450 µl HGM inoculum each day at 4 and 5 days of age. Pigs in the HuNoV group and HGM+HuNoV group were orally inoculated at 6 days of age with 2.74×10^4 viral RNA copies of HuNoV. This dose was determined as 10 ID_{50} for neonatal pigs based on a previous study (29). Four ml of 200 mM $NaHCO_3$ was given 15-20 min prior to HuNoV inoculation to neutralize stomach acid. Pigs were euthanized on PID3 or PID10 for collection of blood, tissues, and intestinal contents.

Assessment of fecal consistency and detection of HuNoV

Fecal consistency and virus shedding was monitored daily after HuNoV inoculation by rectal swab sampling. The fecal consistency scores were as follows: 0, solid; 1, semisolid; 2, pasty; 3, semiliquid; 4, liquid. HuNoV genomes in feces, blood, mononuclear cells, and tissues were detected by a one-step TaqMan qRT-PCR, and HuNoV capsid protein was detected in sections of duodenum and jejunum by immunohistochemistry as described previously (30).

RNAseq library preparation and sequencing

The distal ileum tissue was collected during pig necropsies, snap frozen in liquid nitrogen, and then stored in a -80 °C freezer. Total RNA was isolated from frozen sections using RNeasy Plus Universal Mini kit with RNase-Free DNase set (QIAGEN) per manufacturer's instructions. The library preparation and sequencing were performed at the Virginia Tech Biocomplexity Institute. Briefly, three µg of total RNA was depleted of rRNA using Ribo-Zero Gold rRNA Removal Kit (Illumina), fragmented and converted to cDNA using PrepX RNA-Seq for Illumina Library Kit (Wafergen). The cDNA fragments went through end repair, addition of a single 'A' base, ligation of adapters, and indexed individually. The products were purified and the second strand digested with N-glycosylase, thus resulting in stranded template. The template molecules with the adapters were enriched by 14 cycles of PCR to create the final cDNA library. The 280-300bp cDNA libraries were pooled and sequenced on Illumina NextSeq 500 platform (75 cycles single end), which generated an average of 16.8 million reads per sample.

Transcriptome analysis

RNA-seq libraries were mapped to the pig Ensembl reference genome (Release-91, Sus_scrofa.Sscrofa11.1) using STAR version 2.5.2b (57). FeatureCounts from Subread version 1.5.1 (58) was used to quantify the mapped reads to genomic features from the pig Ensembl gene annotation (Sus_scrofa.Sscrofa11.1.91). DEGs were identified by DESeq2 with the adjusted p-value cutoff of < 0.05 (59). Both raw RNA-seq data and processed gene expression matrix file reported in this study will be publicly available on the NCBI GEO.

Ethical Statement

The stool collection was conducted in accordance with protocols approved by the Institutional Review Boards the Cincinnati Children's Hospital Medical Center (IRB number: 2008-1131) and the Universidad Nacional Autónoma de Nicaragua, León (IRB number: #110), parents or guardians of the children provided written consent for future studies. All animal experiments were conducted in accordance with protocols approved by the Institutional Animal Care and Use Committee at Virginia Tech (IACUC protocols: 14-108-CVM and 17-110-CVM).

Statistics

Pigs were randomly divided into treatment groups upon derivation regardless of gender and body weight, and pigs in each group were randomly assigned for euthanasia on PID3 or PID10. For assessing fecal virus shedding and consistency scores after HuNoV infection, pigs in the PID 10 subgroup contributed data to the PID 3 subgroup. Statistical analysis was performed using GraphPad Prism 6.0 (GraphPad Software) with different significance specified in figure legends, while only P value < 0.05 was considered as statistically significant.

Conflict of interest

The authors declare that they have no conflict of interest.

References

1. Atmar, R. L., Ramani, S. & Estes, M. K. Human noroviruses: recent advances in a 50-year history. *Curr Opin Infect Dis* **31**, 422-432, doi:10.1097/QCO.0000000000000476 (2018).
2. Hall, A. J., Glass, R. I. & Parashar, U. D. New insights into the global burden of noroviruses and opportunities for prevention. *Expert review of vaccines*, 1-3, doi:10.1080/14760584.2016.1178069 (2016).
3. Bartsch, S. M., Lopman, B. A., Ozawa, S., Hall, A. J. & Lee, B. Y. Global Economic Burden of Norovirus Gastroenteritis. *PloS one* **11**, e0151219, doi:10.1371/journal.pone.0151219 (2016).
4. Riddle, M. S. & Walker, R. I. Status of vaccine research and development for norovirus. *Vaccine* **34**, 2895-2899, doi:10.1016/j.vaccine.2016.03.077 (2016).
5. Kuss, S. K. *et al.* Intestinal microbiota promote enteric virus replication and systemic pathogenesis. *Science* **334**, 249-252, doi:10.1126/science.1211057 (2011).
6. Kane, M. *et al.* Successful transmission of a retrovirus depends on the commensal microbiota. *Science* **334**, 245-249, doi:10.1126/science.1210718 (2011).
7. Uchiyama, R., Chassaing, B., Zhang, B. & Gewirtz, A. T. Antibiotic treatment suppresses rotavirus infection and enhances specific humoral immunity. *J Infect Dis* **210**, 171-182, doi:10.1093/infdis/jiu037 (2014).
8. Jones, M. K. *et al.* Enteric bacteria promote human and mouse norovirus infection of B cells. *Science* **346**, 755-759, doi:10.1126/science.1257147 (2014).
9. Baldridge, M. T. *et al.* Commensal microbes and interferon-lambda determine persistence of enteric murine norovirus infection. *Science* **347**, 266-269, doi:10.1126/science.1258025 (2015).
10. Ivanov, II & Honda, K. Intestinal commensal microbes as immune modulators. *Cell Host Microbe* **12**, 496-508, doi:10.1016/j.chom.2012.09.009 (2012).
11. Kumar, A. *et al.* Impact of nutrition and rotavirus infection on the infant gut microbiota in a humanized pig model. *BMC Gastroenterol* **18**, 93, doi:10.1186/s12876-018-0810-2 (2018).
12. Thackray, L. B. *et al.* Oral Antibiotic Treatment of Mice Exacerbates the Disease Severity of Multiple Flavivirus Infections. *Cell reports* **22**, 3440-3453.e3446, doi:10.1016/j.celrep.2018.03.001 (2018).
13. Sullender, M. E. & Baldridge, M. T. Norovirus interactions with the commensal microbiota. *PLoS Pathog* **14**, e1007183, doi:10.1371/journal.ppat.1007183 (2018).
14. Nelson, A. M. *et al.* Disruption of the human gut microbiota following Norovirus infection. *PLoS One* **7**, e48224, doi:10.1371/journal.pone.0048224 (2012).
15. Rodriguez-Diaz, J. *et al.* Relevance of secretor status genotype and microbiota composition in susceptibility to rotavirus and norovirus infections in humans. *Sci Rep* **7**, 45559, doi:10.1038/srep45559 (2017).
16. Kolawole, A. O., Rocha-Pereira, J., Elftman, M. D., Neyts, J. & Wobus, C. E. Inhibition of human norovirus by a viral polymerase inhibitor in the B cell culture system and in the mouse model. *Antiviral Res* **132**, 46-49, doi:10.1016/j.antiviral.2016.05.011 (2016).
17. Lei, S. *et al.* Enterobacter cloacae inhibits human norovirus infectivity in gnotobiotic pigs. *Sci Rep* **6**, 25017, doi:10.1038/srep25017 (2016).

18. Ettayebi, K. *et al.* Replication of human noroviruses in stem cell-derived human enteroids. *Science* **353**, 1387-1393, doi:10.1126/science.aaf5211 (2016).
19. Costantini, V. *et al.* Human Norovirus Replication in Human Intestinal Enteroids as Model to Evaluate Virus Inactivation. *Emerging Infectious Disease journal* **24**, 1453, doi:10.3201/eid2408.180126 (2018).
20. Lei, S., Twitchell, E. & Yuan, L. in *Mechanisms Underlying Host-Microbiome Interactions in Pathophysiology of Human Diseases* (eds Jun Sun & Pradeep K. Dudeja) 55-78 (Springer US, 2018).
21. Kocher, J. *et al.* Intranasal P particle vaccine provided partial cross-variant protection against human GII.4 norovirus diarrhea in gnotobiotic pigs. *J Virol* **88**, 9728-9743, doi:10.1128/jvi.01249-14 (2014).
22. Bui, T. *et al.* Effects of Racecadotril on Weight Loss and Diarrhea Due to Human Rotavirus in Neonatal Gnotobiotic Pigs (Sus scrofa domesticus). *Comp Med* **67**, 157-164 (2017).
23. Yang, X. *et al.* High protective efficacy of rice bran against human rotavirus diarrhea via enhancing probiotic growth, gut barrier function, and innate immunity. *Sci Rep* **5**, 15004, doi:10.1038/srep15004 (2015).
24. Wen, X., Cao, D., Jones, R. W., Hoshino, Y. & Yuan, L. Tandem truncated rotavirus VP8* subunit protein with T cell epitope as non-replicating parenteral vaccine is highly immunogenic. *Human vaccines & immunotherapeutics* **11**, 2483-2489, doi:10.1080/21645515.2015.1054583 (2015).
25. Zhang, H. *et al.* Probiotics and virulent human rotavirus modulate the transplanted human gut microbiota in gnotobiotic pigs. *Gut Pathog* **6**, 39, doi:10.1186/s13099-014-0039-8 (2014).
26. Twitchell, E. L. *et al.* Modeling human enteric dysbiosis and rotavirus immunity in gnotobiotic pigs. *Gut Pathog* **8**, 51, doi:10.1186/s13099-016-0136-y (2016).
27. Miyazaki, A. *et al.* Protein deficiency reduces efficacy of oral attenuated human rotavirus vaccine in a human infant fecal microbiota transplanted gnotobiotic pig model. *Vaccine* **36**, 6270-6281, doi:10.1016/j.vaccine.2018.09.008 (2018).
28. Cheetham, S. *et al.* Pathogenesis of a genogroup II human norovirus in gnotobiotic pigs. *J Virol* **80**, 10372-10381, doi:10.1128/JVI.00809-06 (2006).
29. Bui, T. *et al.* Median infectious dose of human norovirus GII.4 in gnotobiotic pigs is decreased by simvastatin treatment and increased by age. *J Gen Virol* **94**, 2005-2016, doi:10.1099/vir.0.054080-0 (2013).
30. Lei, S. *et al.* Increased and prolonged human norovirus infection in RAG2/IL2RG deficient gnotobiotic pigs with severe combined immunodeficiency. *Sci Rep* **6**, 25222, doi:10.1038/srep25222 (2016).
31. Sender, R., Fuchs, S. & Milo, R. Revised Estimates for the Number of Human and Bacteria Cells in the Body. *PLoS Biol* **14**, e1002533, doi:10.1371/journal.pbio.1002533 (2016).
32. De Vadder, F. *et al.* Gut microbiota regulates maturation of the adult enteric nervous system via enteric serotonin networks. *Proc Natl Acad Sci U S A* **115**, 6458-6463, doi:10.1073/pnas.1720017115 (2018).
33. Obata, Y. & Pachnis, V. The Effect of Microbiota and the Immune System on the Development and Organization of the Enteric Nervous System. *Gastroenterology* **151**, 836-844, doi:10.1053/j.gastro.2016.07.044 (2016).

34. An, R. *et al.* Age-dependent changes in GI physiology and microbiota: time to reconsider? *Gut*, doi:10.1136/gutjnl-2017-315542 (2018).
35. Yuan, L., Jobst, P. M. & Weiss, M. in *Gnotobiotics* (eds Trenton R. Schoeb & Kathryn A. Eaton) 349-368 (Academic Press, 2017).
36. Robinson, C. M., Jesudhasan, P. R. & Pfeiffer, J. K. Bacterial lipopolysaccharide binding enhances virion stability and promotes environmental fitness of an enteric virus. *Cell Host Microbe* **15**, 36-46, doi:10.1016/j.chom.2013.12.004 (2014).
37. Miura, T. *et al.* Histo-blood group antigen-like substances of human enteric bacteria as specific adsorbents for human noroviruses. *J Virol* **87**, 9441-9451, doi:10.1128/jvi.01060-13 (2013).
38. Almand, E. A., Moore, M. D., Outlaw, J. & Jaykus, L. A. Human norovirus binding to select bacteria representative of the human gut microbiota. *PLoS One* **12**, e0173124, doi:10.1371/journal.pone.0173124 (2017).
39. Rubio-del-Campo, A. *et al.* Noroviral p-particles as an in vitro model to assess the interactions of noroviruses with probiotics. *PLoS One* **9**, e89586, doi:10.1371/journal.pone.0089586 (2014).
40. Lei, S. *et al.* High Protective Efficacy of Probiotics and Rice Bran against Human Norovirus Infection and Diarrhea in Gnotobiotic Pigs. *Frontiers in microbiology* **7**, 1699, doi:10.3389/fmicb.2016.01699 (2016).
41. Li, D., Breiman, A., le Pendu, J. & Uyttendaele, M. Binding to histo-blood group antigen-expressing bacteria protects human norovirus from acute heat stress. *Frontiers in microbiology* **6**, 659, doi:10.3389/fmicb.2015.00659 (2015).
42. Jones, M. K. *et al.* Human norovirus culture in B cells. *Nat Protoc* **10**, 1939-1947, doi:10.1038/nprot.2015.121 (2015).
43. Agus, S. G., Dolin, R., Wyatt, R. G., Tousimis, A. J. & Northrup, R. S. Acute infectious nonbacterial gastroenteritis: intestinal histopathology. Histologic and enzymatic alterations during illness produced by the Norwalk agent in man. *Ann Intern Med* **79**, 18-25 (1973).
44. Schreiber, D. S., Blacklow, N. R. & Trier, J. S. The mucosal lesion of the proximal small intestine in acute infectious nonbacterial gastroenteritis. *N Engl J Med* **288**, 1318-1323, doi:10.1056/NEJM197306212882503 (1973).
45. Schreiber, D. S., Blacklow, N. R. & Trier, J. S. The small intestinal lesion induced by Hawaii agent acute infectious nonbacterial gastroenteritis. *J Infect Dis* **129**, 705-708 (1974).
46. Dolin, R., Levy, A. G., Wyatt, R. G., Thornhill, T. S. & Gardner, J. D. Viral gastroenteritis induced by the Hawaii agent. Jejunal histopathology and serologic response. *Am J Med* **59**, 761-768 (1975).
47. Karst, S. M., Wobus, C. E., Goodfellow, I. G., Green, K. Y. & Virgin, H. W. Advances in norovirus biology. *Cell host & microbe* **15**, 668-680, doi:10.1016/j.chom.2014.05.015 (2014).
48. Karandikar, U. C. *et al.* Detection of human norovirus in intestinal biopsies from immunocompromised transplant patients. *J Gen Virol* **97**, 2291-2300, doi:10.1099/jgv.0.000545 (2016).
49. Wilen, C. B. *et al.* Tropism for tuft cells determines immune promotion of norovirus pathogenesis. *Science* **360**, 204-208, doi:10.1126/science.aar3799 (2018).

50. Enosi Tuipulotu, D., Netzler, N. E., Lun, J. H., Mackenzie, J. M. & White, P. A. RNA Sequencing of Murine Norovirus-Infected Cells Reveals Transcriptional Alteration of Genes Important to Viral Recognition and Antigen Presentation. *Front Immunol* **8**, 959, doi:10.3389/fimmu.2017.00959 (2017).
51. Levenson, E. A. *et al.* Comparative Transcriptomic Response of Primary and Immortalized Macrophages to Murine Norovirus Infection. *J Immunol* **200**, 4157-4169, doi:10.4049/jimmunol.1700384 (2018).
52. Hekman, J. P., Johnson, J. L. & Kukekova, A. V. Transcriptome Analysis in Domesticated Species: Challenges and Strategies. *Bioinform Biol Insights* **9**, 21-31, doi:10.4137/BBI.S29334 (2015).
53. Brogan, D. M. & Mossialos, E. A critical analysis of the review on antimicrobial resistance report and the infectious disease financing facility. *Global Health* **12**, 8, doi:10.1186/s12992-016-0147-y (2016).
54. Becker-Dreps, S. *et al.* The Association Between Fecal Biomarkers of Environmental Enteropathy and Rotavirus Vaccine Response in Nicaraguan Infants. *The Pediatric infectious disease journal* **36**, 412-416, doi:10.1097/inf.0000000000001457 (2017).
55. Becker-Dreps, S. *et al.* Gut Microbiome Composition in Young Nicaraguan Children During Diarrhea Episodes and Recovery. *Am J Trop Med Hyg* **93**, 1187-1193, doi:10.4269/ajtmh.15-0322 (2015).
56. Tin, C. M. *et al.* A Luciferase Immunoprecipitation System (LIPS) assay for profiling human norovirus antibodies. *J Virol Methods* **248**, 116-129, doi:10.1016/j.jviromet.2017.06.017 (2017).
57. Dobin, A. *et al.* STAR: ultrafast universal RNA-seq aligner. *Bioinformatics (Oxford, England)* **29**, 15-21, doi:10.1093/bioinformatics/bts635 (2013).
58. Liao, Y., Smyth, G. K. & Shi, W. featureCounts: an efficient general purpose program for assigning sequence reads to genomic features. *Bioinformatics (Oxford, England)* **30**, 923-930, doi:10.1093/bioinformatics/btt656 (2014).
59. Love, M. I., Huber, W. & Anders, S. Moderated estimation of fold change and dispersion for RNA-seq data with DESeq2. *Genome Biol* **15**, 550, doi:10.1186/s13059-014-0550-8 (2014).
60. Leisching G, Wiid I, Baker B. The Association of OASL and Type I Interferons in the Pathogenesis and Survival of Intracellular Replicating Bacterial Species. Front Cell Infect Microbiol. 2017;7:196.
61. Takahashi T, Nakano Y, Onomoto K, Yoneyama M, Ui-Tei K. Virus Sensor RIG-I Represses RNA Interference by Interacting with TRBP through LGP2 in Mammalian Cells. Genes (Basel). 2018;9(10

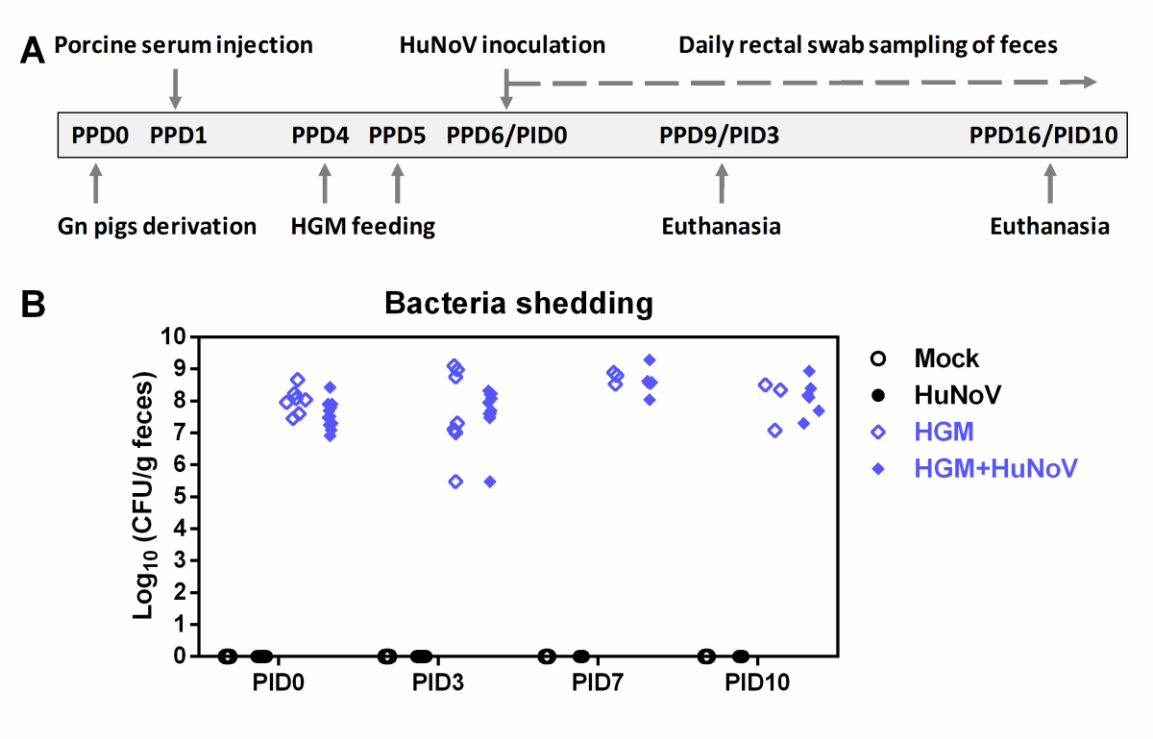

Figure 9 Experimental design and fecal bacteria shedding. (A) Schematic representation of Gn pig study. HGM, human gut microbiota; PPD, post-partum day; PID, post inoculation day. (B) HGM colonization in Gn pigs. The concentrations of culturable aerobic bacteria were measured in serial dilution of pig feces and enumeration of colony forming unit (CFU) grown on LB media agar plates. Data are presented as individual animal data points. Sample sizes are shown in Table 1.

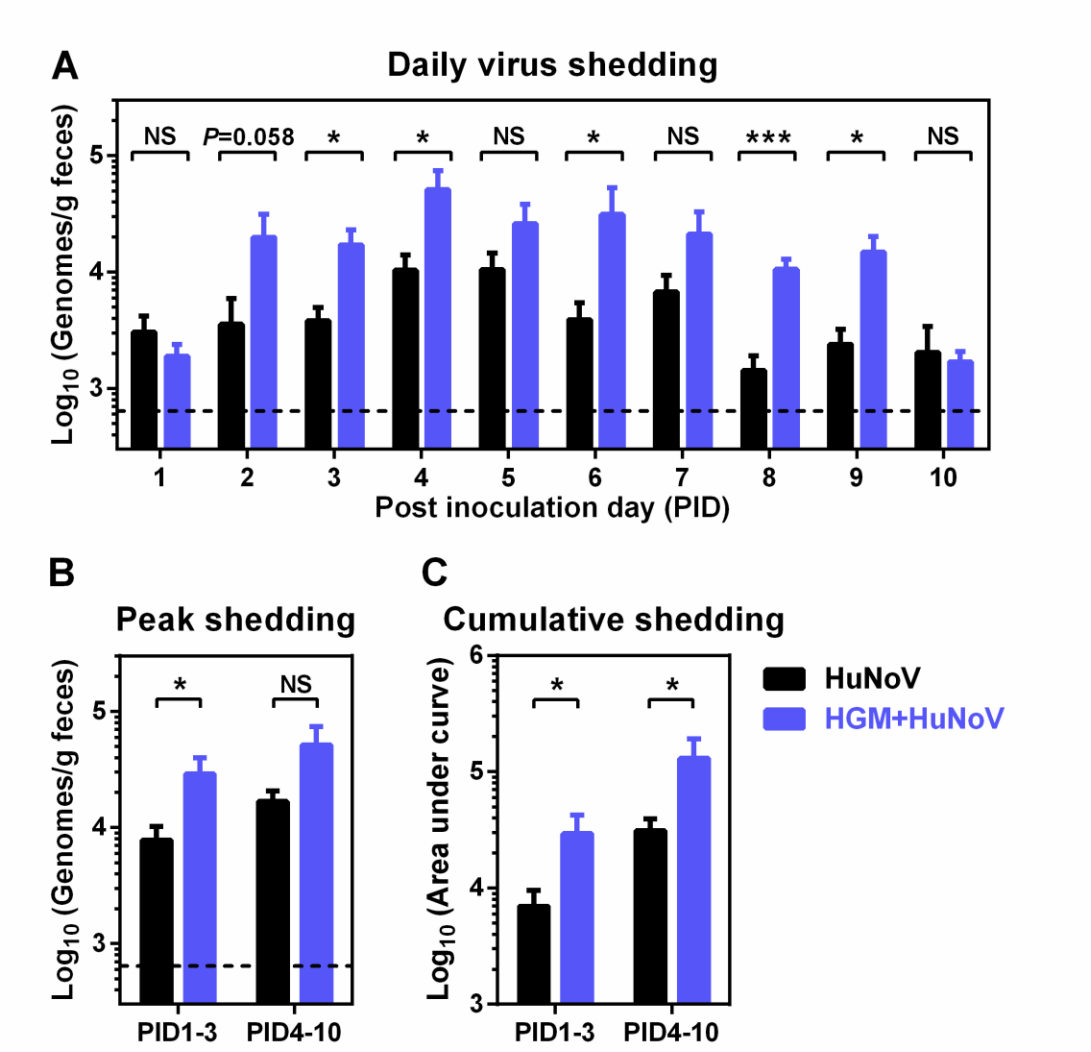

Figure 2. Increased fecal HuNoV shedding in HGM-transplanted pigs. (A) Daily virus shedding was measured from PID1 to PID10 by quantitative reverse transcription polymerase chain reaction (qRT-PCR) to quantify HuNoV genomes in feces. (B) Peak shedding titers during PID1 to PID3 and PID4 to PID10 in individual pigs were present. (C) Individual pigs' cumulative shedding was shown as area under curve based on daily virus shedding in (A). Sample sizes are indicated in Table 1. Dashed line shows the limit of detection. Data are presented as mean ± SEM. Statistical significance was determined by Mann-Whitney test. NS, not significant, $*p < 0.05$, $**p < 0.01$.

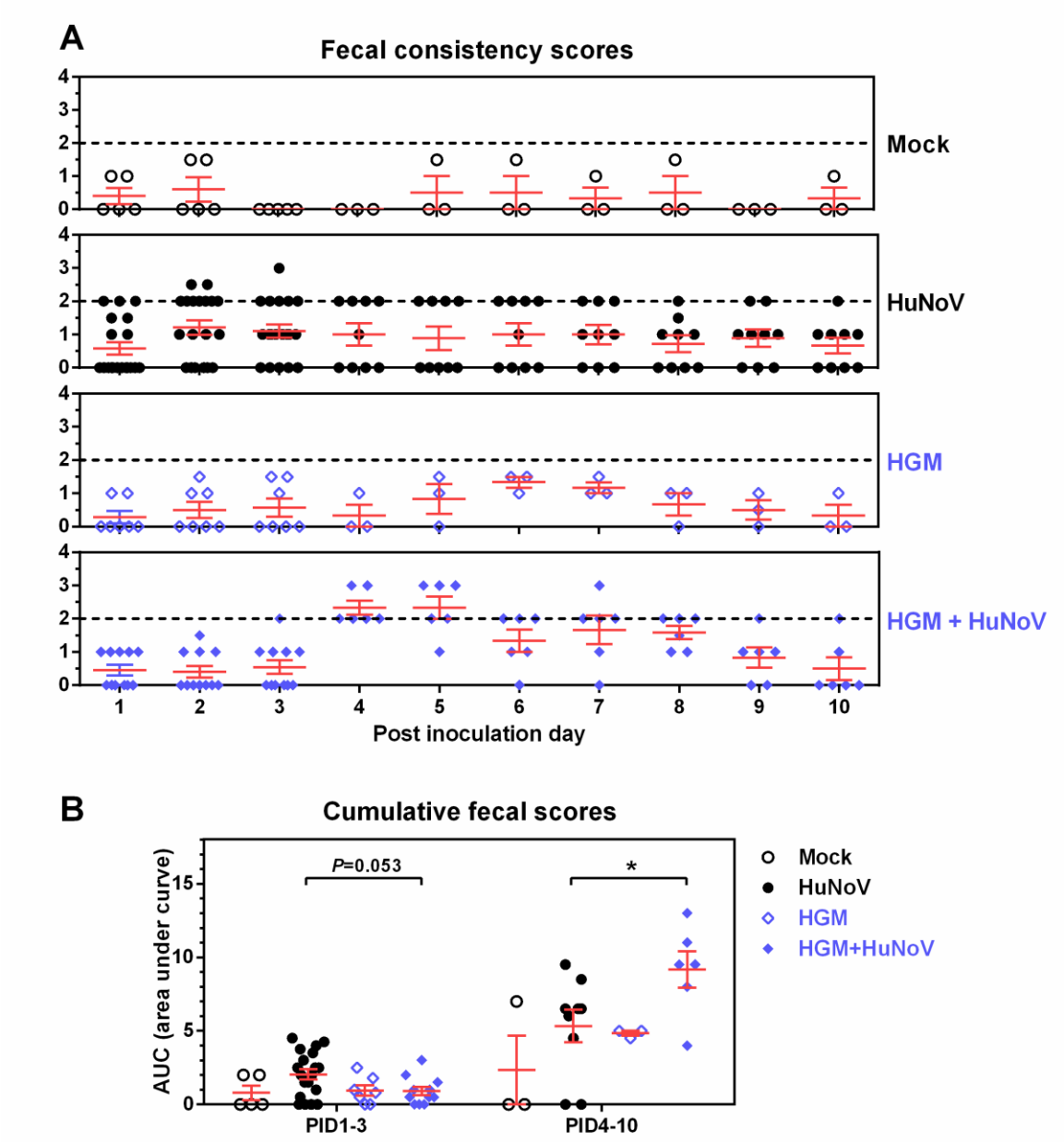

Figure 3. Fecal consistency scores. (A) Daily fecal consistency scores after HuNoV inoculation. Fecal consistency was scored as follows: 0, solid; 1, semisolid; 2, pasty; 3, semiliquid; and 4, liquid. Dashed line shows the threshold of diarrhea. (B) Individual pigs' cumulative fecal scores were shown as area under curve based on daily fecal consistency scores in (A). Data are presented as individual animal data points with mean ± SEM. Statistical significance was determined by Mann-Whitney test, *$p < 0.05$.

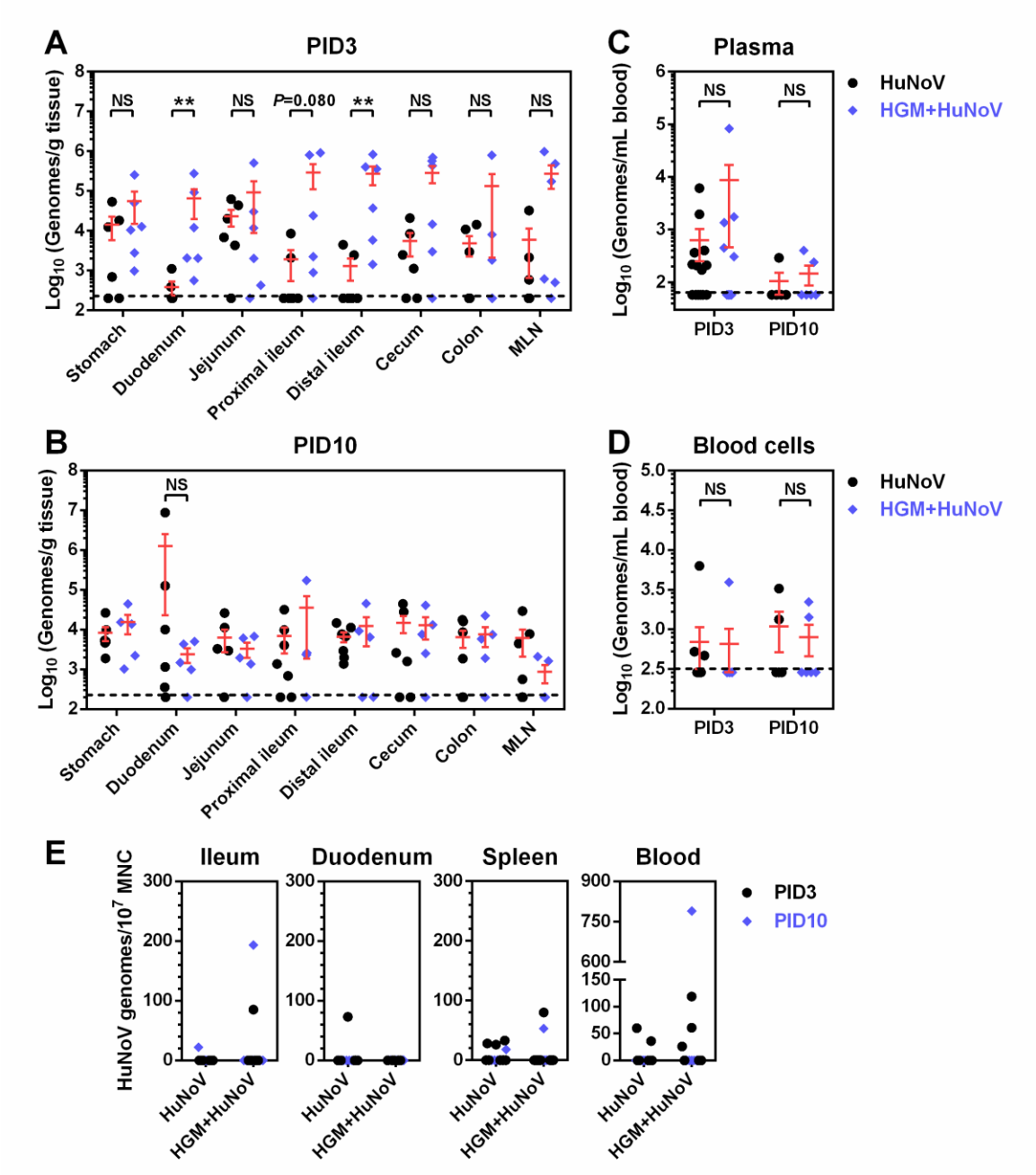

Figure 4 HuNoV distribution in gut tissues, blood, and MNCs. HuNoV genomes in gut tissues from pigs euthanized on PID3 (A) and PID10 (B) were quantified by qRT-PCR. HuNoV genomes in plasma (C), whole blood cells (D), and mononuclear cells (MNCS) were quantified by qRT-PCR. (A-B) HuNoV group size: PID3 $n = 6$, PID10 $n = 7$. HGM+HuNoV group size: PID3 $n = 5$, PID10 $n = 6$. (C-E) Group size were shown in Table 1. Dashed line shows the limit of detection. Data are presented as individual animal data points with mean ± SEM. Statistical significance was determined by Mann-Whitney test. NS, not significant, $*p < 0.05$, $**p < 0.01$.

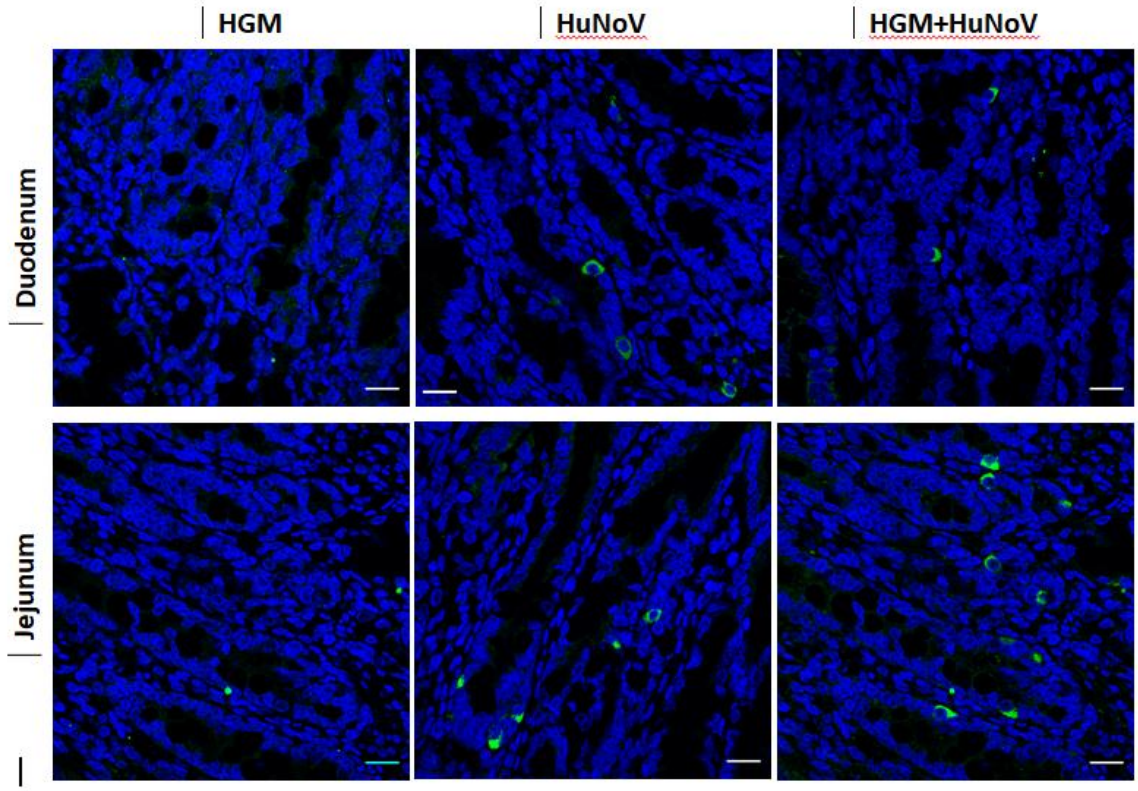

Figure 5 HuNoV infection of enterocytes in HGM-transplanted pigs. HuNoV capsid (bright green) in sections of duodenum (top panel) and jejunum (bottom panel) from Gn pigs euthanized on PID3 were detected by immunohistochemistry. Cell nuclei (blue) were counterstained. Scale bar, 20μm.

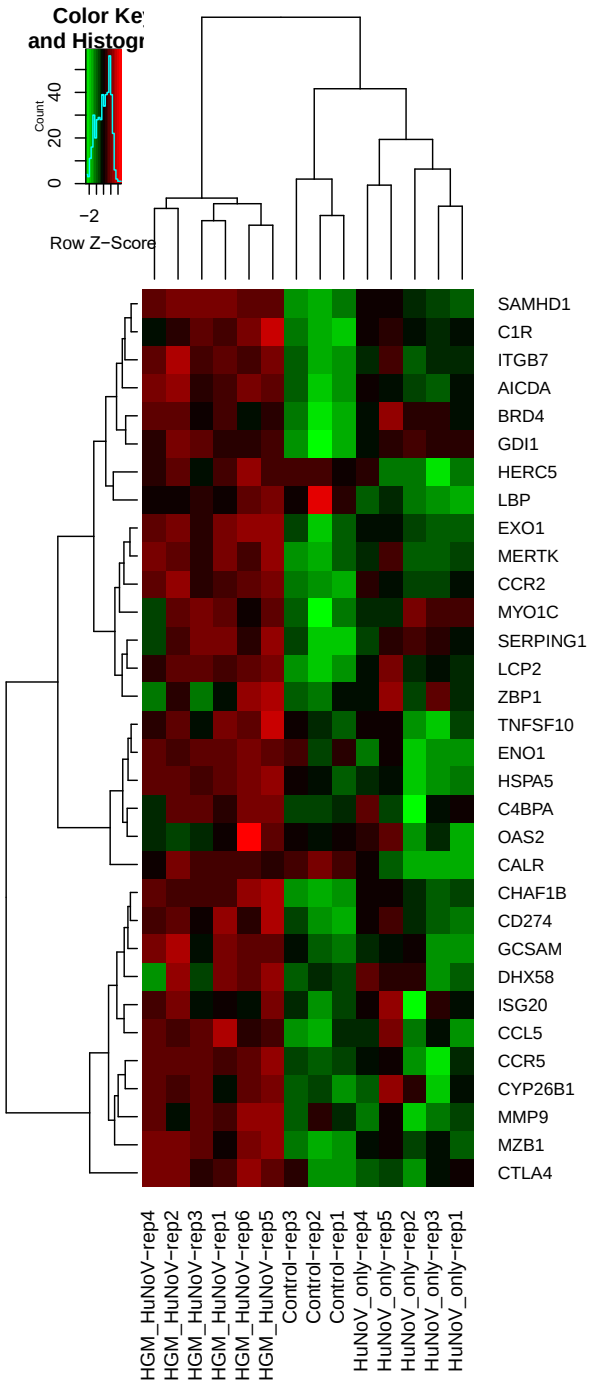

Figure 6　Heat map of immune response related genes.

Table 1 Summary of clinical sign and virus shedding in Gn pigs

Group	Time	*n*	Diarrhea[b]		Virus shedding	
			Pigs with diarrhea (%)*	Mean duration days (SEM[c])**	Pigs with virus shedding (%)*	Mean duration days (SEM)**
Mock	PID1-3	5	0	0	0	0
HuNoV		19	11 (58%)[A]	0.9 (0.2)[A]	16 (84%)	1.5 (0.2)[A]
HGM		7	0	0	0	0
HuNoV+HGM		11	1 (9%)[B]	0.1 (0.1)[B]	11 (100%)	2.4 (0.2)[B]
Mock	PID4-10	3	0	0	0	0
HuNoV		9	7 (78%)	2.0 (0.5)[A]	9 (100%)	4.9 (0.7)[A]
HGM		3	0	0	0	0
HuNoV+HGM		6	6 (100%)	3.8 (0.7)[B]	6 (100%)	6.8 (0.2)[B]

Gn pigs were inoculated with a HuNoV GII.4 2006b variant 092895 at 6 days of age. Rectal swabs were collected daily after inoculation to determine fecal consistency scores and virus shedding.

[b]Fecal consistency was scored as follows: 0, solid; 1, semisolid; 2, pasty; 3, semiliquid; and 4, liquid. Pigs with scores of or over 2 were considered with diarrhea.

[c]SEM, standard error of the mean.

*Fisher's exact test or **Mann-Whitney test was used for statistical analysis. Groups with significant differences ($P<0.05$) were indicated with letters A and B.

Chapter 4 General discussion and future directions

Erica Lynn Twitchell

Department of Biomedical Sciences and Pathobiology

Virginia-Maryland College of Veterinary Medicine,
Virginia Tech, Blacksburg, VA 24061, USA.

The influence of enteric microbiota on viral infection and host response is an active area of research. The findings from my dissertation studies address two questions: 1) what is the role of microbiota-pathogen-host interaction play in the development of host immunity to the pathogen? and 2) what is the role of this interaction play in the virus infectivity and pathogenesis?

In the studies presented here, we showed that pigs colonized by "healthy" infant gut microbiota had a stronger cell-mediated immune response to oral rotavirus vaccination than those pigs colonized by "unhealthy" infant gut microbiota, and certain OTUs were significantly associated with IFN-γ producing T cells at the time of rotavirus challenge. These pigs also had a stronger mucosal immune response based on trends towards higher rotavirus-specific antibody titers in intestinal contents. Vaccinated Gn pigs colonized by "healthy" HGM also had less severe clinical signs compared to "unhealthy" HGM-colonized pigs after rotavirus challenge. These findings confirmed that healthy HGM promotes vaccine induced immunity against enteric infection whereas unhealthy HGM has a detrimental impact on vaccine immunogenicity and protective efficacy.

In the HuNoV study, infection was enhanced in Gn pigs colonized by HGM as these animals had greater titer and duration of virus shedding, and higher intestinal viral titers compared to non-colonized pigs after HuNoV challenge. Clinical signs were also more severe in these animals than HuNoV-only animals on PID 4-10. Multiple genes related to the immune system were highly upregulated in HGM+HuNoV pigs compared to HuNoV-only pigs on PID 3, giving support to the conclusion that HGM influences host immune response. Our findings confirmed that HGM promotes HuNoV intestinal

replication and prolongs the course of HuNoV induced diarrhea. The mechanism behind such effect of HGM is not understood by our study. The host gene expression, especially genes related to the immune system, such as immunoglobulin synthesis and innate viral immunity were enhanced by HGM colonization in HuNoV infected pigs compared to non-HGM transplanted pigs. However, the relationship between the increased HuNoV replication and the immune gene activation needs further investigation.

Given that the composition of the microbiome affects the course of enteric viral disease, it follows that future studies should test the feasibility of altering the microbiome as a means to treat or prevent disease. It is already know that prebiotics and probiotics can influence enteric viral infection. Prebiotics and probiotics are potential agents to purposefully modulate host microbiome and can be used alone or in combination. Modulation of microbiome by probiotics has been studied in Gn pig models. A study in Gn pigs colonized with *Lactobacillus rhamnosus* GG (LGG) and *E.coli* Nissle 1917 (EcN), and fed a diet supplemented with rice bran, showed that the pigs were more protected against rotavirus diarrhea and they had increased growth of probiotic strains compared to probiotic colonized pigs not fed rice bran (1). In another study of HuNoV infection in Gn pigs, animals were colonized with LGG and EcN. It showed that LGG+EcN colonization inhibited viral shedding (2). When dietary rice bran supplementation before and after viral challenge was combined with LGG and EcN colonization, there was a high protective efficacy against diarrhea and viral shedding (2). Rotavirus vaccinated Gn pigs colonized with infant gut microbiota showed that LGG prevented changes in microbiome structure caused by rotavirus challenge that was seen in non-LGG supplemented groups (3). Future studies evaluating intentional microbiome

alteration as a therapeutic or prophylactic measure need to consider potential side effects such as increased risk of certain infections, metabolic diseases, or immune-mediated diseases.

Our studies have demonstrated that Gn pigs are a valuable model for studying the interactions of microbiota, enteric pathogens, and host immune system. Effectively utilizing the Gn pig model in future studies is particularly helpful to address questions in the context of host immune responses such as “Which factors determine the development of microbial gut dysbiosis?” “Which attributes of particular microbes act as probiotics for the development of immune responses?" “Are there particular gut microbes universally correlated with optimal immune responses, and others correlated with insufficient immune responses?”(4)

Future studies assessing intestinal microbiome should also consider viruses, fungi, protozoa, and archaea. Aside from bacteria, there are also viruses, fungi, protozoa, and archaea living among vertebrates. It is expected that interactions between these organisms and commensal bacterial, pathogens, and host are involved in outcomes of disease.

References

1. Yang X, Twitchell E, Li G, Wen K, Weiss M, Kocher J, et al. High protective efficacy of rice bran against human rotavirus diarrhea via enhancing probiotic growth, gut barrier function, and innate immunity. Sci Rep. 2015;5:15004.
2. Lei S, Ramesh A, Twitchell E, Wen K, Bui T, Weiss M, et al. High Protective Efficacy of Probiotics and Rice Bran against Human Norovirus Infection and Diarrhea in Gnotobiotic Pigs. Front Microbiol. 2016;7:1699.
3. Zhang H, Wang H, Shepherd M, Wen K, Li G, Yang X, et al. Probiotics and virulent human rotavirus modulate the transplanted human gut microbiota in gnotobiotic pigs. Gut pathogens. 2014;6:39.
4. Desselberger U. The Mammalian Intestinal Microbiome: Composition, Interaction with the Immune System, Significance for Vaccine Efficacy, and Potential for Disease Therapy. Pathogens. 2018;7(3).